UNIVERSIDADE FEDERAL DE SANTA MARIA
CENTRO DE TECNOLOGIA
DEPARTAMENTO DE ENGENHARIA QUÍMICA
PROGRAMA DE PÓS-GRADUAÇÃO EM ENGENHARIA QUÍMICA

Juliano Missau

VALORIZAÇÃO DE RESÍDUOS DA SERRAGEM DE MADEIRA DE EUCALIPTO A PARTIR DA APLICAÇÃO DA PIRÓLISE

Santa Maria, RS
2022

Juliano Missau

VALORIZAÇÃO DE RESÍDUOS DA SERRAGEM DE MADEIRA DE EUCALIPTO A PARTIR DA APLICAÇÃO DA PIRÓLISE

Tese apresentada ao Curso de Pós-Graduação em Engenharia Química, da Universidade Federal de Santa Maria (UFSM, RS), como requisito parcial para obtenção do título de **Doutor em Engenharia Química.**

Orientador: Prof. Dr. Eduardo Hiromitsu Tanabe
Coorientador: Prof. Dr. Daniel Assumpção Bertuol

Santa Maria, RS
2022

Missau, Juliano
VALORIZAÇÃO DE RESÍDUOS DA SERRAGEM DE MADEIRA DE EUCALIPTO A PARTIR DA APLICAÇÃO DA PIRÓLISE / Juliano Missau.- 2022.
119 p.; 30 cm

Orientador: Eduardo Hiromitsu Tanabe
Coorientador: Daniel Assumpção Bertuol
Tese (doutorado) - Universidade Federal de Santa Maria, Centro de Tecnologia, Programa de Pós-Graduação em Engenharia Química, RS, 2022

1. Serragem de eucalipto 2. Pirólise 3. Biochar 4. Briquetes 5. Material adsorvente I. Hiromitsu Tanabe, Eduardo II. Assumpção Bertuol, Daniel III. Título.

Sistema de geração automática de ficha catalográfica da UFSM. Dados fornecidos pelo autor(a). Sob supervisão da Direção da Divisão de Processos Técnicos da Biblioteca Central. Bibliotecária responsável Paula Schoenfeldt Patta CRB 10/1728.

Juliano Missau

VALORIZAÇÃO DE RESÍDUOS DA SERRAGEM DE MADEIRA DE EUCALIPTO A PARTIR DA APLICAÇÃO DA PIRÓLISE

Tese apresentada ao Curso de Pós-Graduação em Engenharia Química, da Universidade Federal de Santa Maria (UFSM, RS), como requisito parcial para obtenção do título de **Doutor em Engenharia Química.**

Aprovado em 22 de Fevereiro de 2022

Eduardo Hiromitsu Tanabe, Dr. (UFSM)
(Presidente/Orientador)

Daniel Assumpção Bertuol, Dr. (UFSM)
(Coorientador)

Ederson Rossi Abaide, Dr. (UFSM)

Evandro Stoffels Mallmann, Dr. (UFSM)

Jivago Schumacher de Oliveira, Dr. (UFN)

Marco Antônio Siqueira Rodrigues, Dr. (FEEVALE)

Santa Maria, RS
2022

DEDICATÓRIA

Dedico este trabalho ao meu pai Edson Missau, à minha mãe Mirian Missau, ao meu irmão Edson Missau Júnior e à minha irmã Caroline Missau por juntos formarem a melhor família que eu poderia ter pedido a Deus.

AGRADECIMENTOS

Primeiramente a Deus, por tornar tudo possível.

À minha família, meus pais Edson e Mirian, por serem a minha base para tudo, meu porto seguro. Aos meus irmãos Júnior e Caroline, por sempre estarem ao meu lado em todos os momentos, independentemente da situação.

À minha namorada Patrícia, pela amizade, paciência, carinho, amor e companheirismo durante todo o meu doutorado. Agradeço também aos momentos de troca de conhecimento técnico e empréstimos de equipamentos, pois sem isso eu não teria conseguido finalizar o meu estudo.

Aos meus amigos Christian, Dimitri, Giovan, Igor, Leonardo, Marcel, Marcus e Mateus, por formarem a minha segunda família e serem grandes pessoas com quem posso contar sempre.

Aos meus colegas de doutorado pelo ótimo convívio, risadas, momentos de descontração e de ajuda nos obstáculos da vida acadêmica.

Aos meus orientadores, Professores Eduardo Tanabe e Daniel Bertuol, pois além de serem excelentes profissionais, também são grandes pessoas que me ajudaram bastante nos momentos de maior dificuldade técnica e emocional.

Às técnicas de laboratório, Mariana Bassaco e Margiani Fortes, por toda ajuda com as análises e pelos momentos de descontração nos laboratórios.

À Madeireira Haas LTDA pela parceria e oportunidade de estudar aplicações para o campo industrial.

Ao CNPq pelo apoio financeiro.

RESUMO

VALORIZAÇÃO DE RESÍDUOS DA SERRAGEM DE MADEIRA DE EUCALIPTO A PARTIR DA APLICAÇÃO DA PIRÓLISE

AUTOR: Juliano Missau
ORIENTADOR: Prof. Dr. Eduardo H. Tanabe
COORIENTADOR: Prof. Dr. Daniel A. Bertuol

O presente trabalho teve como foco, agregar valor à serragem da madeira de eucalipto, a qual é um resíduo lignocelulósico. Isso foi realizado a partir da aplicação da técnica de pirólise, convertendo a serragem em biochar. Os produtos sólidos (biochar) obtidos da pirólise foram investigados com relação à sua aplicação como briquetes (fins energéticos) e como material adsorvente. Na primeira etapa do trabalho, o biochar foi misturado com outros resíduos aglutinantes tais como cera bruta (resíduos da pirólise de polímeros) e folhas de eucalipto, na presença de amido, para a confecção de briquetes. Os briquetes foram analisados quanto ao seu poder calorífico superior (PCS) e resistência mecânica. O rendimento de biochar obtido na pirólise foi de 35%, e o PCS do mesmo foi de 33,02 MJ/kg a 400 ºC. As proporções de resíduos (cera bruta e/ou folha de eucalipto) avaliadas na composição dos briquetes de carvão foram 10, 20 e 30%. A proporção de amido de milho foi fixada em 8%. Os briquetes com 30% de cera bruta apresentaram o melhor PCS, 23,45 MJ/kg, e maior resistência mecânica ao teste de quebra, 97,81%. Em síntese, foram produzidos briquetes de alta eficiência energética e durabilidade. Na segunda etapa do trabalho, o biochar foi quimicamente ativado com ácido fosfórico (40%) e impregnado com hidróxidos duplos lamelares de cálcio e alumínio (Ca/Al HDL), para melhorar sua capacidade de adsorção. O novo material adsorvente desenvolvido foi aplicado para remover o corante cristal violeta (CV) de soluções aquosas através da operação de adsorção em batelada. Os resultados da caracterização do adsorvente sugeriram que o material foi efetivamente sintetizado e suportado no biochar. Além disso, os experimentos de adsorção indicaram que o pH 8 foi mais adequado para adsorção do corante CV. Na cinética e isoterma de adsorção, os dados experimentais se ajustaram melhor ao modelo cinético de pseudo-segunda ordem e ao modelo isotérmico de Freundlich, respectivamente. O novo adsorvente desenvolvido mostrou uma alta capacidade de adsorção do corante CV alcançando a melhor capacidade de adsorção de 496,55 $mg \cdot g^{-1}$ a 50°C. Com relação as propriedades termodinâmicas, o uso deste adsorvente demonstrou um processo favorável, espontâneo e endotérmico. Nos ciclos de adsorção e dessorção, esse novo material adsorvente manteve 71% da capacidade adsortiva inicial, mesmo após quatro ciclos de reutilização. Com isso, esse novo biochar, quimicamente ativado com ácido fosfórico (40%) e impregnado com Ca/Al HDL, produzido gerou um adsorvente sustentável com alto desempenho para tratamento de efluentes contaminados por corantes.

Palavras-chave: biomassa, serragem de eucalipto, pirólise, biochar, briquetes, material adsorvente.

ABSTRACT

VALORIZATION OF WASTES FROM EUCALYPT WOOD SAWDUST THROUGH THE APPLICATION OF PYROLYSIS

AUTHOR: Juliano Missau
ADVISOR: Prof. Dr. Eduardo H. Tanabe
COADVISOR: Prof. Dr. Daniel A. Bertuol

The present work focused on adding value to the sawdust of eucalypt wood, which is a lignocellulosic waste. This was accomplished by applying the pyrolysis technique, converting sawdust into biochar. The solid products (biochar) obtained from pyrolysis were investigated regarding their application as briquettes (energy purposes) and as adsorbent material. In the first stage of the work, the biochar was mixed with other binder residues such as crude wax (polymer pyrolysis residues) and eucalypt leaves, in the presence of starch, to produce briquettes. The briquettes were analyzed for their higher heating value (HHV) and mechanical strength. The biochar yield obtained in the pyrolysis was 35%, and its HHV was 33.02 MJ/kg at 400 ºC. The proportions of residues (crude wax and/or eucalypt leaf) evaluated in the composition of biochar briquettes were 10, 20 and 30%. The proportion of corn starch was set at 8%. The briquettes with 30% crude wax showed the best HHV, 23.45 MJ/kg, and the highest mechanical resistance to the shatter index test, 97.81%. In summary, briquettes with high energy efficiency and durability were produced. In the second stage of the work, the biochar was chemically activated with phosphoric acid (40%) and impregnated with calcium and aluminum lamellar double hydroxides (Ca/Al LDH), to improve its adsorption capacity. The novel developed adsorbent material was applied to remove the crystal violet (CV) dye from aqueous solutions through the batch adsorption operation. The adsorbent characterization results suggested that the material was effectively synthesized and supported in the biochar. Furthermore, the adsorption experiments indicated that pH 8 was more suitable for adsorption of the CV dye. In the adsorption kinetics and isotherm, the experimental data fit better to the pseudo-second order kinetic model and to the Freundlich isothermal model, respectively. The newly developed adsorbent showed a high adsorption capacity of the CV dye of 496.55 $mg \cdot g^{-1}$ at 50°C. Regarding the thermodynamic properties, the use of this adsorbent demonstrated a favorable, spontaneous and endothermic process. In the adsorption and desorption cycles, this new adsorbent material maintained 71% of the initial adsorptive capacity, even after four cycles of reuse. Therefore, the new biochar, chemically activated with phosphoric acid (40%) and impregnated with Ca/Al LDH, produced generated a sustainable adsorbent with high performance for the treatment of effluents contaminated by dyes.

Keywords: biomass, eucalypt sawdust, pyrolysis, biochar, briquettes, adsorbent material.

LISTA DE FIGURAS

Artigo 1: charcoal briquetting: an environmentally friendly destination for waste materials

Artigo 2: highly efficient adsorbent for removal of crystal violet dye from aqueous solution by caal/ldh supported on biochar

LISTA DE TABELAS

Artigo 1: charcoal briquetting: an environmentally friendly destination for waste materials

Artigo 2: highly efficient adsorbent for removal of crystal violet dye from aqueous solution by CaAl/LDH supported on biochar

SUMÁRIO

1 INTRODUÇÃO

Biomassas lenhosas são amplamente disponíveis ao redor do mundo (KIAN et al., 2018). No Brasil, atualmente, existem 9,85 milhões de hectares de florestas plantadas, sendo 75,2% de eucalipto, destinados à indústria de papel, às serrarias, aos produtos de madeira sólida e processada (OLIVEIRA, 2021).

Entretanto, a grande demanda por produtos oriundos da madeira de eucalipto é acompanhada por uma elevada quantidade de materiais lignocelulósicos gerados, os quais acabam tornando-se resíduos para as empresas, como por exemplo a serragem para as serrarias. Dessa forma, tais resíduos devem ser destinados corretamente para evitarem atenuação de impactos ambientais, como por exemplo contaminação de lençóis freáticos (CHEN et al., 2015).

Uma das corretas formas de destinar resíduos lignocelulósicos ocorre através da aplicação da técnica de pirólise, a qual consiste na degradação térmica de compostos orgânicos em atmosfera inerte. A grande justificativa para a aplicação dessa técnica está na agregação de valor ao resíduo que se usa como matéria-prima. A partir da pirólise de resíduos lignocelulósicos é possível obter três diferentes produtos finais: biochar, bioóleo e gás que possuem diversas aplicações. O biochar pode ser uma fonte importante e alternativa de matéria-prima para fins energéticos e materiais adsorventes (WRÓBLEWSKA et al., 2014).

O biochar é uma fonte potencial de energia e calor, pois é caracterizado por possuir alto teor de carbono com poder calorífico superior na faixa de 17 a 36 MJ/kg (GARCA-PÈREZ; CHAALA e ROY, 2002). No entanto, se for utilizado serragem como matéria-prima da pirólise, o biochar obtido estará na forma de pó, precisando ser aglomerado para facilitar o transporte e armazenamento do produto, se for utilizado para propósitos energéticos (OKOT; BILSBORROW e PHAN, 2019). Isso pode ser obtido pelo processo de briquetagem, que consiste na prensagem do material em pó, em sistema hidráulico ou prensa mecânica, dando origem aos briquetes (SOARES et al., 2015).

Os briquetes são caracterizados como combustíveis sólidos que são ideais para geração de calor em caldeiras industriais, fornos de padarias, entre outros. A produção de briquetes consiste em pressionar o carvão, que está, geralmente, na forma de pequenas partículas ou pó, em equipamentos hidráulicos ou prensas mecânicas para obter um material compacto no formato de pequenos cilindros ou

discos (AL-HAMAMRE et al., 2017). Para melhorar o processo de briquetagem, materiais aglutinantes são utilizados com o objetivo de melhorar a adesão de partículas, estabilidade térmica, resistência à compressão, resistência à abrasão (SETTE et al., 2018). Diversos materiais têm sido usados como aglutinantes, no entanto, não existem estudos que investigaram a aplicação de cera bruta, um subproduto da pirólise de resíduos plásticos, e folhas de eucalipto, considerados resíduos de colheita, misturados com amido de milho para a produção de briquetes de biochar, com o intuito de reduzir o descarte inadequado e proporcionar uma destinação ecologicamente correta para esses resíduos sólidos.

O biochar também é caracterizado por ser uma substância porosa rica em carbono, podendo ser utilizado como material adsorvente em etapas de tratamento de efluentes. Entretanto, dependendo da biomassa, o biochar pode apresentar baixa área superficial. Dessa maneira, o mesmo deve passar por etapas de modificação em sua estrutura para suprir tal deficiência. É possível transformá-lo em carvão ativado, o qual é um material caracterizado por elevadas áreas superficiais, ou impregná-lo com hidróxidos duplos lamelares, para assim maximizar sua eficiência na purificação de resíduos líquidos e gasosos por meio da adsorção (HUANG et al., 2019; YARGICOGLU et al., 2015).

Os carvões ativados podem ter suas propriedades físicas e químicas afetadas pelo grau de ativação, que pode ser feito de maneira física ou química. Na ativação física, temperaturas elevadas e gases são utilizados. Na ativação química, temperaturas menores e um agente químico de desidratação são aplicados (ROCHA et al., 2011).

Outra maneira de modificar a estrutura do biochar é a impregnação com hidróxidos duplos lamelares, visto que melhora o desempenho de adsorção devido à estabilidade aprimorada de partículas, atividade de superfície, densidade de grupo funcional e capacidade de recuperação (YANG et al., 2019). Além disso, outro motivo para impregnar o biochar com HDLs, é que se os HDLs forem usados diretamente como adsorventes, eles podem ser esfoliados durante o processo. Portanto, é mais eficaz utilizá-lo na forma de compósitos com materiais recalcitrantes, como o biochar (MEILI et al., 2019). No entanto, não foram relatados estudos na literatura que efetuassem um pré-tratamento de ativação do biochar bruto, antes de sua impregnação com os HDLs, a fim de aumentar ainda mais a capacidade de adsorção e testá-la na remoção de corantes presentes em soluções aquosas.

Dessa forma, o presente estudo avaliou, no primeiro momento, a produção de biochar, a partir da pirólise da serragem de eucalipto. A aplicação do produto sólido da pirólise foi analisada na confecção de briquetes envolvendo outros resíduos sólidos, cera bruta e folhas de eucalipto, como materiais aglutinantes, com o propósito de destiná-los de maneira ambientalmente correta. Na segunda etapa, foram realizadas modificações na estrutura do biochar, por meio de ativação química seguido da impregnação com hidróxidos duplos lamelares de cálcio e alumínio. A eficiência do novo material adsorvente foi avaliada na remoção do corante cristal violeta, presente em soluções aquosas, através da operação unitária adsorção.

1.1 OBJETIVOS

Os objetivos do presente estudo estão listados a seguir.

1.1.1 Objetivo geral

O objetivo geral desse estudo foi aplicar a técnica de pirólise, como forma de agregar valor à serragem de eucalipto.

1.1.2 Objetivos específicos e metas

Como objetivos específicos desse estudo, destaca-se:

i) Caracterizar a serragem de eucalipto em termos de composição química, perfil de degradação térmico por análise termogravimétrica (TGA), grupos químicos por espectroscopia no infravermelho por Transformada de Fourier (FTIR), teor de umidade, matéria volátil, carbono fixo, cinzas e poder calorífico superior;

ii) Produzir biochar a partir de diferentes temperaturas de pirólise e caracterizá-los em termos de perfil de degradação térmico por análise termogravimétrica (TGA), grupos químicos por espectroscopia no infravermelho por Transformada de Fourier (FTIR), teor de umidade, matéria volátil, carbono fixo, cinzas e poder calorífico superior. Utilizar o biochar produzido na melhor condição de temperatura, em termos de poder calorífico superior e rendimento, para aplicá-lo na confecção de briquetes;

iii) Produzir briquetes, por meio da mistura de biochar e outros resíduos sólidos, cera bruta e folhas de eucalipto, e caracterizá-los em termos de teor de umidade, matéria volátil, carbono fixo, cinzas, poder calorífico superior e resistência mecânica pelo teste de quebra;

iv) Sintetizar um novo material adsorvente, através de modificações na estrutura do biochar, por meio da ativação química com ácido fosfórico, seguido da impregnação com hidróxidos duplas lamelares usando com cátions di e trivalentes, Ca^{2+} e Al^{3+}, respectivamente. Caracterizar o material em termos de espectroscopia no

infravermelho por Transformada de Fourier (FTIR), difração de Raios-X (DRX), microscopia eletrônica de varredura (MEV) e área superficial;

v) Avaliar a eficiência do material adsorvente na remoção do corante cristal violeta presente em soluções aquosas sintéticas. Analisar a influência do pH da solução, a cinética do processo e as isotermas de equilíbrio no processo de adsorção. Testar a regeneração do adsorvente.

2 REVISÃO DA LITERATURA

Neste capítulo será abordado uma breve descrição dos tipos de biomassas, seus principais componentes químicos e o uso da pirólise, tecnologia ambientalmente amigável que pode ser utilizada para a destinação de resíduos lignocelulósicos. Posteriormente, serão expostas duas maneiras de aplicação do biochar, produto sólido obtido pela pirólise de resíduos lignocelulósicos, através da briquetagem, como briquetes, e da adsorção, como material adsorvente por meio de duas formas de modificações em sua estrutura.

2.1 BIOMASSA

A biomassa pode ser definida como uma substância orgânica sólida ou material derivado de organismos vivos, incluindo plantas e animais. Devido à produção massiva de materiais de origem vegetal, principalmente agro-resíduos, aparas de madeira e resíduos florestais, e sua composição química atrativa, uma grande atenção está sendo dada à sua exploração para obtenção de energia e produtos químicos (TUMULURU et al., 2011).

A biomassa derivada de plantas pode ser classificada em dois grupos: a biomassa lenhosa e a biomassa herbácea. A primeira é tipicamente originada de materiais oriundos de árvores e pode ser classificada em resíduos florestais (folhas e galhos), resíduos de serraria (serragem) e restos de madeira (resíduos de construção) (DEMIRBAŞ, 2005). No entanto, este material pode não ser adequado para a preparação de madeira serrada e, assim, é apurado como um potencial recurso renovável pertencente à categoria de materiais lignocelulósicos (DANISH e AHMAD, 2018).

A biomassa herbácea é originária de fontes vegetais, mas possui caule não lenhoso e é coletado como resíduo ao final de cada safra. Culturas agrícolas (ou cereais) e gramíneas são a principal classificação deste tipo de recurso renovável que inclui principalmente palha de trigo, palha de arroz, bambu, etc. (VOGEL e JUNG, 2001). No entanto, ao comparar com a biomassa lenhosa, o material característico contém altos teores de nutrientes e baixos teores de lignina.

2.1.1 Composição química de materiais lignocelulósicos

Os materiais lignocelulósicos são constituídos por três componentes principais: hemiceluloses, celulose e lignina. Os componentes se aglutinam através de ligações covalentes e de pontes de hidrogênio. Assim, a celulose é envolvida pela estrutura densa formada por hemiceluloses e lignina, resultando em uma estrutura altamente complexa e robusta (LUM et al., 2019). A estrutura hierárquica dos materiais lignocelulósicos é apresentada na Figura 1.

Figura 1 - Principais componentes químicos de materiais lignocelulósicos.

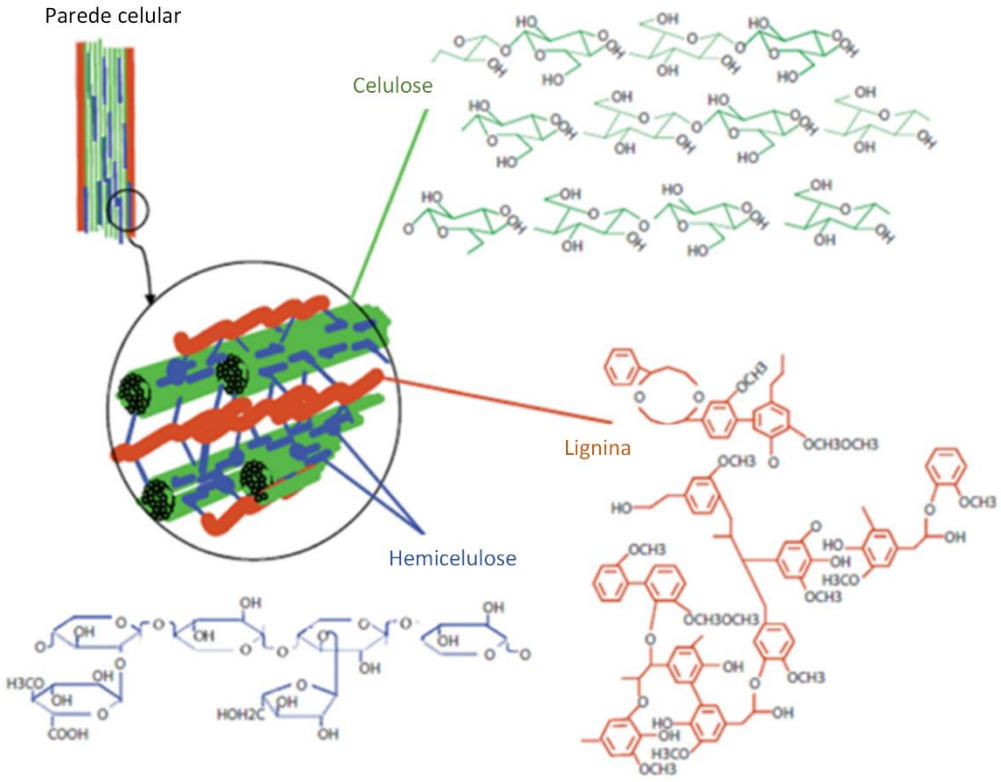

Fonte: Adaptado de WANG; SUN e SUN (2019).

Em média, a proporção quantitativa de hemiceluloses, celulose e lignina na biomassa lenhosa é observada na faixa de 20 a 35, 40 a 50 e 15 a 35%, respectivamente (MACEDO et al., 2008). Porém, a composição química pode variar dependendo de fatores como idade da árvore, ambiente e condição do solo (BALLESTEROS et al., 2018).

A lignina é o polímero aromático, de alto peso molecular, mais abundante na natureza, devido aos seus arranjos moleculares muito complexos (NORMARK et al., 2014). Trata-se de um polímero tridimensional de unidades de fenilpropano ligadas entre si por ligações C – O – C ou C – C. Esses tipos de ligações químicas na lignina dão maior porcentagem de carbono (62% em peso) e menor porcentagem de oxigênio (32% em peso) nas moléculas. Além disso, essas ligações, não apenas se conectam às unidades de fenilpropano, mas também se associam às unidades de hemiceluloses e celulose (CHEN, 2015; BALLESTEROS et al., 2018). Assim, a lignina serve como um material de ligação para a estrutura lignocelulósica (JIBRIL et al., 2008). A composição e estrutura dos componentes da lignina não são uniformes e variam de acordo com o tipo de resíduo lignocelulósico (YÁÑEZ-S et al., 2014).

A celulose é o polímero natural, de maior ocorrência natural no mundo, renovável e sustentável (KIAN et al., 2018). Trata-se de um polímero de alto peso molecular (10^6 kg/mol), homogêneo que contém unidades polissacarídicas lineares parcialmente cristalinas. A celulose é formada por unidades repetidas de β-celobiose, um dissacarídeo formado por duas moléculas de D-glicose, ligadas por ligações glicosídicas β-1,4 (FARIA et al., 2016).

Já, as hemiceluloses consistem em um número menor de unidades sacarídeas em comparação com a celulose. As hemiceluloses são heteropolissacarídeos complexos compostos por polímeros amorfos e ramificados, como: D-glicose, D-galactose, D-manose, D-xilose, L-arabinose, ácido D-glucurônico e ácido 4-O-metil-glucurônico (JIBRIL et al., 2008).

2.1.2 Aplicação dos materiais lignocelulósicos

A biomassa lenhosa encontra-se disponível em abundância ao redor do mundo (KIAN et al., 2018). No Brasil, atualmente, existem 9,85 milhões de hectares de florestas plantadas, sendo 75,2% de eucalipto, destinados à indústria de papel, às serrarias, aos produtos de madeira sólida e processada (OLIVEIRA, 2021).

Entretanto, a grande demanda por produtos oriundos da madeira de eucalipto é acompanhada por uma elevada quantidade de materiais lignocelulósicos gerados, os quais acabam tornando-se resíduos para as empresas, como por exemplo a serragem para as serrarias. Dessa forma, tais resíduos devem ser destinados corretamente para evitarem a atenuação de impactos ambientais, como por exemplo

contaminação de lençóis freáticos (CHEN et al., 2015). Os resíduos lignocelulósicos podem ser uma fonte importante e alternativa de matéria-prima para fins energéticos e materiais adsorventes(WRÓBLEWSKA et al., 2014).

Para fins energéticos, os resíduos lignocelulósicos podem ser utilizados como fontes alternativas de energia, visto que os combustíveis fósseis estão cada vez mais escassos (IBGE, 2019). Dessa forma, a geração de energia pode ser realizada por meio das seguintes maneiras: combustão direta para produzir calor ou conversão em biocombustíveis valiosos usando rotas termoquímicas. O calor gerado pela combustão direta é explorado para aquecimento ou geração de energia imediata. Porém, além do problema óbvio de baixa eficiência do resíduo lignocelulósico bruto, essa abordagem também leva ao acúmulo indesejável de cinzas (WANG et al., 2017).

Já as rotas termoquímicas incluem gaseificação, pirólise, entre outros. A gaseificação é a oxidação parcial de resíduos lignocelulósicos com vapor e ar e tem vários benefícios potenciais em relação à combustão tradicional, principalmente relacionada à possibilidade de combinar temperatura e razão de equivalência para obter um gás de síntese apropriado (WRÓBLEWSKA et al., 2014). A pirólise degrada termicamente, em atmosfera inerte, o resíduo sólido lignocelulósico, gerando produtos sólidos, líquidos e gasosos (WANG et al., 2017).

O biochar, produto sólido da pirólise, além de ser utilizado para fins energéticos, também pode ser aplicado como material adsorvente para purificar efluentes aquosos ou gasosos, porém ele pode ser modificado através de um pré-tratamento, afim de aumentar sua eficiência de purificação nesses efluentes (YARGICOGLU et al., 2015).

2.2 PIRÓLISE

De maneira geral, a pirólise é um processo que engloba um conjunto de reações químicas complexas acompanhadas por transferência de calor e massa. Seu princípio consiste na degradação térmica dos componentes orgânicos de uma determinada matéria-prima em atmosfera inerte. Quando é utilizado biomassa lignocelulósica como matéria-prima, os principais produtos gerados no processo pirolítico são: gases não condensáveis, líquidos (bioóleo) e sólidos (biochar), a partir da decomposição térmica de seus três principais componentes, hemiceluloses, celulose e lignina. Este processo pode ter seus parâmetros ajustados, como

temperatura e tempo de residência, para maximizar o favorecimento de um determinado produto (AL-HAMAMRE et al., 2017; KAN, STREZOV e EVANS, 2016).

Dessa forma, condições de pirólise como temperaturas moderadas e tempos de processo curtos favorecem a produção de líquidos (bioóleo). Altas temperaturas e maior tempo de processo aumentam o favorecimento de gás. Temperaturas mais baixas e tempos de processo mais longos favorecem a produção de biochar (BRIDGWATER, 2012).

A Figura 2 apresenta um fluxograma simplificado da obtenção dos produtos através da pirólise de biomassa.

Figura 2 - Esquema simplificado da pirólise de biomassa com a obtenção de produtos.

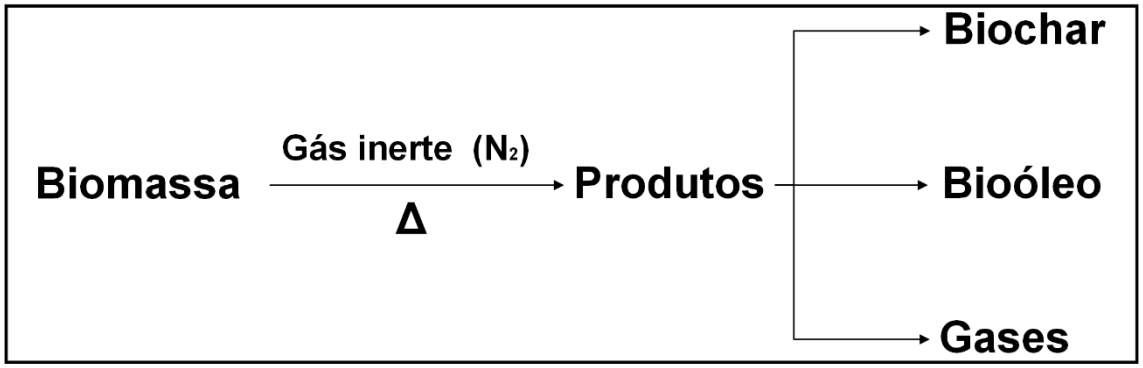

Fonte: Produção do próprio autor.

Em qualquer tipo de pirólise, o princípio sempre será o mesmo, ou seja, a biomassa é degradada termicamente em atmosfera não oxidante, originando os produtos sólido (biochar), líquido (bioóleo) e gasoso (voláteis não condensáveis). No entanto, alguns parâmetros variam de um processo pirolítico para o outro. A Tabela 1 mostra os rendimentos normalmente obtidos para os diferentes tipos de pirólise.

Nos mecanismos de reações da pirólise lenta, pode-se distinguir a seguinte sequência de fenômenos. A aproximadamente 160 °C ocorre praticamente a eliminação total da umidade. Entre 200 e 260 °C decompõem-se a maior parte das hemiceluloses, gerando predominantemente produtos voláteis (CO, CO_2 e vapores condensáveis). Entre 240 a 350 °C, a celulose, que já experimentou algumas transformações químicas, decompõe-se a uma velocidade maior, atingindo um máximo em torno dos 320 °C. Os produtos de decomposição são, principalmente, vapores condensáveis. Neste intervalo de temperatura, a lignina, que sofreu

mudanças em sua estrutura, começa a emitir quantidades significativas de vapores condensáveis a temperaturas superiores a 320°C (BRIDGWATER, 2012).

Tabela 1 - Rendimentos típicos obtidos para diferentes tipos de pirólise.

Modo	**Condição**	**Líquido (%)**	**Sólido (%)**	**Gasoso (%)**
Rápida	~500°C, tempo de residência ~1 s	75	12	13
Intermediária	~500°C, tempo de residência ~10-30 s	50, duas fases	25	25
Carbonização (lenta)	~400°C, tempo de residência de horas/dias	30	35	35
Gaseificação	~750 – 900°C	5	10	85
Torrefação (lenta)	~290°C, tempo de residência ~10-60 min	0 – 5	80	20

Fonte: Adaptado de BRIDGWATER (2003).

2.3 BIOCHAR

Lehmann e Joseph (2009) definiram o biochar como uma substância porosa rica em carbono, de grão fino, que é produzida pela decomposição térmica da biomassa sob condições de oxigênio limitado e a temperaturas relativamente baixas (<700 ºC). Também pode-se definir biochar como o carvão que possui um alto teor de carbono orgânico e é altamente resistente à decomposição (HU et al., 2010).

Diversos estudos que são aplicados à pirólise buscam por fontes alternativas de matérias-primas para a produção de biochar. A Tabela 2 apresenta alguns trabalhos desenvolvidos, contendo os parâmetros de pirólise utilizados para a obtenção do biochar a partir de diferentes biomassas.

Tabela 2 - Resumo de trabalhos de pirólise.

Biomassa	Temperatura final (ºC)	Taxa de aquecimento (ºC/min)	Tempo de residência (min)	Referência
Palha de arroz	300	20	240	(JIANG et al., 2012)
Torta de mamona	300 e 350	30	30 e 60	(SUGUIHIRO et al., 2013)
Cascalho de eucalipto	300 – 700	10	120	(DAWOOD; SEN; PHAN, 2016)
Bagaço de avelã	400 - 700	30	30	(SALLEM-IDRISSI et al., 2016)
Serragem de maçaranduba	500	2	30	(CASTRO et al., 2019)

Fonte: Produção do próprio autor.

As propriedades do biochar dependem principalmente das condições do processo de pirólise e da composição da biomassa utilizada. Dessa forma, o mesmo é caracterizado por apresentar características físicas e químicas particulares, visto que a composição química de cada matéria-prima pode variar, possuindo diferentes teores de lignina, celulose e hemiceluloses. A decomposição térmica remove a umidade e o conteúdo de matéria volátil da biomassa, e o material sólido restante (biochar) tem propriedades diferentes da biomassa original. Diferenças significativas são observadas principalmente na área de superfície, porosidade, estruturas de poros e propriedades físico-químicas (HAYKIRI-ACMA; YAMAN e KUCUKBAYRAK, 2006).

Conforme observado na Tabela 2, o biochar pode ser produzido a partir de uma extensa variedade de biomassa, o que o torna uma ferramenta relativamente econômica e benéfica para o meio ambiente para remediação ambiental, fatos assim estimulam o aumento de sua pesquisa por potenciais aplicações. As aplicações do biochar são muito diversas, indo desde a produção de calor e energia, uso médico, e uso metalúrgico. O biochar também tem sido usado como corretivo do solo para melhorar a sua fertilidade e sequestrar carbono (WEBER e QUICKER, 2018).

Conforme mencionado, o biochar é uma fonte potencial de energia e calor, pois é caracterizado por possuir alto teor de carbono com poder calorífico na faixa de 17 a 36 MJ/kg (GARCA-PÈREZ; CHAALA e ROY, 2002). No entanto, se for utilizado serragem como matéria-prima da pirólise, o biochar obtido estará na forma de pó, e precisará ser aglomerado para facilitar o transporte e armazenamento do produto (OKOT; BILSBORROW e PHAN, 2019). Isso pode ser obtido pelo processo de briquetagem, que consiste na prensagem do material em pó, em sistema hidráulico ou prensa mecânica, dando origem aos briquetes (SOARES et al., 2015).

Na Tabela 3 constam os valores quanto ao percentual de sólido produzido a partir de determinada temperatura e tempo de residência, para alguns tipos de biomassas, bem como seu poder calorífico final. Os experimentos foram relizados utilizando gás nitrogênio como gás inerte.

Tabela 3 - Rendimento de sólidos e respectivo poder calorífico para diferentes biomassas e condições operacionais obtidos após a torrefação.

Biomassa	**T (ºC)**	**t (min)**	**Rendimento de sólido (%)**	**Poder calorífico (MJ/Kg)**	**Referências**
Eucalipto	250	60	83,60	20,60	(LU et al., 2012)
	275	60	75,80	21,50	
	300	60	57,90	23,90	
Casca de arroz	250	60	77,50	15,89	(PIMCHUAI; DUTTA e BASU, 2010)
	270	60	74,25	16,07	
	300	60	58,25	17,59	
Bambu	230	60	49,36	24,31	(ROUSSET et al., 2011a)
	260	60	40,92	26,11	
	290	60	37,98	26,14	

Fonte: Adaptado de NAKASHIMA; LARISSA e HANSTED (2017).

Para outras aplicações, como purificação de gases e águas, dependendo da biomassa, o biochar pode apresentar baixa área superficial. Dessa maneira, o mesmo deve passar por etapas de modificação em sua estrutura para suprir tal deficiência. É possível impregná-lo com hidróxidos duplos lamelares, ou transformá-lo em carvão ativado, o qual é um material caracterizado por altas áreas superficiais e, assim,

possibilitar sua aplicação na purificação de efluentes por adsorção (HUANG et al., 2019; YARGICOGLU et al., 2015).

2.4 BRIQUETAGEM

Briquetagem é a densificação ou compactação de resíduos sólidos lignocelulósicos em um produto de maior densidade do que as matérias-primas. Os briquetes produzidos dependem dos materiais disponíveis localmente, que podem ser bagaço de cana, pó de carvão, casca de café, goma arábica, folhas de árvores, casca de arroz, serragem e outros resíduos de madeira ou subprodutos agrícolas (ROUSSET et al., 2011b). Os briquetes podem ser usados tanto para geração de calor em residências e pequenas indústrias domésticas, ou mesmo para geração de energia em grandes indústrias (ZHENG et al., 2006).

Uma das grandes vantagens da briquetagem é a possibilidade de aproveitamento de resíduos lignocelulósicos carbonizados em geral. Assim, além da produção de briquetes de resíduos lignocelulósicos in natura, existe a briquetagem de carvão vegetal, na qual consegue-se um combustível com homogeneidade granulométrica. Dessa forma, uma maior densidade e resistência à geração de finos é garantida. A densificação proporciona um combustível sólido com maior concentração energética por unidade de volume, que, aliado à resistência adquirida, viabiliza técnica e economicamente o transporte a distâncias maiores (SETTE et al., 2018).

Diversos parâmetros como granulometria, pressão de prensagem, tempo de prensagem, prensagem a frio ou prensagem a quente, umidade e, principalmente, o material utilizado como aglutinante são avaliados no processo de briquetagem. Aglutinantes são materiais que desempenham um papel fundamental no processo de produção de briquetes. Eles são utilizados com o objetivo de melhorar a adesão de partículas, estabilidade térmica, resistência à compressão, resistência à abrasão e conteúdo energético dos briquetes (ROUSSET et al., 2011b).

Os aglutinantes podem ser materiais inorgânicos ou orgânicos. Os aglutinantes orgânicos (resíduos lignocelulósicos, amido e alcatrão, por exemplo) geram briquetes com bom desempenho de aglomeração e alta resistência ao esmagamento e resistência à ruptura (MASSARO, SON e GROVEN, 2014). Já os aglutinantes inorgânicos (cal, gesso, argila, cimento e silicato de sódio, por exemplo) são

caracterizados por seu baixo custo e boa hidrofilicidade, porém geram briquetes com elevado teor de cinzas. A escolha desse material é feita geralmente em função do gasto e da qualidade final desejada (SETTE et al., 2018). Na Tabela 4 são apresentados alguns materiais que já foram utilizados como aglutinante, durante a briquetagem de biochar.

Tabela 4 - Materiais utilizados como aglutinantes e suas concentrações avaliadas.

Aglutinantes	**Proporção avaliada (%)**	**Referências**
Resíduos de polietileno de baixa densidade	5, 7, 10 e 15	(MASSARO, SON e GROVEN, 2014)
Melaço, amido e óleo de pirólise	8 e 10	(ADELEKE et al., 2019)
Cera de parafina	15	(FLORENTINO-MADIEDO et al., 2018)
Resíduos plásticos	10	(ARANSIOLA et al., 2019)

Fonte: Produção do próprio autor.

Conforme apresentado na Tabela 4, diversos materiais podem ser utilizados como aglutinantes, de maneira separada ou em conjunto, formando uma mistura de diferentes proporções para a fabricação de briquetes de biochar. No entanto, não foram encontrados estudos investigando a aplicação de cera bruta e folhas de eucalipto, como resíduos misturados com amido de milho, para a produção de briquetes de biochar, a fim de reduzir o descarte inadequado e proporcionar uma destinação ambientalmente correta para esses resíduos sólidos.

A cera bruta é um subproduto originado da pirólise de resíduos plásticos, e é composta principalmente de parafina. Esse resíduo sólido tem sido relatado com um poder calorífico superior de, aproximadamente, 46 MJ/kg (WILLIAMS, 2020). As folhas de eucalipto são consideradas resíduos de colheita que não devem ser depositadas no solo, pois contêm elevada concentração de nutrientes que podem afetar o equilíbrio do solo e comprometer a produtividade local (ZAITON et al., 2020). As folhas de eucalipto podem ser destinadas à produção de óleo, utilizado como intensificador de sabor e aroma, a partir de procedimentos complexos de extração (extração a vapor,

hidrodestilação ou extração por fluido supercrítico) (ZHAO e ZHANG, 2014). No entanto, uma aplicação fácil e simples de folhas de eucalipto ainda pode ser estudada.

Os briquetes de carvão comerciais apresentam geralmente forma quadrada, com os cantos arredondados (tipo almofada), conforme Figura 3, volume de 30 cm^3 e densidade na faixa de 0,4 a 0,7 g/cm^3 (MWAMPAMBA, OWEN e PIGAHT, 2013). Os equipamentos industriais utilizados na confecção destes briquetes são prensas de rolos rotativos, Figura 4. Pela sua elevada capacidade de produção, podem atingir até 5 toneladas/hora (ADELEKE et al., 2019).

Figura 3 - Briquete comercial de carvão vegetal.

Fonte: Produção do próprio autor.

Figura 4 - Prensa de rolos rotativos para produção de briquetes de carvão vegetal.

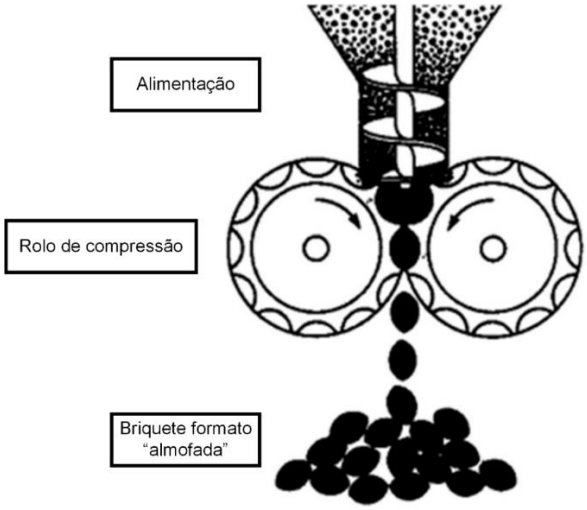

Fonte: Adaptado de (FLORENTINO-MADIEDO et al., 2018).

Em nível laboratorial, os materiais que formam o briquete são moldados utilizando um molde de aço, resistente à compressão. Assim, ocorre a formação de briquetes no formato cilíndrico, conforme Figura 5 e Figura 6, respectivamente (SOARES et al., 2015).

Figura 5 - Molde de aço para produção de briquetes em laboratório.

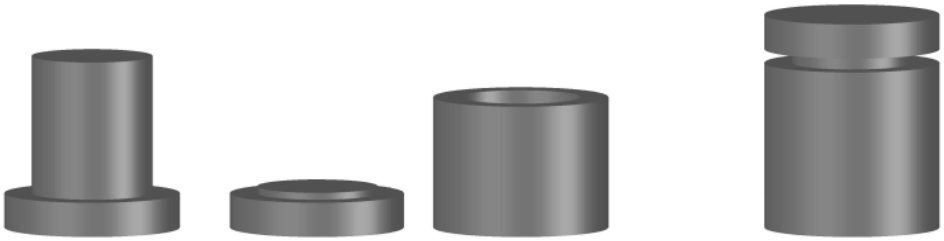

Fonte: Produção do próprio autor.

Figura 6 - Briquete produzido em laboratório através de molde cilíndrico.

Fonte: Produção do próprio autor.

2.5 ADSORÇÃO

Diversos processos físicos, químicos e biológicos são aplicados para o tratamento de efluentes aquosos industriais, incluindo extração de solvente, precipitação química, fotocatálise, filtração por membrana, troca iônica, adsorção e tratamento eletroquímico (JANA; PURKAIT e MOHANTY, 2010; MUNTEAN et al., 2013; YI et al., 2015). No entanto, dentre os processos citados, a adsorção destaca-se como um dos métodos mais eficazes, devido à sua alta eficiência, facilidade de operação, reutilização e custo relativamente baixo, pois utiliza como materiais

adsorventes de baixo valor agregado como materiais carbonáceos, minerais de argila e óxi-hidróxidos de metal, além disso, apresenta um baixo consumo energético em sua operação (GUPTA; ALI, 2008).

A adsorção é um fenômeno físico-químico em que ocorre a transferência de massa no qual determinados componentes presentes em uma fase líquida ou gasosa, chamada de adsorbato, concentram-se nas superfícies do material sólido, chamado de adsorvente. Dessa forma, a separação dos componentes da fase fluída é ocasionado (MASEL, 1996). Como o adsorbato concentra-se na superfície do adsorvente, quanto maior for essa área superficial, maior será a eficiência da adsorção em purificar o fluido em questão.

O grau de interação pelo qual as moléculas de adsorbatos são acumuladas nos adsorventes define a natureza e o tipo de adsorção, como fisissorção (adsorção física) ou quimissorção (adsorção química). A fissorção é a adsorção na qual as interações moleculares entre as moléculas de adsorbato e o adsorvente são governadas principalmente pelas forças de van der Waals e interações eletrostáticas de polarização, dipolo e quadrupol, enquanto a quimissorção é a adsorção que ocorre se houver ligações químicas entre as moléculas de adsorvato e o adsorvente com calor de adsorção na mesma ordem de grandeza dos calores de reação (superior a 20 kcal/mol) e geralmente são irreversíveis (AGBOOLA e BENSON, 2021). Etapas de dessorção são realizadas para analisar se um processo é reversível, nas quais se tenta a liberação completa do adsorbato da fase sólida (adsorvente) após a etapa de adsorção (TÜKMEN et al., 2010).

As características do adsorvente, adsorbato e das condições operacionais do processo afetam a capacidade de adsorção de um líquido sobre um sólido. Dessa forma, fatores como área superficial do adsorvente, pH, temperatura, e concentração das soluções a serem tratadas, e o tempo de contato entre adsorbato e adsorvente influenciam o processo de adsorção (RUTHVEN, 1984).

Devido a adsorção ocorrer na superfície de um sólido, a área superficial é uma das principais características que afeta a capacidade adsortiva de um determinado adsorvente, ou seja, a quantidade adsorvida por unidade de massa de adsorvente é maior quanto mais finamente estiver dividido o adsorvente, e quanto mais poroso for o material (SEKAR; SAKTHI e RENGARAJ, 2004). O pH da solução influencia o grau de adsorção, pois o processo ocorre devido as forças intermoleculares e a presença de íons na solução. A alteração do pH provoca mudanças no processo adsortivo por

meio da dissociação de grupos funcionais nos locais ativos da superfície adsorvente, levando a uma posterior mudança na cinética da reação e nas características de equilíbrio do processo de adsorção (RUTHVEN, 1984). O aumento da temperatura ocasiona o aumento da velocidade de difusão das moléculas de adsorbato, devido à diminuição da viscosidade da solução (DOĞAN et al., 2006).

O tempo de contato entre adsorbato e adsorvente também influencia no processo adsorção, visto que a rápida remoção dos poluentes e o alcance de equilíbrio em um curto período de tempo demonstram a eficiência do adsorvente. As espécies podem ser adsorvidas mais rapidamente, dependendo da natureza adsorção. Na adsorção física, a maioria das espécies são adsorvidas em um curto intervalo de tempo. Porém, na adsorção química, a forte ligação química do poluente adsorvido com o adsorvente exige um maior tempo de contato para que o equilíbrio seja atingido (MALL; SRIVASTAVA e AGARWAL, 2006).

2.5.1 Cinética de adsorção

A cinética de adsorção descreve a velocidade com as quais as moléculas do adsorbato são adsorvidas pelo adsorvente, sendo de fundamental importância para o projeto de sistemas de tratamento de efluentes, pois possibilita a determinação do tempo de equilíbrio e da velocidade em que ocorre a adsorção (NASCIMENTO et al., 2014).

A dinâmica do processo de adsorção em sólidos porosos inicia com a difusão do adsorbato em solução para a superfície externa do adsorvente, seguida da adsorção nos sítios da superfície externa e da difusão das moléculas da superfície para o interior do sólido até o sítio de adsorção (poros), por fim, ocorre a adsorção das moléculas nos sítios ativos disponíveis na superfície interna (NASCIMENTO et al., 2014).

Diversos modelos cinéticos podem ser utilizados para descrever a adsorção de um adsorbato sobre um adsorvente. No entanto, os modelos de pseudo-primeira ordem e pseudo-segunda ordem são comumente empregados para o ajuste dos dados experimentais para a cinética de adsorção (ROCHA et al., 2012).

O modelo de adsorção de pseudo-primeira ordem, conforme Equação 1, assume que a taxa de variação do soluto adsorvido com o tempo é diretamente

proporcional à diferença entre a quantidade de soluto adsorvida no equilíbrio, q_1, e a quantidade adsorvida num tempo *t* qualquer, q_t (LAGERGREN, 1898).

$$q_t = q_1(1 - e^{-k_1.t}) \quad (1)$$

onde q_t é a quantidade adsorvida no tempo *t* (mg g^{-1}), q_1 é a quantidade adsorvida no equilíbrio (mg g^{-1}), k_1 é a constante de velocidade de adsorção de pseudo-primeira ordem (min^{-1}) e *t* é o tempo (min).

O modelo de pseudo-segunda ordem, conforme Equação 2, é baseado na capacidade de adsorção do adsorvente e relata o comportamento do processo em toda a faixa de tempo de contato, assumindo que a velocidade de adsorção é diretamente proporcional ao quadrado de sítios disponíveis (HO; MCKAY, 1999).

$$q_t = \frac{k_2.t.q_2^2}{(1 + k_2.t.q_2)} \quad (2)$$

onde q_t é a quantidade adsorvida no tempo *t* (mg g^{-1}), q_2 é a quantidade adsorvida no equilíbrio (mg g^{-1}), k_2 é a constante da taxa de adsorção de pseudo–segunda ordem (g mg^{-1} min^{-1}) e *t* é o tempo (min).

2.5.2 Isotermas de adsorção

A eficiência do processo de adsorção pode ser avaliada através das isotermas, as quais fornecem dados de equilíbrio, que são utilizados para avaliar a capacidade de diferentes materiais sólidos porosos em adsorver um determinado adsorbato. As isotermas relacionam a quantidade do material adsorvido (q_e em mg g^{-1}) e a concentração de equilíbrio na fase fluida (C_e em mg L^{-1}) em temperatura constante (DĄBROWSKI, 2001).

As isotermas podem ser classificadas de acordo com as formas de suas curvas, conforme Figura 7.

Figura 7 - Isotermas de adsorção.

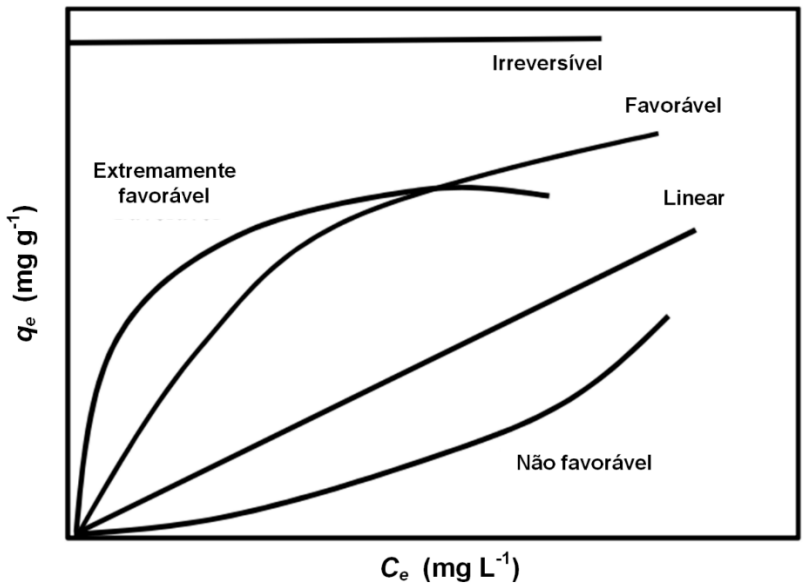

Fonte: Adaptado de MCCABE; SMITH e HARRIOTT (2004).

De acordo com as curvas apresentadas na Figura 7, na isoterma linear a quantidade adsorvida é proporcional à concentração do fluido, característica comum de superfícies homogêneas. Nas isotermas favoráveis, grandes quantidades podem ser adsorvidas com baixas concentrações e nas isotermas não favoráveis, não apresentarem boa capacidade de adsorção a baixas. A isoterma do tipo irreversível é independente da concentração do adsorbato no equilíbrio (MCCABE; SMITH e HARRIOTT, 2004).

Alguns modelos matemáticos são usados para descrever o comportamento do adsorbato durante o processo de adsorção, porém, os mais utilizados são os modelos de Langmuir e de Freundlich (ROCHA et al., 2012).

O modelo de Langmuir assume que a adsorção se procede em monocamada em uma superfície homogênea do adsorvente, onde os sítios de adsorção são energeticamente equivalentes, nos quais as moléculas são adsorvidas uma de cada vez em cada sítio e, as mesmas não interagem com as moléculas adsorvidas nos sítios vizinhos. A isoterma de Langmuir pode ser representada pela Equação 3 (LANGMUIR, 1918).

$$q_e = \frac{q_m k_L C_e}{1 + k_L C_e} \tag{3}$$

onde q_m é a capacidade máxima de adsorção (mg g^{-1}) e k_L é a constante de Langmuir (L mg^{-1}), que expressa a afinidade entre o adsorvente e o adsorbato.

O modelo de Freundlich assume que a adsorção ocorre em uma superfície heterogênea do material adsorvente, em multicamadas e, que a quantidade de adsorbato adsorvido aumenta infinitamente com a concentração do mesmo. A isoterma de Freundlich pode ser representada pela Equação 4 (FREUNDLICH, 1906).

$$q_e = k_F C_e^{1/nF} \quad (4)$$

onde k_F é a constante de Freundlich (mg g^{-1}) (mg $L^{-1})^{-1/nF}$, e *1/nF* é o fator de heterogeneidade.

O parâmetro n_F pode variar de 0 a 1, apresentando uma maior heterogeneidade quanto mais próximo for de zero (RANGABHASHIYAM et al., 2014).

2.5.3 Materiais adsorventes

Para que um material possa ser utilizado como adsorvente, o mesmo deve possuir uma estrutura porosa, acarretando em uma elevada área superficial (MCCABE; SMITH e HARRIOTT, 2004). Em detrimento do elevado custo que o carvão ativado comercial detém, inúmeras modificações têm sido desenvolvidas para que o biochar possa ser otimizado e aplicado como material adsorvente em processos de adsorção, garantindo boa eficiência na remoção de determinados contaminantes. Dentre as modificações propostas de melhoramento do biochar estão a ativação e a impregnação de sua superfície com hidróxidos duplos lamelares (HUANG et al., 2019)(YARGICOGLU et al., 2015).

2.5.3.1 Carvão ativado

Carvão ativado é um material de natureza amorfa que detém elevada porosidade e área superficial, resultante de um processo de ativação do material rico em carbono. Resíduos sólidos lignocelulósicos com alto teor de carbono (50 a 90%) são adequado precursores para produzir carvão ativado (DAZA; MENDIOROZ e PAJARES, 1986). Grande área superficial pode fazer com que o carvão ativado seja

um excelente adsorvente. Esses materiais são úteis para uma aplicação extensiva em operações de separação, descoloração, desodorização, purificação e filtração (BANSAL e GOYAL, 2005). A composição química, bem como os métodos e condições do processo utilizados durante a ativação desses resíduos, desempenham um papel importante na formação de poros, volume de poros e área superficial (BÓTA et al., 1997).

Existem dois métodos de ativação de resíduos lignocelulósicos: método de ativação física, em que vapor, nitrogênio e dióxido de carbono são utilizados para redução leve da matéria carbonosa. Enquanto, no método de ativação química, um agente químico de desidratação é aplicado para ativar o resíduo lignocelulósico (SOARES et al., 2015).

A ativação física é normalmente realizada em duas etapas. Na primeira etapa, a carbonização ocorre para eliminar as matérias voláteis em baixas temperaturas da matéria-prima. Considerando que, na segunda etapa, a ativação da substância carbonizada (intermediária rica em carbono) obtida ocorra a uma temperatura muito elevada, de 700 °C a 1100 °C. O uso de gases de arraste inertes durante a carbonização e o processo de ativação impedem a formação de CO_2 e geram poros de diversos tamanhos no carvão ativado. A queima do carbono fibroso do resíduo lignocelulósico pode ser evitada na presença de gás, como vapor, N_2, CO_2, Ar ou suas misturas. Normalmente, o N_2 é o gás mais comumente usado como atmosfera gasosa durante o processo de ativação, porque pode repelir o oxigênio gasoso da câmara de pirólise. O gás nitrogênio é limpo, fácil de manusear e disponível a baixo custo (ILOMUANYA et al., 2017). A otimização de rendimento da ativação física pode ser feita através da avaliação dos parâmetros como tempo de carbonização, temperatura de ativação e vazão de gás de arraste (DANISH e AHMAD, 2018).

Os métodos de ativação química envolvem a impregnação do material de partida com um agente químico de desidratação antes ou depois da etapa de carbonização. O agente químico é usado para desidratar o resíduo lignocelulósico. Uma variedade de produtos químicos pode ser utilizada como agentes de ativação tais como ácido sulfúrico, ácido nítrico, ácido fosfórico, cloreto de zinco, hidróxido de potássio, hidróxido de sódio, carbonato de cálcio, etc. Os agentes químicos facilitam o desenvolvimento dos poros no carvão ativado usando degradação, desidratação e complexação com moléculas de carbono orgânico de materiais precursores. A ativação química é realizada a uma temperatura mais baixa comparada a uma

ativação física, porque a interação química entre o resíduo químico precursor e os agentes ativadores compensa esse intervalo de temperatura (BÓTA et al., 1997).

A ativação química tem inúmeros benefícios em comparação com a ativação física. Na ativação química, os processos de carbonização e ativação são combinados em uma etapa que economiza a energia térmica durante a síntese. Além disso, a ativação química é conduzida a uma temperatura mais baixa em comparação com a ativação física, assim, também economiza energia. Os outros grandes benefícios do uso do processo de ativação química são maior rendimento, menor tempo de ativação, incorporação de grupos funcionais adequados e maior área de superfície do carvão ativado. A principal desvantagem do processo de ativação química é o custo dos produtos químicos, e é necessário realizar uma etapa adicional de lavagem de carvão ativado com água quente e fria para eliminar o excesso de produtos químicos não reagidos e subprodutos químicos (LAMINE et al., 2014).

A Tabela 5 apresenta as diversas condições de ativação das diferentes espécies de carvão ativado obtidos a partir de resíduos lignocelulósicos, bem como a área superficial obtida em cada caso.

Tabela 5 - Parâmetros de carbonização e de ativação para a produção de carvões ativados a partir de resíduos lignocelulósicos.

Resíduos lignocelulósicos	**Tipo de ativação**	**Temperatura taxa de aquecimento tempo de carbonização**	**Temperatura taxa de aquecimento tempo de ativação**	**Gás de arraste**	**Área Superficial (m^2 g^{-1})**	**Referências**
Diafragmas de *Elaeis guineensis*	Física	400 ºC 10 ºC min^{-1} 240 min	600 ºC 40 ºC min^{-1} 120 min	N_2	1496,00	(ILOMUANYA et al., 2017)
Diafragmas de *Elaeis guineensis*	Química com H_3PO_4	400 ºC 10 ºC min^{-1} 240 min	600 ºC 40 ºC min^{-1} 120 min	N_2	2153,00	
Sabugo de milho	Química com $ZnCl_2$	500 °C 10 ºC min^{-1} 180 min	ND	N_2	501,00	(MACIÁ-AGULLÓ et al., 2004)
Serragem de *Apuleia leiocarpa*	Física	500 ºC 1,65 ºC min^{-1} 30 min	850 ºC 10 ºC min^{-1} 60 min	CO_2	564,90	(LAMINE et al., 2014)
Serragem de pinus	Física	ND	800 ºC 10 ºC min^{-1} 60 min	CO_2	352,00	(NOWICKI e PIETRZAK, 2010)
Lascas de eucalipto	Física	400 ºC 25 ºC min^{-1} 60 min	900 ºC 25 ºC min^{-1} 60 min	Mistura N_2 e CO_2	1491,00	(ILOMUANYA et al., 2017)

Fonte: Produção do próprio autor.

2.5.3.2 Hidróxidos duplos lamelares

Diferentes modificações do biochar têm sido sugeridas a fim de melhorar seu desempenho na remoção de contaminantes da água. A adição de diferentes componentes ao biochar melhora as funcionalidades da sua superfície, que por sua vez, melhora o desempenho de adsorção para uma ampla gama de contaminantes, embora possa ocasionalmente diminuir a porosidade em compósitos de biochar projetados por meio do bloqueio dos poros (XIANG et al., 2020).

O grande foco de pesquisa para o biochar é a montagem de HDLs como uma abordagem benéfica para sintetizar compostos mineral-biochar, visto que melhora o desempenho de adsorção devido à estabilidade aprimorada de partículas, atividade de superfície, densidade de grupo funcional e capacidade de recuperação (YANG et al., 2019). Outro motivo para impregnar o biochar com HDLs, é que se os HDLs forem usados diretamente como adsorventes, eles podem ser esfoliados durante o processo. Portanto, é mais eficaz utilizá-lo na forma de compósitos com materiais recalcitrantes, como o biochar (MEILI et al., 2019). Além disso, os compósitos de biochar/HDL apresentam potencial de degradação fotocatalítica de poluentes orgânicos, em particular de antibióticos (GHOLAMI et al., 2020).

Os HDLs também são conhecidos como argilas aniônicas, do tipo hidrotalcita (hidroxicarboneto de magnésio e alumínio), consistindo em camadas positivas empilhadas, que são separadas e neutralizadas por ânions trocáveis nas galerias interlamelares (YAN; WU e JIN, 2016). Esses compostos são representados pela fórmula geral $[M^{2+}_{1-x}\ M^{3+}_{x}(OH)_2]^{+x}\ (A^{-m})_{x/m}\cdot nH2O]$, na qual M^{2+} e M^{3+} são cátions metálicos di e trivalentes, respectivamente, A^{-m} representa um ânion intercalado com carga m, X é a razão entre os cátions di e trivalentes e n é o número de mols de água (THEISS; AYOKO e FROST, 2016).

Os HDLs são montados por uma ligação não covalente, onde o lamelar principal carregado positivamente inclui cátions di ou trivalentes e ânions nas entre camadas não estruturais juntamente com moléculas de água (MISHRA; DASH e PANDEY, 2018).

A estrutura dos HDLs pode ser interpretada como uma derivação da brucita ($Mg(OH)_2$), onde os íons Mg^{2+} estão localizados no centro dos octaedros com ânions hidroxila em seus vértices (DOS SANTOS LINS et al., 2019). Esses octaedros

compartilham suas bordas, formando camadas planas de carga neutra que são mantidas empilhadas por meio de ligações de hidrogênio. Quando os íons divalentes são substituídos por íons trivalentes, uma carga residual positiva é gerada na lamela. Essa carga é compensada pelos ânions intercalados, que, juntamente com as moléculas de água, promovem o empilhamento das camadas duplas de hidróxidos com domínio interlamelar, conforme apresentado na Figura 8.

Figura 8 - Representação estrutural de hidróxidos duplos lamelares.

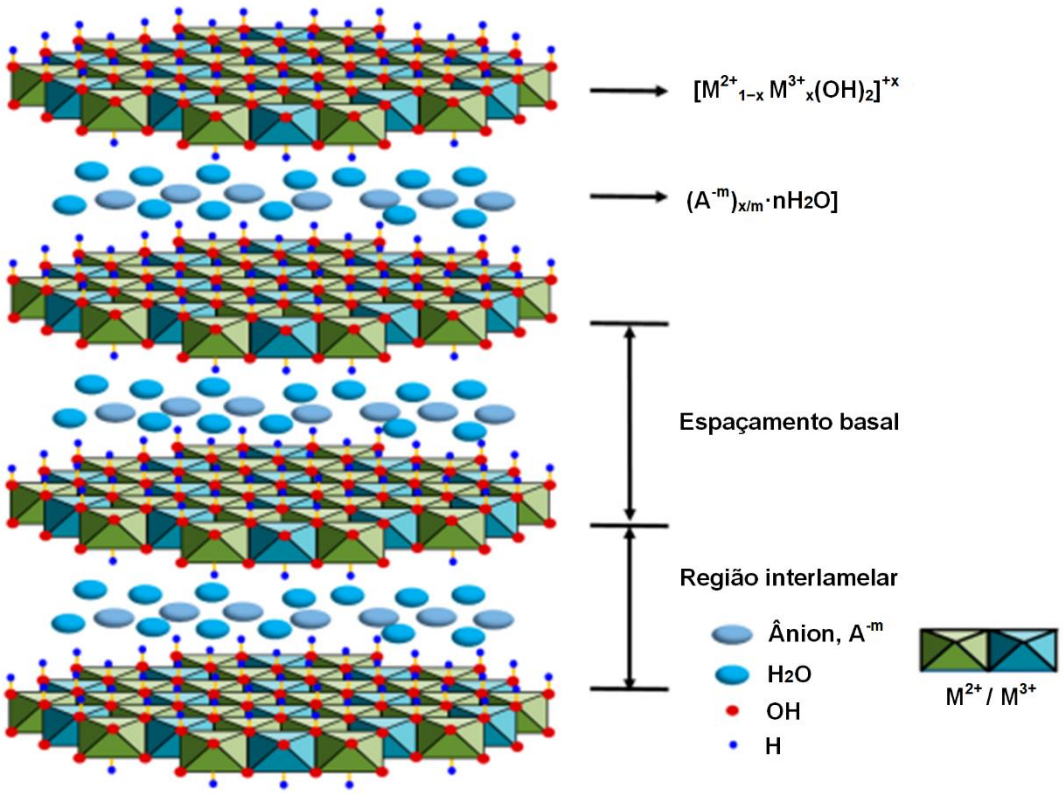

Fonte: Adaptado de STAMATE et al., (2020).

Dentre as propriedades que tornam os HDLs como excelentes materiais compósitos tem-se a síntese fácil e direta, estrutura lamelar em camadas uniformemente distribuídas, presença de grupos hidroxila na superfície, fácil sintonia, ânions intercalados com espaços entre camadas, alta estabilidade química e térmica, alta capacidade e compatibilidade para intercalar várias biomoléculas inorgânicas e orgânicas (DAUD et al., 2019).

Além disso, os HDLs são alcalinos e carregados positivamente devido à natureza dos cátions metálicos e das ligações Metal-O, que proporcionam interações eletrostáticas com poluentes aniônicos, cobrindo assim a limitação do biochar (HUANG et al., 2019). Por outro lado, o uso de HDLs como adsorventes, sem um suporte como o biochar, pode limitar a eficácia para adsorver diversos poluentes (JIA et al., 2019). Portanto, a montagem de HDLs suportados em biocarvões torna-se uma estratégia benéfica tanto para o biochar quanto para os HDLs, em termos de remoção de numerosos contaminantes da água por adsorção.

2.5.3.2.1 Métodos de síntese do HDL

Vários metais catiônicos di e trivalentes têm sido empregados para adaptar os compósitos de biochar de HDL. Os cátions metálicos divalentes mais comuns são os de Mg, Mn, Fe, Co, Ni, Cu, Zn e Ca. Já, os cátions trivalentes são os de Al, Cr, Mn, Fe, Co e Ni.

As técnicas de síntese também variam entre si para influenciar o objetivo final da aplicação composta. Três métodos diferentes têm sido usados para a síntese de compósitos de HDL-biochar; 1) pré-revestir a matéria-prima com HDL e pirólise após a precipitação, 2) aplicação direta de biochar à mistura precursora de cátions e síntese de HDL, e 3) síntese de HDL na mistura precursora de biochar-cátion e pirólise novamente. No entanto, apenas um estudo individual relata o uso dos dois últimos métodos de síntese para preparar compósitos, o que permite a comparação das técnicas (WANG et al., 2016).

O método de síntese de co-precipitação em fase líquida para a síntese de HDLs tem sido amplamente divulgado; no entanto, em alguns casos, a co-precipitação foi usada como método de pré-revestimento na biomassa, antes da pirólise (HUANG et al., 2019; MEILI et al., 2019). Acima de tudo, a composição e estrutura dos HDLs são governadas pelos métodos de síntese. A co-precipitação, síntese hidrotérmica, hidrólise de ureia, método sol-gel estão entre os métodos mais comuns que são usados para a síntese de HDLs (THEISS; AYOKO e FROST, 2016). Dentre os métodos citados, a co-precipitação é frequentemente descrita como um método de “uma só etapa” devido à sua simplicidade e custo-benefício (BUKHTIYAROVA, 2019).

Na literatura, encontram-se as seguintes combinações de compósitos de HDLs suportados em biocarvões e o contaminante avaliado, conforme Tabela 6.

Tabela 6 - Estudos de HDLs suportados em biocarvões já publicados com seus respectivos contaminantes tratados.

Materiais compósitos	**Resíduos tratados**	**Referências**
Biochar/MgAl-HDL	Azul de metileno	(MEILI et al., 2019)
Biochar/MgFe-HDL	As (V)	(GUO et al., 2019)
Biochar/CuAl-HDL	Fosfato	(HU et al., 2018)
Biochar/FeAl-HDL	Fosfato	(PENG et al., 2019)
Biochar/NiFe-HDL	Fosfato	(YANG et al., 2019)
Biochar/MnAl-HDL	Cu (II)	(WANG et al., 2018)
Biochar/MnFe-HDL	Cd (II)	(GUO et al., 2019)
Biochar/ZnAl-HDL	Fosfato	(YANG et al., 2019)

Fonte: Produção do próprio autor.

Os estudos destacados na Tabela 6 impregnaram os HDLs na estrutura de um biochar bruto. No entanto, através dos experimentos de regeneração dos materiais adsorventes, foi observado uma redução em suas capacidades adsortivas, devido à

desintegração do HDL. No entanto, a eficiência de adsorção foi melhor favorecida pela presença do biochar. Dessa forma, existe uma lacuna na literatura ainda a ser estudada, que permite aplicar um pré-tratamento de ativação do biochar, antes de impregná-lo com HDL, a fim de manter a alta capacidade de adsorção para mais ciclos de regeneração. Além disso, nenhuma pesquisa disponível foi conduzida para investigar a adsorção do corante cristal violeta utilizando Ca^{2+} e Al^{3+}, como cátions di e trivalentes, suportados em um biochar previamente tratado por ativação química.

3 ARTIGO 1: CHARCOAL BRIQUETTING: AN ENVIRONMENTALLY FRIENDLY DESTINATION FOR WASTE MATERIALS

O artigo a seguir foi publicado na revista ENVIRONMENTAL ENGINEERING SCIENCE (ISSN: 1557-9018). DOI: 10.1089/ees.2021.0043

Charcoal briquetting: an environmentally friendly destination for waste materials

Juliano Missau[a*], Daniel Assumpção Bertuol[a], Eduardo Hiromitsu Tanabe[a]

[a] Environmental Processes Laboratory (LAPAM), Chemical Engineering Department, Federal University of Santa Maria – UFSM, Avenida Roraima 1000, 97105-900, Santa Maria, RS, Brazil

Abstract Inappropriate disposal of solid waste materials leads to environmental problems. Therefore, the present work promoted the novelty of an environmentally friendly destination of the waste materials such as crude wax, a by-product from pyrolysis of high-density polyethylene (HDPE) used packaging, and eucalypt leaves (a harvest residue). It was investigated the application of these waste materials, each one blended with corn starch, in the production of charcoal briquettes. The briquettes were analyzed in terms of its higher heating value (HHV) and mechanical resistance. Charcoal was produced from the pyrolysis of eucalypt sawdust biomass. The charcoal yield obtained was 35%, and the HHV was 33.02 MJ/kg at 400 ºC. This temperature was ideal for the production of charcoal, aiming to minimize energy and yield losses. The waste materials proportions evaluated in the composition of charcoal briquettes were 10, 20, and 30%. The corn starch proportion was fixed at 8%. The results showed that briquettes with 30% crude wax presented the best HHV, 23.45 MJ/kg, and greater shatter index, 97.80%. Satisfactory HHV were also achieved with 10% eucalypt leaves, 21.52 MJ/kg. In summary, the waste materials promoted charcoal briquettes with excellent results, providing it high energy efficiency and durability. Therefore, in order to minimize solid inadequate deposition, this study showed that crude wax and eucalypt leaves could be efficiently destinated for charcoal briquetting.

Keywords: Eucalypt sawdust biomass, pyrolysis, crude wax, eucalypt leaves, waste binders blend, charcoal briquettes.

3.1 INTRODUCTION

Plastics and wood materials dependence increases annually, due to accelerating consumer demands (Thomas et al. 2020). The intensive manufacture of products from these materials leads to enormous generation of solid wastes, such as used packaging, harvest residues and by-products, whose inappropriate disposal contributes to environmental problems (contamination of the oceans and groundwater). Therefore, environmental correct destination or recycling these residue materials can minimize such problems (Zhihua Chen et al. 2015; Saleem, Adil, and Mckay 2018).

Among the recycling techniques of solid wastes, pyrolysis stands out due to low requirement for raw materials, simplicity, and low energy consumption (Guo et al. 2020). It is a thermal degradation of organic compounds in an inert atmosphere, and does not require additional chemicals. In this process, three different final products are obtained: solid, liquid, and non-condensable gases (Al-salem et al. 2017). Temperature, heating rate, and time are among the most important parameters in the pyrolysis process (Rafiq et al. 2016).

HDPE in used packaging, eucalypt leaves and sawdust are examples of solid wastes from plastic and wood materials, respectively. Pyrolysis of HDPE in used packaging is mainly developed to produce oil, used as a fuel. However, crude wax and non-condensable gases are the by-products of this process (Williams 2020). The crude wax is composed mainly of paraffin, and it has been reported with a HHV of approximately 46 MJ/kg. Waxes have a variety of applications, such as fuels, useful feedstock chemicals, fruit coating and surface polishing.(Aguado et al. 2002; Rahman et al. 2018). Nevertheless, previous purification treatment is required for the removal of impurities (fillers, metals, etc.) (Missau, Bertuol, and Tanabe 2020). Applications of the crude wax obtained from the HDPE pyrolysis, without purification steps, have not yet been investigated in the literature, leaving a gap to be studied.

Eucalypt leaves are considered harvest residues that should not be deposited in the soil, as they contain a higher concentration of nutrients that can affect the balance of soil and compromising the local productivity (Zaiton et al. 2020). Eucalypt

leaves can be destinated for oil production, used as flavor and aroma enhancers, from complex extraction procedures (steam extraction, hydro-distillation or supercritical fluid extraction) (Zhao and Zhang 2014). However, an easy and simpler application of eucalypt leaves still can be studied.

The pyrolysis of eucalypt sawdust, a by-product from the manufacture of cellulose products, results in charcoal in a powder form, tar, and non-condensable gases (de Jesus et al. 2019). The charcoal displays significant superiority, compared with original eucalypt sawdust, in terms of energy density, convenient storage, transportation, and as an alternative to fossil fuels energy generation (Domingues et al. 2017). In addition, the use of charcoal can alleviate problems due to fossil fuel shortages as well as environmental problems (air pollution arising from the emissions of particulates and gaseous pollutants such as NO_x and SO_x) (Crespo et al. 2017).

However, the charcoal obtained by the pyrolysis of sawdust is in powder form, and it needs to be agglomerated to facilitate transport and storage of the product (Okot, Bilsborrow, and Phan 2019). This can be achieved by briquetting process, consisting of pressing the powder material in a hydraulic system or a mechanical press (Soares et al. 2015). Parameters evaluated in the briquetting technique include granulometry, pressing pressure, pressing time, cold or hot pressing, moisture content, and the material used as a binder (Xiao et al. 2015).

Binder materials are essential in the charcoal briquette production, as they are used to improve particle adhesion, thermal stability, compressive strength, abrasion resistance, and the energy content of the briquette. Several studies have reported the use of binders separately or together, forming a blend, with different proportions for the manufacture of charcoal briquettes (Muazu and Stegemann 2017; Aransiola et al. 2019; Simonelli et al. 2017; Florentino-Madiedo et al. 2018). However, to the best of our knowledge, there have been no studies investigating the application of crude wax and eucalypt leaves, as waste materials blended with corn starch, to produce charcoal briquettes in order to reduce the inadequate disposal and to provide an environmentally friendly destination for these solid wastes.

Therefore, the novelty of the present work was to investigated the effect of crude wax and eucalypt leaves in improving the energy content of charcoal briquettes. Firstly, charcoal production was established from the pyrolysis of eucalypt sawdust. The influence of pyrolysis temperature was evaluated in terms of yield and HHV of the charcoal produced. Subsequently, charcoal briquettes were developed by adding

crude wax and eucalypt leaves in different proportions, in a blend with corn starch. Finally, charcoal briquettes were characterized through proximate analysis, HHV, and determinations of the shatter index and relaxed density. The results of this study may serve as a reference for future research and applications.

3.2 MATERIALS AND METHODS

3.2.1 Materials

Eucalyptus saligna sawdust and eucalypt leaves were kindly donated by the company Madeireira Haas (Venâncio Aires, Rio Grande do Sul, Brazil). Crude wax was obtained as a byproduct from pyrolysis of HDPE waste and was characterized in a previous work (Missau, Bertuol, and Tanabe 2020). Corn starch was purchased from the company Maiscerta (Rio do Sul, Santa Catarina, Brazil).

3.2.2 Characterization of the materials

The samples of eucalypt leaves were previously dried for 24 h in 105 ºC to remove the water content using a muffle furnace (Model 1109, Ind. Magnus, Brazil), then crushed in a knife mill (Model N150, Rone, Brazil) fitted with a 10 mm mesh. Finally, the eucalypt leaves particles were size-segregated in order to obtain a mean particle size of 6.5 mm (Rahaman and Salam 2017).

The average particle size of the eucalypt sawdust was measured by granulometric distribution analysis, according to ASTM D-293-96. For this, a 30 g quantity of the sample was stirred using an electromagnetic stirrer (Model VP-01, Bertel, Brazil) and was passed through sieves with mesh sizes of 12, 16, 20, 30, 40, 50, 70, 100, 140, and 200 (Aleixo et al. 2015). The Sauter mean diameter (*ds*) of the eucalypt sawdust was determined according to Equation 1 (Kunii and Levenspiel 1991).

$$d_s = 1/(\sum \frac{\Delta\Phi_i}{Dp_i}) \quad (1)$$

where, $\Delta\Phi_i$ is the ratio of the mass retained by each sieve and Dp_i (mm) is the mean diameter in the sieve range.

The eucalypt sawdust chemical components were quantified in terms of total extractives (TAPPI T264 cm-97 standard method, adapted), Klason lignin (TAPPI T222 om-98 standard method), and holocellulose and alpha cellulose (TAPPI T203 cm-99 standard method). The hemicellulose content was calculated as the difference between holocellulose and alpha cellulose (Coldebella et al. 2018).

The thermal degradation profiles of the eucalypt sawdust, torrefied sawdust, and charcoal samples were obtained using a TGA-50 analyzer (Shimadzu, Japan). Approximately 10 mg of the samples was placed inside the alumina pans and heated from room temperature to 1000 ºC at a heating rate of 10 ºC/min, under an inert atmosphere of analytical grade N_2, 5.0 (99.999% purity), and flow rate of 100 mL/min (Zhihua Chen et al. 2015). The chemical groups present in the materials were investigated using FTIR spectroscopy (Prestige 21, Shimadzu, Japan), between the bands of 800 and 2000 cm^{-1}, in order to identify changes in lignin, cellulose, and hemicellulose (Wang et al. 2017).

The moisture content (MC), volatile matter (VM), ash content (AC), and fixed carbon (FC) values of the eucalypt sawdust, torrefied sawdust, charcoal, and charcoal briquette samples were determined by heating in a muffle furnace (Model 1109, Ind. Magnus, Brazil). Firstly, the samples were oven dried at 105˚C for 24 h, and then heated in a covered crucible inside the muffle furnace at 950˚C for 6 min. The resulting loss of mass refers to VM. The samples were then returned to the muffle furnace and heated in an open crucible at 750˚C for 6 h. The mass of material remaining after incineration refers to AC. For all the materials, FC was calculated according to Equation 2 (Thabuot et al. 2015).

$$FC\ (\%) = 100 - (VM + AC) \quad (2)$$

The HHVs of the eucalypt sawdust, torrefied sawdust, charcoal, and charcoal briquette samples were determined as established by ABNT NBR-8633, using a calorimetric bomb (Model 6400, Parr Instruments) (Zhiwen Chen et al. 2018).

The charcoal briquettes density was calculated using Equation 3.

$$Density = {}^{Mb}/_{Vb} \quad (3)$$

where, *Mb* is the briquette mass (kg) and *Vb* is the briquette volume (m^3) (Manyuchi, Mbohwa, and Muzenda 2018).

The relaxed density of the briquettes was measured 72 h after removal from the mold (Tembe, Otache, and Ekhuemelo 2014). The briquette strength was investigated

by the shatter index technique, with the briquette being allowed to fall onto a concrete floor from a height of 1 m. The briquette fraction remaining was used to determine the durability index, according to Equations 4 and 5 (Kaliyan and Vance Morey 2009).

$$Percentage\ weight\ loss = \frac{Initial\ weight\ before\ shattering - Weight\ after\ shattering}{Initial\ weight\ of\ briquette\ before\ shattering} \quad (4)$$

$$Shatter\ resistance = 100 - Percentage\ weight\ loss \quad (5)$$

3.2.3 Pyrolysis experiments

Pyrolysis tests were performed, in triplicate, using a system consisting of a gas supply unit and a vertical pyrolysis reaction unit, as shown in Figure 1. The samples were previously dried at 105 °C for 24 h to remove the water content (Sette et al. 2017).

The temperature has been reported to be the main parameter influencing the pyrolysis (Kumar and Bhattacharya 2020). Therefore, improvement of the pyrolysis process to obtain a charcoal with greater HHV considered the effect of the process temperature. The temperatures selected (250, 300, 350, 400, and 450 ºC) were based on the TGA analysis of the eucalypt sawdust. The values of the other parameters established during the pyrolysis experiments were fixed based on preliminary tests. The fixed values were as follows: heating rate of 15 °C min^{-1}, process time of 30 min, nitrogen flow of 50 mL min^{-1}, and mass of 100 g of the sample to be pyrolyzed (Zhiwen Chen et al. 2018). The charcoal yield obtained at each temperature was also evaluated.

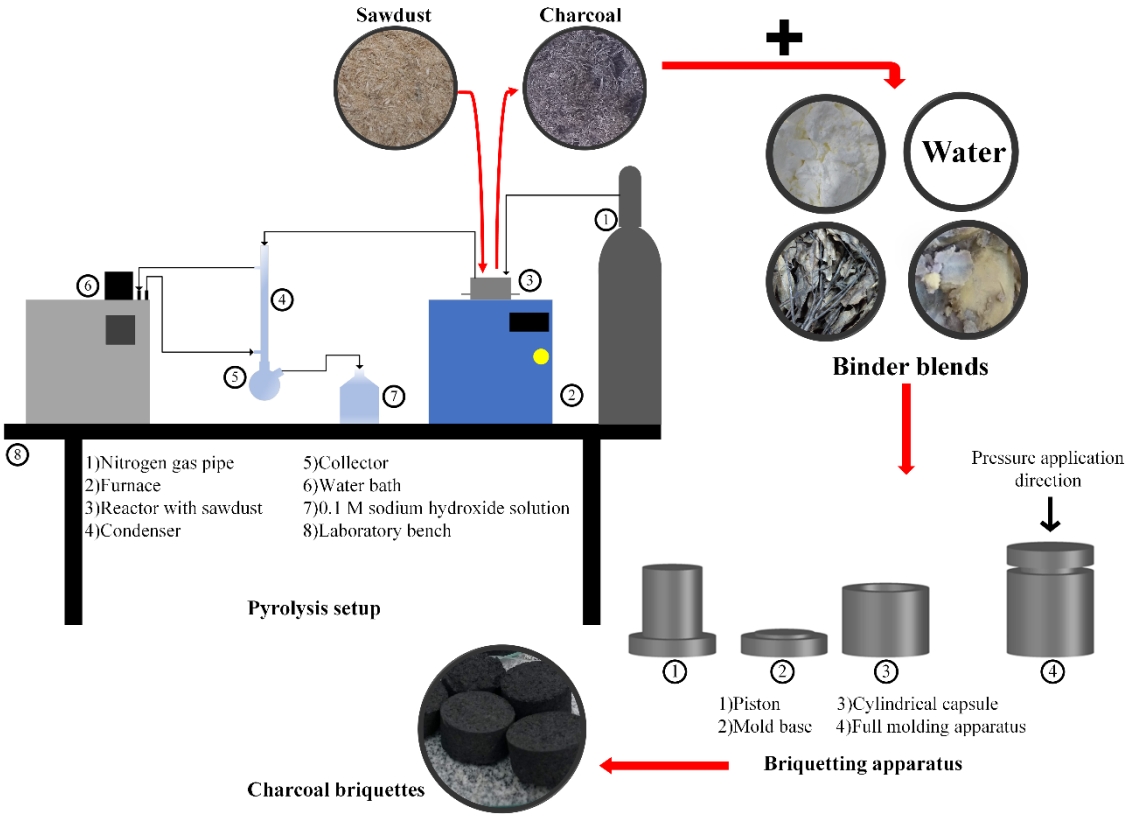

Figure 1 - Preparation of charcoal briquettes developed in this study.

The pyrolysis experiments were performed according to the following steps: (I) the stainless steel reactor was filled with 100 g of eucalypt sawdust; (II) the reactor was placed inside the furnace and the pyrolysis temperature was adjusted; (III) the nitrogen gas piping and the pyrolysis products output pipe were connected at the top of the reactor; (IV) the temperature of the cooling water supplied to the condenser was adjusted to 20 ºC. Tar was collected in a glass collector attached at the bottom of the condenser. Any non-condensable vapors were neutralized in a 0.1 M sodium hydroxide solution, prior to release to the atmosphere (Adam, Afzal, and Bennamoun 2017). The charcoal was trapped within the reactor and was removed after cooling to room temperature, under a nitrogen atmosphere (Wu et al. 2018). The mass of each product obtained was measured. The amount of gases was calculated by mass balance.

3.2.4 Preparation of waste materials-corn starch blends and briquetting

Charcoal powder, corn starch and the waste materials were homogeneously mixed, after which water was added and stirred properly to activate the binders for agglomeration (Adeleke et al. 2019). During mixing, the water content was adjusted in order to obtain particle agglomeration after addition of the matrix-forming compound, based on preliminary tests. The waste materials (crude wax and eucalypt leaves) proportions evaluated were 10, 20, and 30% of the entire briquette weight, based on studies reported in the literature (Jibril et al. 2008). The corn starch proportion was fixed at 8%, based on previous work, in order to improve the mechanical resistance of the charcoal briquettes (Jesús Rangel et al. 2016). The briquette mass established was 4.5 g, which satisfactorily filled the molds employed. All the constituents were measured in weight percent. The labeling and composition of the briquette samples are shown in Table 1. All the experiments were performed in triplicate.

Table 1 - Composition of the charcoal briquettes.

Briquette	Charcoal (wt%)	Corn starch (wt%)	Crude wax (wt%)	Eucalypt leaf
CBCS	92	8	-	-
CBCW-10	82	8	10	-
CBCW-20	72	8	20	-
CBCW-30	62	8	30	-
CBEL-10	82	8	-	10
CBEL-20	72	8	-	20
CBEL-30	62	8	-	30

Charcoal briquette with crude wax/corn starch blend – CBCW;
Charcoal briquette with eucalypt leaves/corn starch blend – CBEL;
Charcoal briquette with corn starch – CBCS.

After mixing all the materials, the mixture was filled into a steel compression mold suitable for forming cylindrical briquettes with a diameter of 35 mm and a height of 20 mm, as shown in Figure 1. The steel apparatus was coupled to a laboratory hydraulic press (Model MA098/A, Marconi, Brazil) and a pressure of 5 MPa under 10 s was applied for compaction of the material. This applied pressure value was chosen, because the use of higher pressures led to difficulty in removing the briquette from the mold. Subsequently, the briquettes were placed in a muffle furnace (Model 1109, Ind. Magnus, Brazil) at 60 °C (the melting temperature of the crude wax) for 12 h. This procedure was important for melting the wax and reducing the moisture in the

briquettes, in order to ensure consistent internal strength and satisfactory combustion (Ku Ahmad, Sazali, and Kamarolzaman 2018). The complete process developed in this study is also shown in Figure 1.

3.3 RESULTS AND DISCUSSION

3.3.1 Characterization of the materials

Figure 2 shows the particle size distribution of the eucalypt sawdust, revealing the presence of particles of different sizes, which is an important factor for the production of briquettes.

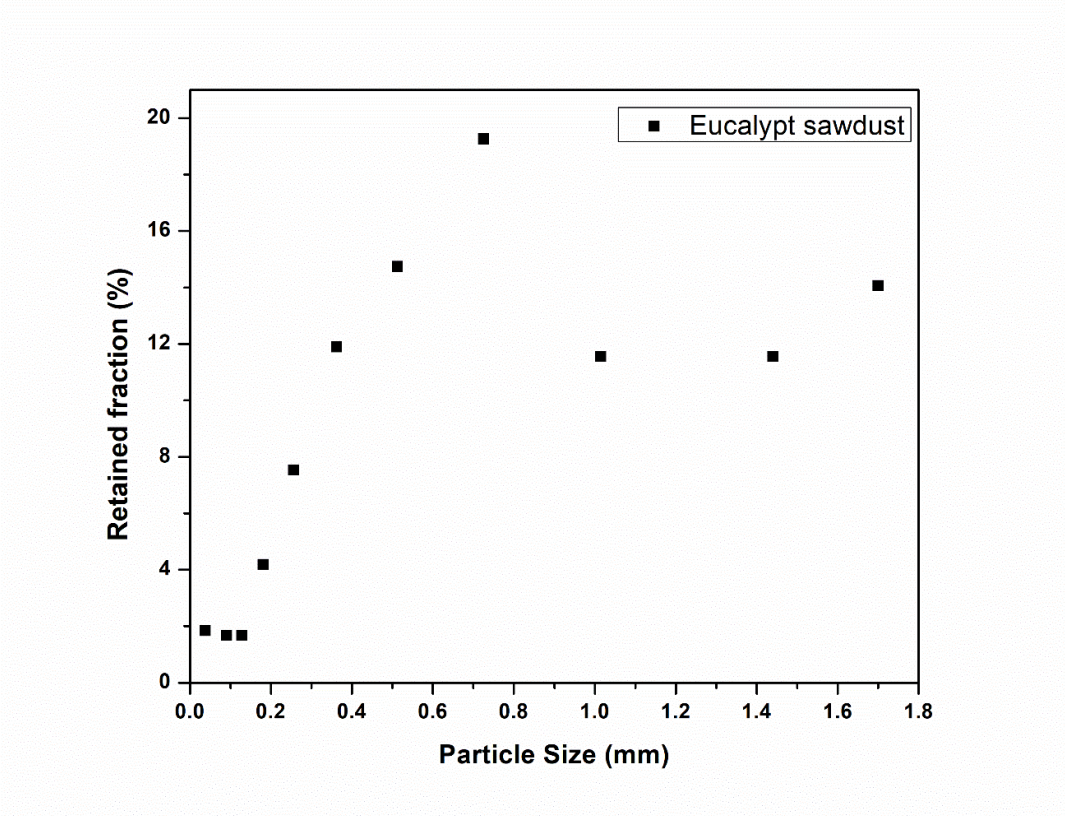

Figure 2 - Eucalypt sawdust particle size distribution.

For these solid fuels, the agglomerated material becomes more compacted when particles of different sizes are present, because the spaces between them are filled more easily, making inter-particle bonding with nearly no inter-particle spaces. Consequently, greater densification of the material results in higher energy efficiency (Kaliyan and Vance Morey 2009; Zepeda-cepeda et al. 2021).

Table 2 - Retained mass/mean particle diameter of the eucalypt sawdust.

Tyler/Mesh	Dp_i (mm)	$\Delta\Phi_i$	$\Delta\Phi_i/Dp_i$ (mm^{-1})	d_s (mm)
12	1.7000	0.1407	0.0828	
16	1.4400	0.1156	0.0803	
20	1.0150	0.1156	0.1139	
30	0.7250	0.1926	0.2657	
40	0.5125	0.1474	0.2876	
50	0.3625	0.1189	0.3281	0.4014
70	0.2560	0.0754	0.2944	
100	0.1810	0.0419	0.2314	
140	0.1280	0.0168	0.1309	
200	0.0905	0.0168	0.1851	
Base	0.0375	0.0184	0.4913	
Total	-	1	2.4914	

The 12, 16, 20, 30, 40, and 50 mesh sieves retained 83.08% of the initial sample mass. Acicular or very large particles were retained by the larger mesh sieves. On the other hand, very small particles passed easily through the sieves and were collected at the base. The Sauter mean diameter (*ds*) of the eucalypt sawdust sample was around 0.40 mm, calculated according to Equation 1, using the results shown in Table 2. Similar results were reported in another work, involving an eucalypt sawdust diameter of 0.35 mm (Jesús Rangel et al. 2016).

Analysis of the chemical composition of eucalypt sawdust is very important for its use in thermochemical processes, since it is related to the energy efficiency. This analysis indicates that the direct use of solid lignocellulosic wastes (SLW) to generate energy can present poor efficiency. The chemical composition results for the eucalypt sawdust (Table 3) showed that cellulose and hemicellulose contributed around 70% of the mass (Butterman and Castaldi 2010).

Table 3 - Eucalypt sawdust chemical composition.

Components analyzed	Composition (%)
Holocellulose	68.81 ± 0.38
Alpha cellulose	38.71 ± 2.77
Hemicellulose	30.10 ± 1.99
Klason lignin	17.90 ± 1.18
Total extractives	13.29 ± 0.09

When eucalypt sawdust biomass is used directly to generate heat, it presents low energy efficiency, due to the large quantity of volatile materials in its composition (Gominho et al. 2012) . Therefore, pyrolysis was used to improve the energy efficiency of the eucalypt sawdust.

Figure 3 shows the results of thermogravimetric analysis of the eucalypt sawdust, torrefied sawdust, and charcoal samples. The profile for the eucalypt sawdust showed three main stages of mass loss: drying (up to 105 °C), devolatilization (200-500 °C), and increased charcoal formation (>500 °C) (Tai and Chen 2016). Continuous heating led to the formation of ash.

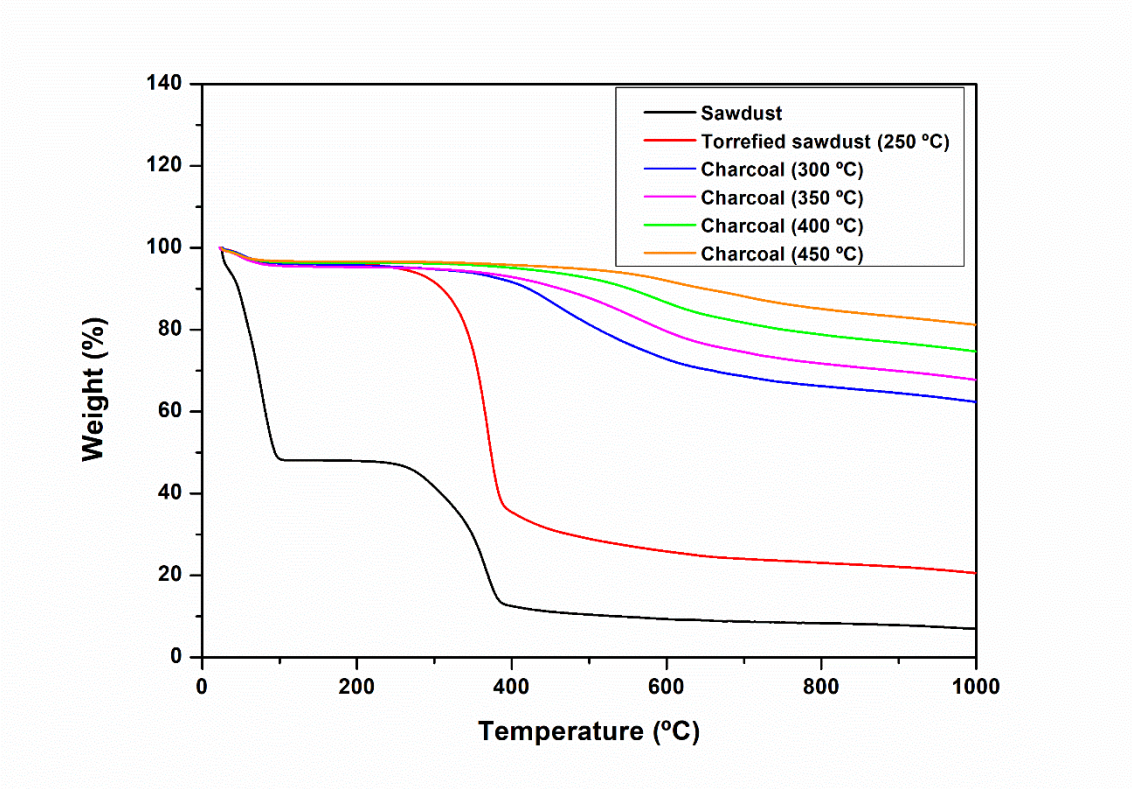

Figure 3 - TGA curves for the eucalypt sawdust, torrefied sawdust, and charcoal samples.

The mass loss for the drying stage showed that the eucalypt sawdust contained approximately 50% water in its composition. The greatest decomposition, associated with devolatilization, was between around 250 and 400 ºC, involving the thermal degradation of hemicellulose, cellulose, and lignin. As reported previously, the degradation processes of hemicellulose, cellulose, and lignin occur in the temperature ranges 200-260, 240-300, and >280 ºC, respectively (Sallem-Idrissi et al. 2016; Boumanchar et al. 2017). Above 400 ºC, the devolatilization step was no longer evident

for the charcoal samples. This behavior showed a greater degradation of volatile matter with increasing temperature, in agreement with other studies (Poletto et al. 2010; Unpinit et al. 2015).

Based on the results of the thermogravimetric analysis of the eucalypt sawdust, the following batch pyrolysis temperatures were chosen: 250, 300, 350, 400, and 450 °C. A temperature of 450 ºC was included in the procedure, because the mass and heat transfers in batch pyrolysis processes may differ from those suggested by thermogravimetric analysis (due to mass differences of the samples used in the two procedures).

The samples were submitted to FTIR analysis to identify changes in the bands corresponding to lignin, cellulose, and hemicellulose (between 800 and 2000 cm^{-1} (Wang et al. 2017)) caused by increase of the eucalypt sawdust pyrolysis temperature, comparing the spectra for the eucalypt sawdust, torrefied sawdust, and charcoal samples (Figure 4).

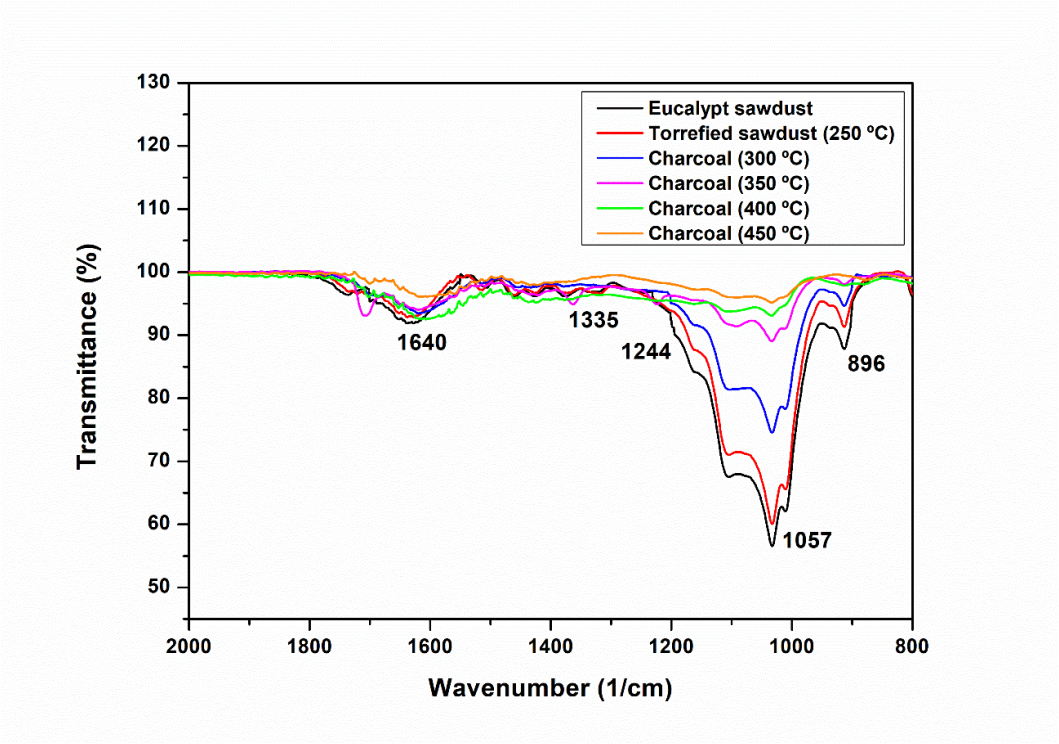

Figure 4 - FTIR spectra of the eucalypt sawdust, torrefied sawdust, and charcoal samples.

A band located at 1640 cm^{-1} corresponded to C=C stretching of the aromatic rings of lignin. Increase of the temperature led to decreased intensity of this peak in the sample spectra. A band at 1057 cm^{-1} could be attributed to C-O-C stretching, while

a peak at 896 cm^{-1} was associated with cellulose C-H rocking vibration (de Figueredo et al. 2017). Decreased intensities were observed for the bands at 1335-1244 cm^{-1}. The reduction of the band at 1244 cm^{-1} suggested disruption or weakening of the interaction between lignin and hemicellulose, due to the temperature increase. This behavior also occurred with cellulose and lignin, leading to decreased intensity of the band at 1335 cm^{-1} (Castoldi et al. 2017).

The FTIR spectra for the sawdust and charcoal samples confirmed that the pyrolysis temperature affected degradation of the hemicellulose, as well as part of the cellulose and lignin present in the eucalypt sawdust.

3.3.2 Effect of pyrolysis temperature on charcoal characteristics

3.3.2.1 Effect of pyrolysis temperature on charcoal yield

The eucalypt sawdust samples were pyrolyzed during 30 min at 250, 300, 350, 400, and 450 °C, using a heating rate of 15 °C min^{-1} and a nitrogen gas flow rate of 50 mL min^{-1}. The pyrolysis heating rate and time were based on preliminary tests and other studies. Kwapinski et al. (2010) mentioned the use of low heating rates to maximize solid product yields. Longer operating times favor the pyrolysis reactions, causing greater degradation of the components (including hemicellulose, cellulose, and lignin) of solid lignocellulosic wastes (Kan, Strezov, and Evans 2016). Therefore, in order to minimize the energy losses of the pyrolysis process, a treatment time of 30 min was set as ideal, in order to favor the charcoal production.

The pyrolysis temperature typically changes the yield and properties of the charcoal produced. The results showed a charcoal yield of 82%, 42%, 35.5%, 35%, and 32% for the pyrolysis temperatures of 250 ºC, 300 ºC, 350 ºC, 400 ºC and 450 ºC, respectively. It was observed that the charcoal yield decreased sharply as the temperature was increased from 250 to 300 °C, followed by a gradual decrease up to 400 °C, after which it remained fairly stable. Angin (2013) also reported that increase of the pyrolysis temperature from 400 to 600 ºC led to a lower yield of charcoal obtained from pyrolysis of safflower seed press cake, with values of around 34 and 27%, respectively. Demirbas (1997) also mentioned that the charcoal yield decreased from 43.5 to 31.0% for walnut shell with increase of the temperature from 275 to 875 ºC.

Although a high final value (82% of the mass remaining) was obtained at 250 ºC, this did not mean that the entire eucalypt sawdust sample had been transformed into charcoal. Katyal, Thambimuthu, and Valix (2003) observed that a high yield of biochar at a low temperature (250 ºC) indicated that the material had been only partially pyrolyzed. Therefore, the use of 250 °C for 30 min was insufficient to completely pyrolyze the eucalypt sawdust biomass. Hence, the eucalypt sawdust was only torrefied.

Increase of the temperature to 300 °C led to a 58% loss of mass, leaving 42% of charcoal. The high degradation of the eucalypt sawdust biomass at this temperature was characteristic of the devolatilization stage. Under this condition, the eucalypt sawdust was converted into charcoal, due to the degradation of hemicellulose and cellulose (Boumanchar et al. 2017).

With further increase of the temperature (to 350, 400, and 450 °C), the decomposition of the lignocellulosic structure became more abrupt. According to Fu et al. (2012), the mass decrease may be due to greater primary decomposition of the wood at higher temperatures, or to secondary decomposition of the charcoal. Consequently, the amounts of charcoal obtained at the end of the tests were 35.5, 35, and 32% for temperatures of 350, 400, and 450 °C, respectively. These results were consistent with the amounts of charcoal obtained from other biomasses reported in earlier studies (Sun et al. 2017; Yorgun and Yildiz 2015).

3.3.2.2 Effect of pyrolysis temperature on charcoal HHV

The results of proximate and HHV analysis of the eucalypt sawdust, torrefied sawdust, and charcoal samples obtained at different pyrolysis temperatures are presented in Table 4. Increase of the pyrolysis temperature to 450 ºC led to an increase of the HHV from 19.47 to 33.88 MJ/kg (an approximately 74% increase). Park and Jang (2012) attributed such behavior to the release of volatile matter during pyrolysis for the production of charcoal from rice husks, wood chips, and wood pellets. Opposite trends were observed for HHV and VM (Figure 5), with VM decreasing rapidly between 250 and 300 ºC, while HHV increased. This is the temperature range in which the thermal degradation of cellulose occurs. When the pyrolysis temperature was increased further, a small difference in the charcoal HHV was observed between 400

and 450 ºC. Uzun, Pütün, and Pütün (2007) concluded that this feature was due to the removal of volatile matter during the degradation of hemicellulose and cellulose. This behavior was also evidenced from the results of the analyses using TGA (Figure 3) and FTIR (Figure 4).

Table 4 - HHV and proximate analysis of the eucalypt sawdust, torrefied sawdust, and charcoal samples.

Samples	MC (%)	VM (%)	AC (%)	FC (%)	HHV (MJ/kg)
Eucalypt sawdust	11.57 ± 0.39	85.99 ± 0.38	0.37 ± 0.01	13.64 ± 0.39	19.47 ± 0.21
Torrefied sawdust (250 ºC)	1.76 ± 0.28	75.31 ± 0.43	3.69 ± 0.11	20.99 ± 0.37	21.93 ± 0.34
Charcoal (300 ºC)	2.43 ± 0.12	33.47 ± 0.51	1.19 ± 0.13	65.34 ± 0.55	29.68 ± 0.30
Charcoal (350 ºC)	2.31 ± 0.10	28.44 ± 0.45	1.29 ± 0.09	70.28 ± 0.42	31.10 ± 0.33
Charcoal (400 ºC)	2.31 ± 0.11	18.36 ± 0.47	1.11 ± 0.10	80.53 ± 0.50	33.02 ± 0.25
Charcoal (450 ºC)	2.47 ± 0.09	14.38 ± 0.39	1.12 ± 0.14	84.51 ± 0.42	33.88 ± 0.27
Commercial eucalypt charcoal	-	-	-	-	32.08 ± 0.17

MC: moisture content; VM: volatile matter; AC: ash content; FC: fixed carbon.

As the pyrolysis temperature was increased from 250 to 450 ºC, the FC contents of the charcoals increased, with FC as high as 84.51% achieved for charcoal pyrolyzed at 450 ºC. The trends for HHV and FC were similar, as also shown in Figure 5. This was expected, because the increased devolatilization during pyrolysis resulted in charcoal that was predominantly carbon. These findings were generally in agreement with results reported in the literature (Angin and Şensöz 2014). He et al. (2018) found that increase of the pyrolysis temperature, with the release of VM and increase of FC, led to a higher degree of carbonization, higher C content in the charcoal, and a substantial decrease of the O content, which together acted to increase the HHV.

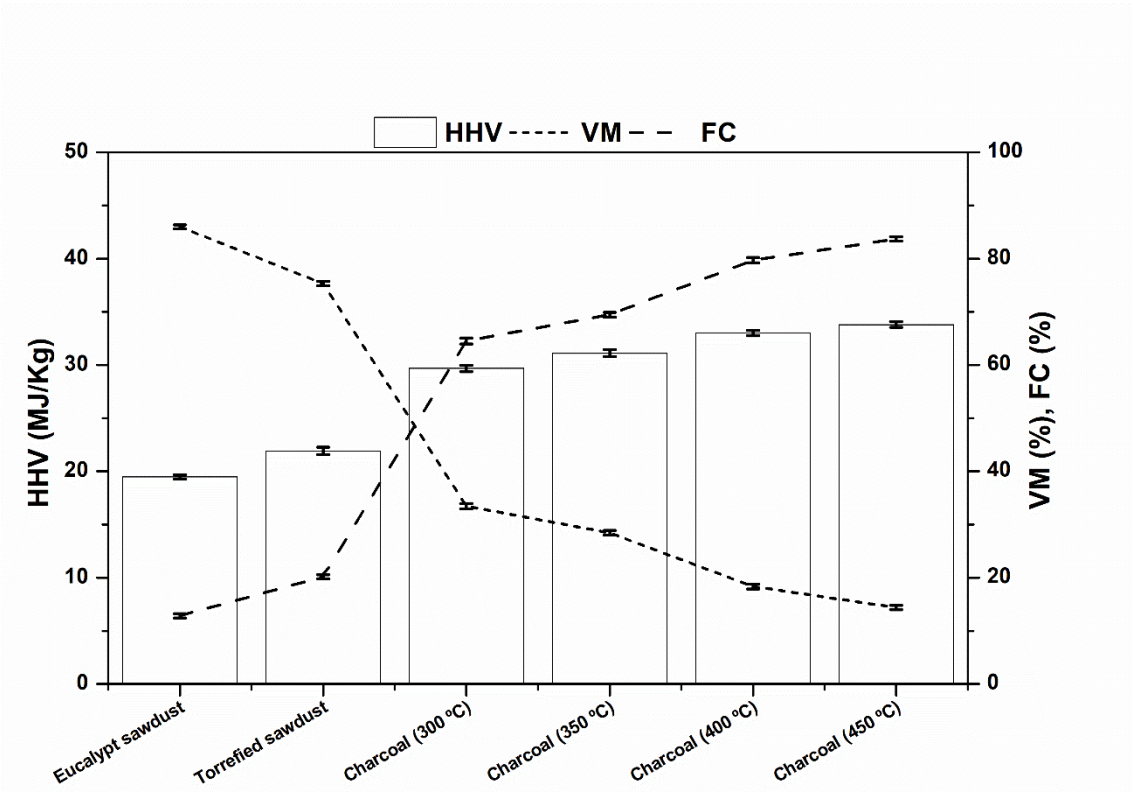

Figure 5 - Relationship between HHV, VM and FC for the eucalypt sawdust, torrefied sawdust, and charcoal samples.

Hence, after evaluating the effects of the pyrolysis temperature on the charcoal yield and HHV, a temperature of 400 ºC was considered ideal in the subsequent studies of the briquetting process. This choice took into consideration the energy savings during the pyrolysis process, since the increase in HHV was only 0.86 MJ/kg between temperatures of 400 and 450 ºC, as shown in Table 4. Another reason for the choice of a temperature of 400 ºC concerned the charcoal yield obtained. The charcoal yield was approximately 35% at 400 ºC, while it decreased to 32% at 450 ºC. It was also found that the HHV for the charcoal obtained at 400 ºC was 5% higher than for the commercial eucalypt charcoal.

3.3.3 Effects of the waste materials-corn starch blends on charcoal briquette production

The applications of the waste materials, crude wax (by-product from pyrolysis of HDPE used packaging) and eucalypt leaves (harvest residue), were investigated in the production of charcoal briquettes. This procedure could be a simple and easily final

destination of these residues, in order to reduce environmental problems caused by their inappropriate disposal.

Table 5 and Figure 6 presents the results of the proximate and HHV analyses of the charcoal briquettes produced in this study, respectively.

Table 5 - Proximate analyses of the charcoal briquettes.

Briquettes	VM (%)	AC (%)	FC (%)	MC (%)
CBCS	69.29 ± 0.15	3.65 ± 0.43	27.06 ± 0.53	1.64 ± 0.03
CBCW-10	69.85 ± 0.86	3.12 ± 0.20	27.03 ± 0.71	0.79 ± 0.13
CBCW-20	64.75 ± 0.49	2.38 ± 0.15	32.87 ± 0.32	1.23 ± 0.12
CBCW-30	56.46 ± 0.76	1.74 ± 0.03	41.80 ± 0.49	1.70 ± 0.11
CBEL-10	61.68 ± 0.94	3.81 ± 0.35	34.51 ± 0.80	1.36 ± 0.15
CBEL-20	64.99 ± 0.85	5.09 ± 0.38	29.92 ± 0.87	2.89 ± 0.14
CBEL-30	69.87 ± 0.93	5.91 ± 0.47	24.22 ± 0.95	3.50 ± 0.18

MC: moisture content; VM: volatile matter; AC: ash content; FC: fixed carbon.

The crude wax and eucalypt leaves proportions had effects on the VM, FC, and HHV of the briquettes. The FC content is one of the major contributors to the HHV of charcoal briquettes, while a lower VM content provides briquettes that are more suitable for combustion (Ikelle and Philip Ivoms 2014). Increase of the proportion of crude wax from 10 to 30% resulted in VM decreasing by 13%, while the FC content and HHV increased by 15 and 16%, respectively. The best HHV (23.45 MJ/kg) was obtained with 30% proportion of crude wax. These features were possibly related to carbon chain length of this waste material. It is reported that crude wax consists of hydrocarbon chains with a wide distribution of molecular weights, which include compounds between C_9 and C_{60} (Berrueco et al. 2002). Therefore, the longer the carbon chain, the higher the fixed carbon content. For this reason, the increase in HHV can be observed as the proportion of crude wax in the composition of the charcoal briquette increases.

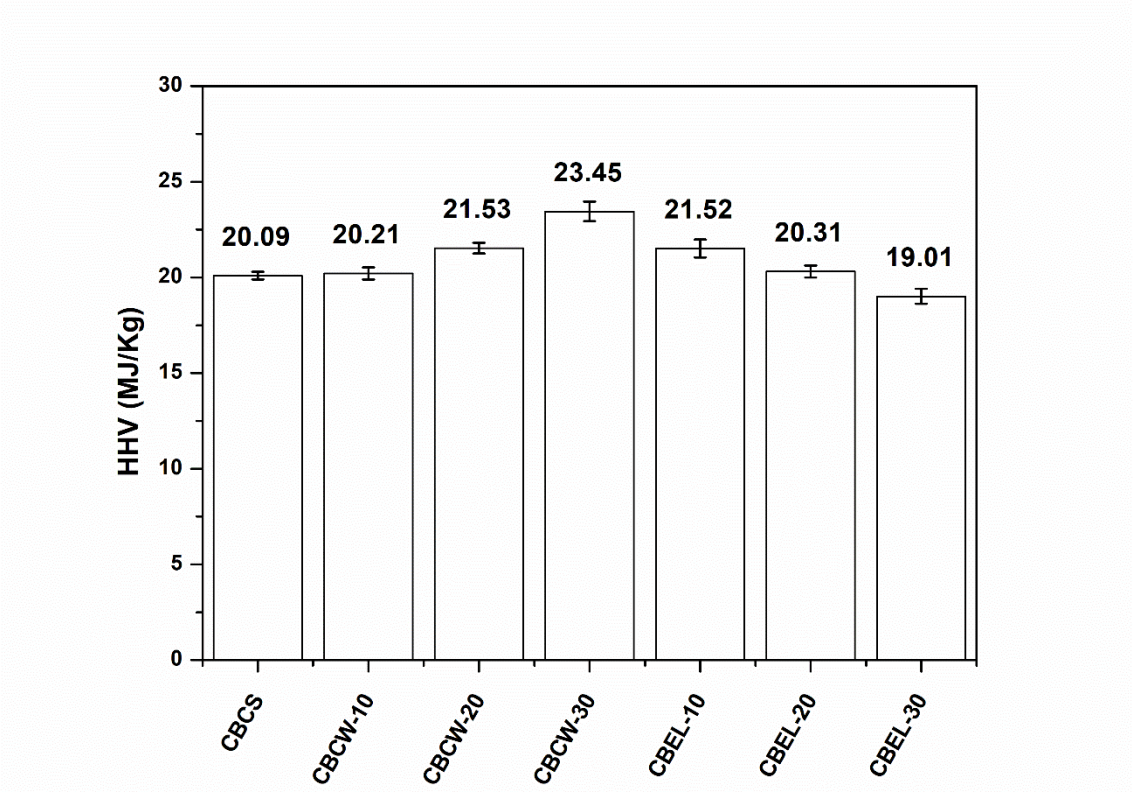

Figure 6 - HHV analyses of the charcoal briquettes.

The briquettes with eucalypt leaves achieved the best result of HHV (21.52 MJ/Kg) with the lowest proportion tested (10%). This behavior can be justified by the composition of the eucalypt leaf, which is an organic harvest residue composed mainly of volatile matter. Therefore, as a higher amount of eucalypt leaves is added, there is an increase in the presence of volatile compounds in the briquette, negatively affecting its HHV (Zhao and Zhang 2014).

Table 6 shows the HHV of charcoal briquettes obtained using other biomasses and binders, compared to those produced in this study. It was observed that the briquettes CBCW-30 and CBEL-10 presented satisfactory energy efficiency compared with several other charcoal briquettes already studied. Carnaje et al. (2018) reported similar results for charcoal briquettes produced using a water hyacinth (*Eichhornia crassipes*) and molasses blend, achieving HHV of 16.60 MJ/kg. Guo et al. (2020) reported similar HHV behavior with increase of the proportion of a sodium hydroxide-corn starch blend, resulting in HHV of 22.12 MJ/kg. However, the CBCW-30 formulation produced here presented the best HHV (23.45 MJ/kg), compared to the other briquettes. This HHV was 17 and 50% higher, respectively, compared to the CBCS briquette produced in this study and a briquette produced using a blend of

glycerin and corn starch (Simonelli et al. 2017). It was also 8 and 11% higher than the HHV obtained for the CBEL-10 briquette produced in this study and a commercial briquette, respectively.

Table 6 - Comparison of the HHV values for charcoal briquettes produced with different binders.

Binders	HHV (MJ/kg)	Reference
Blend of crude wax and corn starch (CBCW-30)	23.45	This study
Blend of sodium hydroxide and corn starch	22.12	(Guo et al. 2020)
Blend of eucalypt leaf and corn starch (CBEL-10)	21.52	This study
Commercial	21.15	-
Corn starch (CBCS)	20.09	This study
Cassava starch	19.95	(Arellano, Kato, and Bacani 2015)
Clay	19.46	(Gebresas et al. 2015)
Blend of water hyacinth and molasses	16.60	(Carnaje et al. 2018)
Corn cob	14.84	(Ikelle and Philip Ivoms 2014)
Blend of glycerin and corn starch	11.80	(Simonelli et al. 2017)

Figure 7 and Figure 8 presents the results for the mechanical resistance (shatter index and relaxed density, respectively) evaluations of the charcoal briquettes. The shatter index provides a direct means of gauging the strength of briquettes for the purposes of handling, transportation, and storage (Kpalo et al. 2020). The CBCW-30 formulation presented a shatter index of 97.80%, which was close to the value of 98.94% for the CBCS briquette. The behavior observed for CBCW-30 could be explained by the high agglomeration capacity of the material, as well as the fact that the crude wax was a partially solid material at room temperature. According to Borowski, Stępniewski, and Wójcik-Oliveira (2017), the shatter index of briquettes should be at least 90%, in order to avoid damage from handling. However, it was observed that the briquettes resulting from the blend of eucalypt leaves and corn starch showed values below this limit. Except CBEL-10, which exceeded 90%, reaching a value of 91.75%. The CBEL-20 and CBEL-30 were not able to retain 90% of the

briquettes' initial mass in solid form. According to Rahaman and Salam (2017), it can be explained by the small particles size of the eucalypt leaves (6.5 mm). Smaller particles are capable of producing briquettes of lower shatter index compared to higher particles even at lower pressure.

Therefore, the blend of crude wax and corn starch produced a charcoal briquette that was harder to disintegrate than the one blended with eucalypt leaves and corn starch.

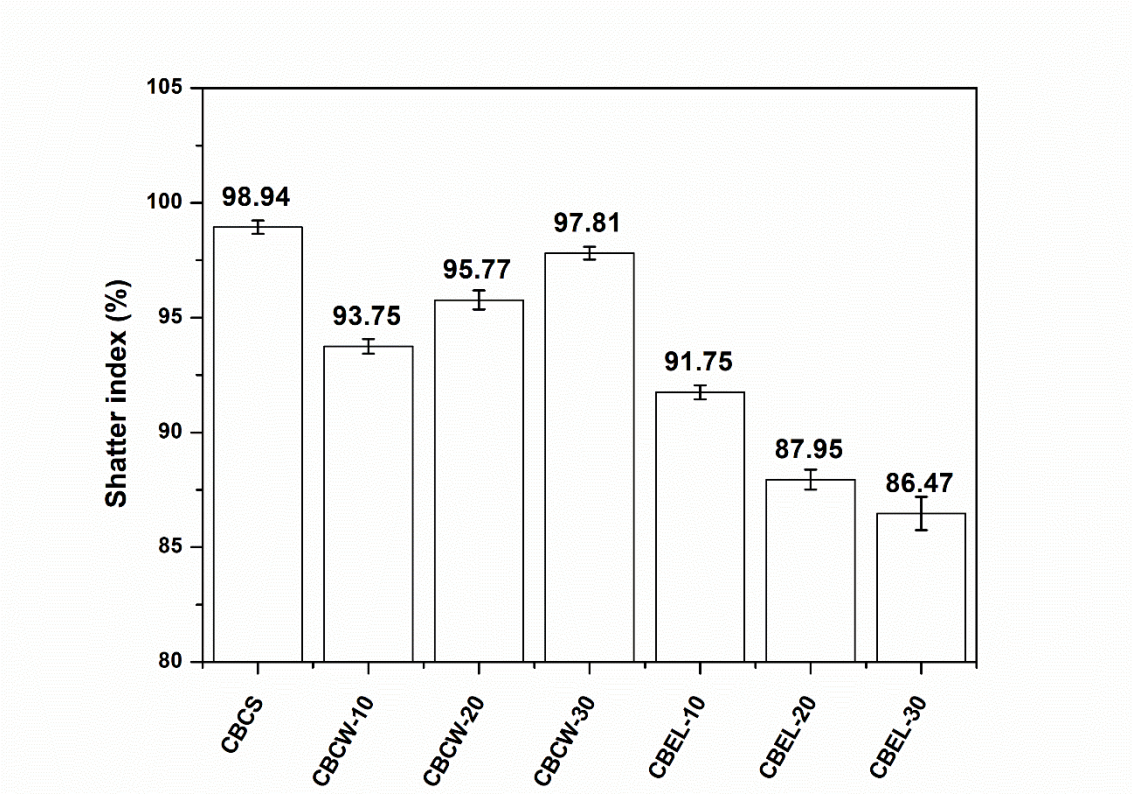

Figure 7 - Shatter index of the charcoal briquettes.

In terms of relaxed density, it was observed that increase of the proportion of crude wax led to higher relaxed density of the briquettes. Consequently, the CBCW-30 briquette presented the best result (713.70 kg/m³). This could be explained by the fact that a higher binder proportion leads to tighter packing of the particles of the charcoal briquette material, due to reduction of the void ratio, consequently increasing the briquette density (Olugbade, Ojo, and Mohammed 2019). The relaxed densities obtained for the briquettes in this study were consistent with the work of Mitchual, Frimpong-Mensah, and Darkwa (2013), who reported that the densities of briquettes produced using a hydraulic piston press are usually lower than 1,000 kg/m^3. According

to Davies and Davies (2013), high density briquettes tend to have a longer burning time and release more heat than briquettes with low density, with the lower weight of the latter resulting in their rapid exhaustion during combustion.

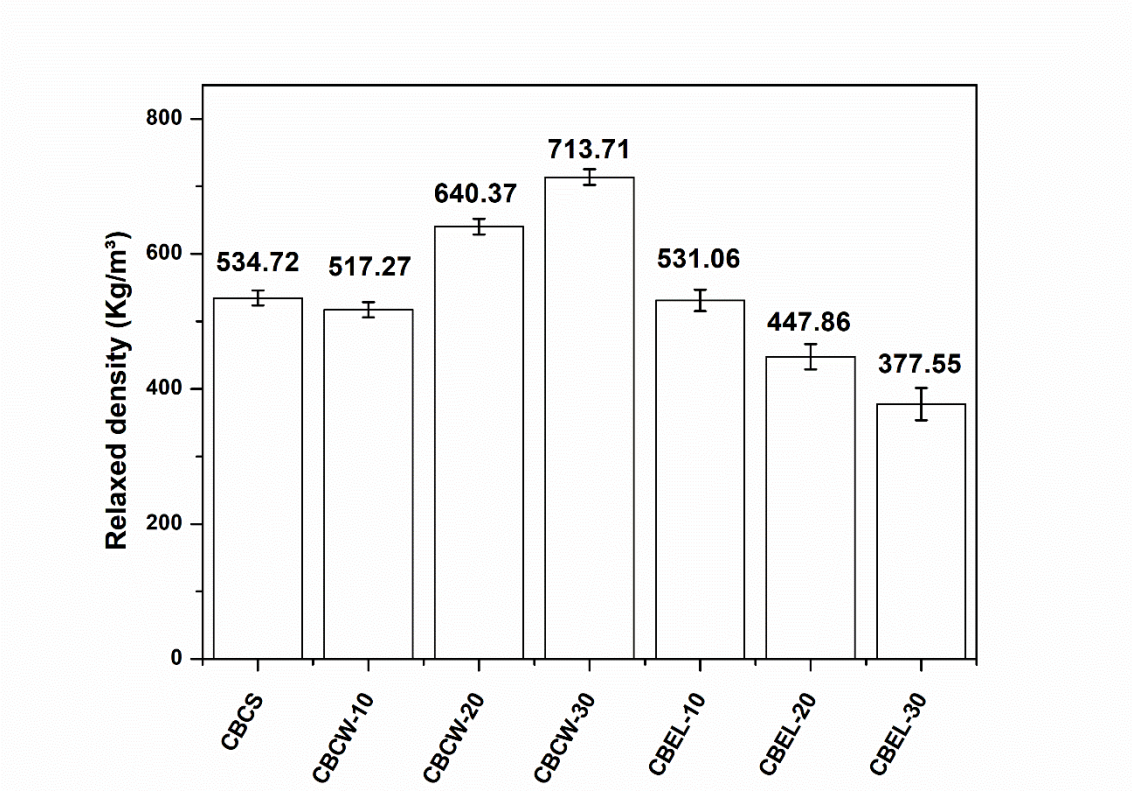

Figure 8 - Relaxed density of the charcoal briquettes.

In summary, the results presented in this work showed that crude wax and eucalypt leaves, each one blended with corn starch, for the bonding of charcoal obtained from pyrolysis of eucalypt sawdust at a temperature of 400 ºC, had a positive effect on the energy efficiency of the briquettes. The HHV of 23.45 and 21.52 MJ/kg obtained with 30% of crude wax and 10 % of eucalypt leaves, respectively, was higher than for a commercial briquette and others reported in the literature. In addition to enhancing the HHV, the waste materials also provided good results in terms of the shatter index of the final solid biofuel.

Therefore, the assays elaborated in this study allowed to obtain results showing that the waste materials, crude wax (a by-product from pyrolysis of HDPE used packaging) and eucalypt leaves (a harvest residue), could be used in the production of charcoal briquettes, in order to reduce the solid wastes inappropriate disposal.

Besides the briquetting process was simple and easily, it provided charcoal briquettes with high energy efficiency and durability enhancement.

3.4 CONCLUSIONS

The intensive manufacture of products from plastic and wood materials leads to enormous generation of solid wastes, such as used packaging, harvest residues, and by-products. The inappropriate disposal of this materials contributes to environmental problems. Therefore, a simple and easy final destination for the waste materials, crude wax (a by-product from pyrolysis of HDPE used packaging) and eucalypt leaves (a harvest residue), blended with corn starch, can be applied in the production of charcoal briquettes.

Firstly, pyrolysis was applied to convert eucalypt sawdust biomass to charcoal. The influence of the pyrolysis temperature was analyzed in terms of charcoal yield and HHV. The production of charcoal briquettes was carried out using the charcoal obtained at a pyrolysis temperature of 400 ºC, with the aim of saving energy and ensuring a satisfactory charcoal yield. At this temperature, the charcoal yield was 35% and the HHV was 33.02 MJ/kg, which was 5% higher than obtained for a commercial eucalypt charcoal.

The effect of the waste materials, crude wax and eucalypt leaves, each one blended with corn starch, was investigated in terms of the charcoal briquette energy efficiency and mechanical resistance. The results obtained, in terms of HHV, were compared with those for other charcoal briquettes produced using different binders, reported previously in the literature. Satisfactory results for HHV and mechanical resistance were achieved for the charcoal briquette produced using a blend of 30% crude wax and 8% corn starch. The HHV (23.45 MJ/kg) was 11% higher than for the commercial briquette and 50% higher than for a briquette blended with glycerin, reported in a published study. The results obtained for the shatter index (97.80%) and relaxed density (713.70 kg/m^3) confirmed the good mechanical resistance of the final product. The charcoal briquettes with eucalypt leaves also presented good results in terms of HHV, 21.52 MJ/kg, and mechanical strength.

In this way, the use of the waste materials, crude wax and eucalypt leaves, presented satisfactory results, confirming that they can be used to increase the energy efficiency and durability of charcoal briquettes in a simple, efficient, and easily

procedure. Therefore, this study promoted a novelty for the environmentally friendly destination of these materials, in order to minimize the environmental problems faced in the current days.

Acknowledgments

The authors are grateful for the financial support provided by CNPq (National Council of Scientific and Technological Development), CAPES (Brazilian Agency for Improvement of Graduate Personnel), FAPERGS (Foundation for Research Support of the State of Rio Grande do Sul), SDECT (Department of Economic Development, Science and Technology of the State of Rio Grande do Sul) and MADEIREIRA HAAS LTDA.

Authorship confirmation statement: All authors contributed equally to this study.
Author(s') disclosure statement(s): No competing financial interests exist.
Funding: Funding was provided by CNPq (National Council of Scientific and Technological Development).

3.5 REFERENCES

Adam, Arshad, Muhammad T Afzal, and Lyes Bennamoun. 2017. "Pyrolysis of Corn Stalk Biomass Briquettes in a Scaled-up Microwave Technology." *Bioresource Technology* 233: 353–62. https://doi.org/10.1016/j.biortech.2017.02.113.

Adeleke, A.A., J.K. Odusote, O.A. Lasode, P.P. Ikubanni, M. Malathi, and D. Paswan. 2019. "Densification of Coal Fines and Mildly Torrefied Biomass into Composite Fuel Using Different Organic Binders." *Heliyon* 5 (7): e02160. https://doi.org/10.1016/j.heliyon.2019.e02160.

Aguado, Roberto, Martín Olazar, María J. San José, Beatriz Gaisán, and Javier Bilbao. 2002. "Wax Formation in the Pyrolysis of Polyolefins in a Conical Spouted Bed Reactor." *Energy and Fuels* 16 (6): 1429–37. https://doi.org/10.1021/ef020043w.

Al-salem, S M, A Antelava, A Constantinou, G Manos, and A Dutta. 2017. "A Review on Thermal and Catalytic Pyrolysis of Plastic Solid Waste." *Journal of Environmental Management* 197 (1408): 177–98. https://doi.org/10.1016/j.jenvman.2017.03.084.

Aleixo, Diego, Fabio Minoru Yamaji, João Lúcio De Barros, Alessandra Luzia, and Gabriela Tamy Nakashima. 2015. "Caracterização de Biomassas Para a

Briquetagem.” *Floresta*, no. 2014: 713–22. https://doi.org/10.5380/rf.v45i4.39700.

Angin, Dilek. 2013. “Effect of Pyrolysis Temperature and Heating Rate on Biochar Obtained from Pyrolysis of Safflower Seed Press Cake.” *Bioresource Technology* 128: 593–97. https://doi.org/10.1016/j.biortech.2012.10.150.

Angin, Dilek, and Sevgi Şensöz. 2014. “Effect of Pyrolysis Temperature on Chemical and Surface Properties of Biochar of Rapeseed (Brassica Napus L.).” *International Journal of Phytoremediation* 16 (7–8): 684–93. https://doi.org/10.1080/15226514.2013.856842.

Aransiola, E.F., T.F. Oyewusi, J.A. Osunbitan, and L.A.O. Ogunjimi. 2019. “Effect of Binder Type, Binder Concentration and Compacting Pressure on Some Physical Properties of Carbonized Corncob Briquette.” *Energy Reports* 5: 909–18. https://doi.org/10.1016/j.egyr.2019.07.011.

Arellano, Gino Martin T, Yuji S Kato, and Florinda T Bacani. 2015. “Evaluation of Fuel Properties of Charcoal Briquettes Derived From Combinations of Coconut Shell , Corn Cob and Sugarcane Bagasse.” *DLSU Research Congress 2015* 3: 1–6.

Berrueco, Cesarb, E. J. Mastral, E. Esperanza, and J. Ceamanos. 2002. “Production of Waxes and Tars from the Continuous Pyrolysis of High Density Polyethylene. Influence of Operation Variables.” *Energy and Fuels* 16 (5): 1148–53. https://doi.org/10.1021/ef020008p.

Borowski, Gabriel, Witold Stępniewski, and Katarzyna Wójcik-Oliveira. 2017. “Effect of Starch Binder on Charcoal Briquette Properties.” *International Agrophysics* 31 (4): 571–74. https://doi.org/10.1515/intag-2016-0077.

Boumanchar, Imane, Younes Chhiti, Fatima Ezzahrae M’hamdi Alaoui, Amal El Ouinani, Abdelaziz Sahibed-Dine, Fouad Bentiss, Charafeddine Jama, and Mohammed Bensitel. 2017. “Effect of Materials Mixture on the Higher Heating Value: Case of Biomass, Biochar and Municipal Solid Waste.” *Waste Management* 61: 78–86. https://doi.org/10.1016/j.wasman.2016.11.012.

Butterman, Heidi C., and Marco J. Castaldi. 2010. “Biomass to Fuels: Impact of Reaction Medium and Heating Rate.” *Environmental Engineering Science* 27 (7): 539–55. https://doi.org/10.1089/ees.2009.0372.

Carnaje, Naomi P., Romel B. Talagon, Jose P. Peralta, Kalpit Shah, and Jorge Paz-Ferreiro. 2018. “Development and Characterisation of Charcoal Briquettes from Water Hyacinth (Eichhornia Crassipes)-Molasses Blend.” *PLoS ONE* 13 (11): 1–14. https://doi.org/10.1371/journal.pone.0207135.

Castoldi, Rafael, Vanesa G. Correa, Gutierrez Rodrigues de Morais, Cristina G.M. de Souza, Adelar Bracht, Rosely A. Peralta, Regina F. Peralta-Muniz Moreira, and Rosane M. Peralta. 2017. “Liquid Nitrogen Pretreatment of Eucalyptus Sawdust and Rice Hull for Enhanced Enzymatic Saccharification.” *Bioresource Technology* 224: 648–55. https://doi.org/10.1016/j.biortech.2016.11.099.

Chen, Zhihua, Quanjie Zhu, Xun Wang, Bo Xiao, and Shiming Liu. 2015. “Pyrolysis Behaviors and Kinetic Studies on Eucalyptus Residues Using Thermogravimetric Analysis.” *Energy Conversion and Management* 105: 251–59. https://doi.org/10.1016/j.enconman.2015.07.077.

Chen, Zhiwen, Mingfeng Wang, Enchen Jiang, Donghai Wang, Ke Zhang, Yongzhi Ren, and Yang Jiang. 2018. “Pyrolysis of Torrefied Biomass.” *Trends in Biotechnology*, 1–12. https://doi.org/10.1016/j.tibtech.2018.07.005.

Coldebella, Rodrigo, Bruna Mohr Giesbrecht, Angelo Fernando de Oliveira Saccol, Marina Gentil, and Cristiane Pedrazzi. 2018. “Propriedades Físicas e Químicas Da Madeira de Maclura Tinctoria (L.) D. Don Ex Steud.” *Revista Ciência Da Madeira - RCM* 9 (1): 54–61. https://doi.org/10.12953/2177-6830/rcm.v9n1p54-61.

Crespo, Yasiel Arteaga, Reinier Abreu Naranjo, Yudel García Quitana, Caio Glauco Sanchez, and Elisabete Maria Saraiva Sanchez. 2017. “Optimisation and Characterisation of Bio-Oil Produced by Acacia Mangium Willd Wood Pyrolysis.” *Wood Science and Technology* 51 (5): 1155–71. https://doi.org/10.1007/s00226-017-0913-x.

Davies, R. M., and O. A. Davies. 2013. “Physical and Combustion Characteristics of Briquettes Made from Water Hyacinth and Phytoplankton Scum as Binder.” *Journal of Combustion* 2013. https://doi.org/10.1155/2013/549894.

Demirbas, Ayhan. 1997. “Calculation of Higher Heating Values of Biomass Fuels.” *Fuel* 76 (5): 431–34. https://doi.org/10.1080/15567036.2015.1115924.

Domingues, Rimena R., Paulo F. Trugilho, Carlos A. Silva, Isabel Cristina N.A. De Melo, Leónidas C.A. Melo, Zuy M. Magriotis, and Miguel A. Sánchez-Monedero. 2017. “Properties of Biochar Derived from Wood and High-Nutrient Biomasses with the Aim of Agronomic and Environmental Benefits.” *PLoS ONE* 12 (5): 1–19. https://doi.org/10.1371/journal.pone.0176884.

Figueredo, Natália Aragão de, Liovando Marciano da Costa, Leônidas Carrijo Azevedo Melo, Evair Antônio Siebeneichlerd, and Jairo Tronto. 2017. “Characterization of Biochars from Different Sources and Evaluation of Release of Nutrients and Contaminants.” *Revista Ciencia Agronomica* 48 (3): 395–403. https://doi.org/10.5935/1806-6690.20170046.

Florentino-Madiedo, L., E. Díaz-Faes, R. García, and C. Barriocanal. 2018. “Influence of Binder Type on Greenhouse Gases and PAHs from the Pyrolysis of Biomass Briquettes.” *Fuel Processing Technology* 171 (September 2017): 330–38. https://doi.org/10.1016/j.fuproc.2017.11.029.

Fu, Peng, Song Hu, Jun Xiang, Lushi Sun, Sheng Su, and Jing Wang. 2012. “Evaluation of the Porous Structure Development of Chars from Pyrolysis of Rice Straw: Effects of Pyrolysis Temperature and Heating Rate.” *Journal of Analytical and Applied Pyrolysis* 98: 177–83. https://doi.org/10.1016/j.jaap.2012.08.005.

Gebresas, Alula, Haftom Asmelash, Hadush Berhe, and Tsegay Tesfay. 2015.

"Briquetting of Charcoal from Sesame Stalk." *Journal of Energy* 2015: 1–6. https://doi.org/10.1155/2015/757284.

Gominho, Jorge, Ana Lourenc, Isabel Miranda, and Helena Pereira. 2012. "Chemical and Fuel Properties of Stumps Biomass from Eucalyptus Globulus Plantations." *Industrial Crops and Products* 39: 12–16. https://doi.org/10.1016/j.indcrop.2012.01.026.

Guo, Zhenkun, Jianjun Wu, Yixin Zhang, Feng Wang, Yang Guo, Kening Chen, and Hu Liu. 2020. "Characteristics of Biomass Charcoal Briquettes and Pollutant Emission Reduction for Sulfur and Nitrogen during Combustion." *Fuel* 272 (March): 117632. https://doi.org/10.1016/j.fuel.2020.117632.

He, Xinyan, Zhaoxia Liu, Wenjuan Niu, Li Yang, Tan Zhou, Di Qin, Zhiyou Niu, and Qiaoxia Yuan. 2018. "Effects of Pyrolysis Temperature on the Physicochemical Properties of Gas and Biochar Obtained from Pyrolysis of Crop Residues." *Energy* 143: 746–56. https://doi.org/10.1016/j.energy.2017.11.062.

Ikelle, Ikelle Issie, and Ogah Sule Philip Ivoms. 2014. "Determination of the Heating Ability of Coal and Corn Cob Briquettes." *IOSR Journal of Applied Chemistry* 7 (2): 77–82. https://doi.org/10.9790/5736-07217782.

Jesus, Márcia Silva de, Angélica de Cássia Oliveira Carneiro, Clara Lisseth Mendoza Martinez, Benedito Rocha Vital, Antônio Policarpo Souza Carneiro, and Maíra Reis de Assis. 2019. "Thermal Decomposition Fundamentals in Large-Diameter Wooden Logs during Slow Pyrolysis." *Wood Science and Technology* 53 (6): 1353–72. https://doi.org/10.1007/s00226-019-01133-9.

Jesús Rangel, M., Marina Hornus, Fernando E. Felissia, and María C. Area. 2016. "Hydrothermal Treatment of Eucalyptus Sawdust for a Forest Biorefinery." *Cellulose Chemistry and Technology* 50 (5–6): 521–28.

Jibril, Baba, Omar Houache, Rashid Al-Maamari, and Badir Al-Rashidi. 2008. "Effects of H3PO4 and KOH in Carbonization of Lignocellulosic Material." *Journal of Analytical and Applied Pyrolysis* 83 (2): 151–56. https://doi.org/10.1016/j.jaap.2008.07.003.

Kaliyan, Nalladurai, and R. Vance Morey. 2009. "Factors Affecting Strength and Durability of Densified Biomass Products." *Biomass and Bioenergy* 33 (3): 337–59. https://doi.org/10.1016/j.biombioe.2008.08.005.

Kan, Tao, Vladimir Strezov, and Tim J. Evans. 2016. "Lignocellulosic Biomass Pyrolysis: A Review of Product Properties and Effects of Pyrolysis Parameters." *Renewable and Sustainable Energy Reviews* 57: 1126–40. https://doi.org/10.1016/j.rser.2015.12.185.

Katyal, Surinder, Kelly Thambimuthu, and Marjorie Valix. 2003. "Carbonisation of Bagasse in a Fixed Bed Reactor: Influence of Process Variables on Char Yield and Characteristics." *Renewable Energy* 28 (5): 713–25. https://doi.org/10.1016/S0960-1481(02)00112-X.

Kpalo, Sunday Yusuf, Mohamad Faiz Zainuddin, Latifah Abd Manaf, and Ahmad Muhaimin Roslan. 2020. “Production and Characterization of Hybrid Briquettes from Corncobs and Oil Palm Trunk Bark under a Low Pressure Densification Technique.” *Sustainability (Switzerland)* 12 (6). https://doi.org/10.3390/su12062468.

Ku Ahmad, Kz, Khaziq Sazali, and A. A. Kamarolzaman. 2018. “Characterization of Fuel Briquettes from Banana Tree Waste.” *Materials Today: Proceedings* 5 (10): 21744–52. https://doi.org/10.1016/j.matpr.2018.07.027.

Kumar, Abhishek, and Tanushree Bhattacharya. 2020. *Biochar: A Sustainable Solution*. *Environment, Development and Sustainability*. Springer Netherlands. https://doi.org/10.1007/s10668-020-00970-0.

Kunii, Daizo, and Octave Levenspiel. 1991. *Fluidization Engineering*. 2nd ed. Butterworth-Heinemann. https://doi.org/https://doi.org/10.1016/C2009-0-24190-0.

Kwapinski, W., C. M.P. Byrne, E. Kryachko, P. Wolfram, C. Adley, J. J. Leahy, E. H. Novotny, and M. H.B. Hayes. 2010. “Biochar from Biomass and Waste.” *Waste and Biomass Valorization* 1 (2): 177–89. https://doi.org/10.1007/s12649-010-9024-8.

Manyuchi, M. M., C. Mbohwa, and E. Muzenda. 2018. “Value Addition of Coal Fines and Sawdust to Briquettes Using Molasses as a Binder.” *South African Journal of Chemical Engineering* 26 (September): 70–73. https://doi.org/10.1016/j.sajce.2018.09.004.

Missau, Juliano, Daniel Assumpcção Bertuol, and Eduardo Hiromitsu Tanabe. 2020. “Development of a Nanostructured Filter for Pyrolysis Wax Purification: Effects of Particulate Filter Aids.” *Particuology*. https://doi.org/10.1016/j.snb.2019.127065.

Mitchual, Stephen J., Kwasi Frimpong-Mensah, and Nicholas A. Darkwa. 2013. “Effect of Species, Particle Size and Compacting Pressure on Relaxed Density and Compressive Strength of Fuel Briquettes.” *International Journal of Energy and Environmental Engineering* 4 (1): 1–6. https://doi.org/10.1186/2251-6832-4-30.

Muazu, Rukayya Ibrahim, and Julia A. Stegemann. 2017. “Biosolids and Microalgae as Alternative Binders for Biomass Fuel Briquetting.” *Fuel* 194: 339–47. https://doi.org/10.1016/j.fuel.2017.01.019.

Okot, David K, Paul E Bilsborrow, and Anh N Phan. 2019. “Briquetting Characteristics of Bean Straw-Maize Cob Blend.” *Biomass and Bioenergy* 126 (May): 150–58. https://doi.org/10.1016/j.biombioe.2019.05.009.

Olugbade, Temitope, Oluwole Ojo, and Tiamiyu Mohammed. 2019. “Influence of Binders on Combustion Properties of Biomass Briquettes: A Recent Review.” *Bioenergy Research*, 241–59. https://doi.org/10.1007/s12155-019-09973-w.

Park, Sang Woo, and Cheol Hyeon Jang. 2012. “Effects of Pyrolysis Temperature on

Changes in Fuel Characteristics of Biomass Char." *Energy* 39 (1): 187–95. https://doi.org/10.1016/j.energy.2012.01.031.

Poletto, Matheus, Juliane Dettenborn, Vinícios Pistor, Mara Zeni, and Ademir José Zattera. 2010. "Materials Produced from Plant Biomass.Part I: Evaluation of Thermal Stability and Pyrolysis of Wood." *Materials Research* 13 (3): 375–79. https://doi.org/10.1590/S1516-14392010000300016.

Rafiq, Muhammad Khalid, Robert Thomas Bachmann, Muhammad Tariq Rafiq, Zhanhuan Shang, Stephen Joseph, and Ruijun Long Long. 2016. "Influence of Pyrolysis Temperature on Physico-Chemical Properties of Corn Stover (Zea Mays l.) Biochar and Feasibility for Carbon Capture and Energy Balance." *PLoS ONE* 11 (6): 1–17. https://doi.org/10.1371/journal.pone.0156894.

Rahaman, Sheikh Aminur, and P. Abdul Salam. 2017. "Characterization of Cold Densified Rice Straw Briquettes and the Potential Use of Sawdust as Binder." *Fuel Processing Technology* 158: 9–19. https://doi.org/10.1016/j.fuproc.2016.12.008.

Rahman, D R S Shofiur, Kelly Hawboldt, Robert Helleur, and Stephanie Macquarrie. 2018. "Pyrolysis of Waste Plastic Fish Bags (Polyethylene and Polypropylene) to Useable Fuel Oil." *Harris Centre - MMSB WASTE MANAGEMENT RESEARCH APPLIED RESEARCH FUND*. https://www.mun.ca/harriscentre/reports/HAWBOLDT_Waste_16-17.pdf.

Saleem, Junaid, Muhammad Adil, and Gordon Mckay. 2018. "Oil Sorbents from Plastic Wastes and Polymers : A Review." *Journal of Hazardous Materials* 341: 424–37. https://doi.org/10.1016/j.jhazmat.2017.07.072.

Sallem-Idrissi, Naïma, Caroline Vanderghem, Tiphanie Pacary, Aurore Richel, Damien P. Debecker, Jacques Devaux, and Michel Sclavons. 2016. "Lignin Degradation and Stability: Volatile Organic Compounds (VOCs) Analysis throughout Processing." *Polymer Degradation and Stability* 130: 30–37. https://doi.org/10.1016/j.polymdegradstab.2016.05.028.

Sette, Carlos Roberto, Pedro Augusto Fonseca Lima, Domingos Manuel Mendes Lopes, Pedro Vilela Gondim Barbosa, Ademilson Coneglian, and Rogério De Araújo Almeida. 2017. "Characterization of Biomass, Charcoal and Briquette of Phyllostachys Aurea Carr. Ex A. & C. Rivière." *Scientia Forestalis/Forest Sciences* 45 (116): 619–28. https://doi.org/10.18671/scifor.v45n116.03.

Simonelli, George, Guilherme Souza Rodrigues, Leonardo José Helmer, Mário César Moro Devens, and Paulo Ricardo Fraga Fonseca. 2017. "Produção De Briquetes Para Queima Utilizando Finos Da Produção De Carvão Vegetal E Glicerina." *Holos* 1: 325. https://doi.org/10.15628/holos.2017.4559.

Soares, L.S.a, V.A.S.a Moris, F.M.b c Yamaji, and J.M.F.a c Paiva. 2015. "Use of Waste Coffee Grounds and Sawdust in Briquettes Molding and Evaluation of Properties." *Revista Materia* 20 (2): 550–60. https://doi.org/10.1590/S1517-707620150002.0055.

Sun, Junna, Fuhong He, Yinghua Pan, and Zhenhua Zhang. 2017. “Effects of Pyrolysis Temperature and Residence Time on Physicochemical Properties of Different Biochar Types.” *Acta Agriculturae Scandinavica Section B: Soil and Plant Science* 67 (1): 12–22. https://doi.org/10.1080/09064710.2016.1214745.

Tai, Hua Shan, and Chun Yu Chen. 2016. “Kinetic Study of Copyrolysis of Waste Polyethylene Terephthalate, Polylactic Acid, and Rice Straw.” *Environmental Engineering Science* 33 (9): 671–80. https://doi.org/10.1089/ees.2015.0522.

Tembe, ET, PO Otache, and DO Ekhuemelo. 2014. “Density, Shatter Index, and Combustion Properties of Briquettes Produced from Groundnut Shells, Rice Husks and Saw Dust of *Daniellia Oliveri*.” *Journal of Applied Biosciences* 82 (1): 7372. https://doi.org/10.4314/jab.v82i1.7.

Thabuot, Mallika, Thanchanok Pagketanang, Kasidet Panyacharoen, Pisit Mongkut, and Prasong Wongwicha. 2015. “Effect of Applied Pressure and Binder Proportion on the Fuel Properties of Holey Bio-Briquettes.” *Energy Procedia* 79: 890–95. https://doi.org/10.1016/j.egypro.2015.11.583.

Thomas, Paul, Nelson P. Rumjit, Chin W. Lai, Mohd R.B. Johan, and Manickam P. Saravanakumar. 2020. “Polymer-Recycling of Bulk Plastics.” *Encyclopedia of Renewable and Sustainable Materials*, 432–54. https://doi.org/10.1016/b978-0-12-803581-8.10765-9.

Unpinit, Tanakorn, Thanaporn Poblarp, Narongrit Sailoon, Prasong Wongwicha, and Mallika Thabuot. 2015. *Fuel Properties of Bio-Pellets Produced from Selected Materials under Various Compacting Pressure*. *Energy Procedia*. Vol. 79. Elsevier B.V. https://doi.org/10.1016/j.egypro.2015.11.551.

Uzun, Başak Burcu, Ayşe Eren Pütün, and Ersan Pütün. 2007. “Composition of Products Obtained via Fast Pyrolysis of Olive-Oil Residue: Effect of Pyrolysis Temperature.” *Journal of Analytical and Applied Pyrolysis* 79 (1-2 SPEC. ISS.): 147–53. https://doi.org/10.1016/j.jaap.2006.12.005.

Wang, Shurong, Gongxin Dai, Haiping Yang, and Zhongyang Luo. 2017. “Lignocellulosic Biomass Pyrolysis Mechanism : A State-of-the-Art Review.” *Progress in Energy and Combustion Science* 62: 33–86. https://doi.org/10.1016/j.pecs.2017.05.004.

Williams, Paul T. 2020. “Hydrogen and Carbon Nanotubes from Pyrolysis-Catalysis of Waste Plastics: A Review.” *Waste and Biomass Valorization*, no. 0123456789. https://doi.org/10.1007/s12649-020-01054-w.

Wu, Shunyan, Shouyu Zhang, Caiwei Wang, Chen Mu, and Xiaohe Huang. 2018. “High-Strength Charcoal Briquette Preparation from Hydrothermal Pretreated Biomass Wastes.” *Fuel Processing Technology* 171 (July 2017): 293–300. https://doi.org/10.1016/j.fuproc.2017.11.025.

Xiao, Xiaodi, Chunming Li, Ping Ya, Jin He, Yansheng He, and X Tony Bi. 2015. “Industrial Experiments of Biomass Briquettes as Fuels for Bulk Curing Barns Industrial Experiments of Biomass Briquettes as Fuels for Bulk Curing Barns.”

International Journal of Green Energy 12: 1061–65. https://doi.org/10.1080/15435075.2014.891119.

Yorgun, Sait, and Derya Yildiz. 2015. “Slow Pyrolysis of Paulownia Wood: Effects of Pyrolysis Parameters on Product Yields and Bio-Oil Characterization.” *Journal of Analytical and Applied Pyrolysis* 114: 68–78. https://doi.org/10.1016/j.jaap.2015.05.003.

Zaiton, Samdin, Mohd Razali Sheriza, Rosman Ainishifaa, Khaw Alfred, and Kamaruddin Norfaryanti. 2020. “Eucalyptus in Malaysia: Review on Environmental Impacts.” *Journal of Landscape Ecology* 13 (2): 79–94. https://doi.org/10.2478/jlecol-2020-0011.

Zepeda-cepeda, Christian Osvaldo, Rodolfo Goche-t, Celina Palacios-mendoza, Oswaldo Moreno-anguiano, N Daniel, and Maginot Ngangyo Heya. 2021. “Effect of Sawdust Particle Size on Physical , Mechanical , and Energetic Properties of Pinus Durangensis Briquettes.” *Applied Sciences (Switzerland)* 11. https://doi.org/https://doi.org/ 10.3390/app11093805.

Zhao, Suwei, and Dongke Zhang. 2014. “Supercritical CO2 Extraction of Eucalyptus Leaves Oil and Comparison with Soxhlet Extraction and Hydro-Distillation Methods.” *Separation and Purification Technology* 133: 443–51. https://doi.org/10.1016/j.seppur.2014.07.018.

4 ARTIGO 2: HIGHLY EFFICIENT ADSORBENT FOR REMOVAL OF CRYSTAL VIOLET DYE FROM AQUEOUS SOLUTION BY CAAL/LDH SUPPORTED ON BIOCHAR

O artigo a seguir foi publicado na revista APPLIED CLAY SCIENCE (ISSN: 0169-1317). DOI: 10.1016/j.clay.2021.106297

Highly efficient adsorbent for removal of Crystal Violet Dye from Aqueous Solution by CaAl/LDH supported on Biochar

Juliano Missau[a*], Daniel Assumpção Bertuol[a], Eduardo Hiromitsu Tanabe[a]

[a] Environmental Processes Laboratory (LAPAM), Chemical Engineering Department, Federal University of Santa Maria – UFSM, Avenida Roraima 1000, 97105-900, Santa Maria, RS, Brazil

Abstract

This work presents the development of a novel highly efficient adsorbent produced from CaAl/LDH supported on biochar chemically activated with phosphoric acid [CaAl/Biochar(H_3PO_4)] in order to maintain a great adsorbent capacity and prevent LDH disintegration. Its adsorptive efficiency was compared to an adsorbent formed from CaAl/LDH supported on untreated biochar (CaAl/Biochar). Biochar was produced from the pyrolysis of *Eucalyptus saligna* sawdust. The adsorbents were applied to remove crystal violet (CV) dye from aqueous solutions in a batch adsorption process. The adsorbents were characterized by Fourier transform infrared spectroscopy (FT-IR), X-ray diffraction (XRD), Brunauer–Emmett–Teller (BET) and scanning electron microscopy (SEM). Adsorption kinetics, isotherms and thermodynamics were evaluated. The characterization results suggested that the CaAl/LDH was successfully synthesized and supported on biochar. The results indicate that pH 8 was more suitable for CV dye adsorption, with an adsorptive capacity over 101 mg g^{-1} for CaAl/Biochar(H_3PO_4). Furthermore, adsorption experimental data fitted well with the pseudo-second order kinetics model and the Freundlich isotherm model. It was

obtained a maximum adsorption capacity of 496.55 $mg \cdot g^{-1}$ at 50°C. For CaAl/Biochar(H_3PO_4), the thermodynamic results revealed a favorable, spontaneous and endothermic process. In addition, the results showed that the pre-treatment of the biochar with phosphoric acid maintained 71% of the initial adsorptive capacity even after four cycles of reuse. Therefore, CaAl/Biochar(H_3PO_4) is a sustainable adsorbent with high performance for CV contaminated wastewater treatment and groundwater remediation.

Keywords
Water treatment, Crystal violet dye, Biochar, CaAl-layered double hydroxides, Adsorption

4.1 INTRODUCTION

Over time providing good quality water worldwide has become a challenging problem. Due to exponential population growth, irrigation practices and rapid industrialization, contamination of water resources by various chemical and biological agents is increasing at a threatening rate (Puri and Sumana, 2018). Among the various water pollutants, the effluents released by the dyeing industries stands out. These effluents are very colorful and can be very toxic to aquatic life in the receiving waters, because even solutions containing dyes in low concentrations promote changes in the color of the water, decreasing the penetration of sunlight, which can end up interfering in photosynthesis (Panic and Velickovic, 2014).

In addition to the generation of environmental problems, dyes are also associated with risks to human health (Burakov et al., 2018). Among the dyes used industrially, crystal violet (CV) is considered one of the most dangerous dyes, because it is mutagenic, carcinogenic, non-biodegradable and can persist in the environment for a long time (Gao et al., 2016; Shoukat et al., 2017). CV is a common type of dye widely used by the paper and textile industry, and is also used as a biological dye and dermatological agent in human and veterinary medicine (Zhang et al., 2014). Therefore, the removal of CV dyes before discharge becomes a major research subject.

Different water decolorization approaches for dyes removal from industrial effluents have been developed and employed in the last few years, including solvent

extraction, chemical precipitation, photocatalysis, nanofiltration, ion exchange, adsorption and electrochemical treatment (Jana et al., 2010; L. Chen et al., 2018; Liu et al., 2018; Peres et al., 2018). However, the adsorption operation presents advantages in terms of cost, flexibility and simplicity (Dotto et al., 2015).

In the adsorption process, the selection of a suitable adsorbent material is the main challenge. A wide range of adsorbents including zeolites, agriculture wastes and biochar already have been reported for the removal of dyes (Brião et al., 2017; Chakraborty et al., 2011; Loulidi et al., 2020; Yek et al., 2020). Nevertheless, compared to other materials, the use of biochar to remove pollutants from aqueous solutions also allows the achievement of five complementary objectives, such as: wastewater treatment, groundwater remediation, waste management, carbon sequestration and production of energy (X. Tan et al., 2016). However, pristine biochar, which is a carbon-rich material produced by biomass pyrolysis in an inert atmosphere, may present limited capacity to adsorb pollutants, due to several factors, including its physical and chemical properties, that vary according to the raw material, technologies and conditions of pyrolysis (Angin and Şensöz, 2014; Tan et al., 2015). Therefore, the functionalization and modification of the biochar as a composite material is a first order concern.

The addition of different components to the pristine biochar can improve the functionality of its surface, which in turn improves the adsorption performance for a wide range of contaminants (Xiang et al., 2020). In this way, the incorporation of double layered hydroxides (LDHs) supported on biochar have received a great prominence as a potential adsorbent for water contaminants removal.

LDH are classified as a clay consisting of stacked of positive layers separated by interlamellar region constituted of anions and water. Its general formula is $[M^{+2}_{1-x}M^{+3}_{x}(OH)_2]^{+x}\ A^{-n}_{x/n}\cdot mH_2O$, where M^{+2} is a divalent metal, M^{+3} a trivalent metal and A^{-n}, an anion n valent; usually where the ratio between M^{+2}/M^{+3} is $0.1 \leq x \leq 0.5$ molecules (Yan et al., 2016). These materials have the ability to incorporate negatively charged species in their interlayer region to neutralize the positive charges of the lamellae through the ion exchange mechanism. Furthermore, LDHs have low cost of raw material, easy synthesis and high adsorption capacity (Guo et al., 2017). However, if LDHs are used directly as adsorbents they can be exfoliated during the process. Therefore, it is more effective to use it in the form of composites with recalcitrant materials, such as biochar (Meili et al., 2019).

Several studies have already reported the use of LDH supported in biochar to remove contaminants from aqueous solutions through the adsorption process (Yu and Zhu, 2018; Jia et al., 2019; X. fei Tan et al., 2016). However, it was observed, through the regeneration experiments of the adsorbent, a reduction in its adsorptive capacity, due to the disintegration of LDH. Nevertheless, the adsorption efficiency of the composite was better favored by the presence of the biochar. In this way, a pre-treatment of the carbon rich material can be performed in order to maintain the high adsorption capacity for more recovery cycles. Furthermore, to the best of our knowledge, no available research has been conducted to investigate the adsorption of the crystal violet dye in CaAl/LDH supported on pristine and previously treated biochar.

The present study aimed to evaluate the adsorption efficiency of the crystal violet dye by CaAl/LDH supported on pristine biochar and chemically activated biochar with phosphoric acid. The synthesized adsorbents were characterized using Fourier transform infrared spectroscopy (FT-IR), X-ray diffraction (XRD), scanning electron microscopy (SEM), and Brunauer–Emmett–Teller (BET) measurement techniques to examine the surface and structure properties after the inclusion of CaAL/LDH layers into both biochar. In the adsorption study, the effects of pH (2.0 to 10.0) were evaluated. Kinetic curves were studied using pseudo−first order (PFO) and pseudo−second order (PSO) models. Isotherms were constructed at different temperatures (30–50ºC) and the curves were fitted with Freundlich and Langmuir models. The standard values of Gibbs free energy (ΔG^0), enthalpy (ΔH^0) and entropy (ΔS^0) changes were estimated. In addition, the effect of ionic strength and reusable property of the CaAl/LDH supported on chemically activated biochar with phosphoric acid were also studied.

4.2 MATERIALS AND METHODS

4.2.1 Materials

Eucalyptus saligna sawdust was kindly donated by the company Madeireira Haas (Venâncio Aires, Rio Grande do Sul, Brazil). For the chemical activation of eucalypt sawdust was used phosphoric acid (H_3PO_4 - 85%, Mw = 98.00, Neon/Brazil). For the synthesis of CaAl-LDH/biochar(H_3PO_4) and CaAl-LDH/biochar the following analytical reagents grade were used: calcium chloride dihydrate ($CaCl_2.2H_2O$, Mw =

147.01, Dinâmica/Brazil), aluminum chloride hexahydrate ($AlCl_2.6H_2O$, Mw = 241.43, Alphatec/Brazil) and sodium hydroxide (NaOH, Mw = 58.44, Dinâmica/Brazil). The adsorbate solutions were produced in various concentrations using the crystal violet dye ($C_{25}H_{30}N_3Cl$) (Neon/Brazil).

4.2.2 Materials characterization

The characteristics of the produced materials and pure biochar were assessed by the following techniques: X–ray diffraction (XRD), Fourier Transform Infrared Spectroscopy (FT–IR), scanning electron microscopy (SEM) and nitrogen adsorption isotherms by the Brunauer, Emmet and Teller (BET). The samples crystallinity was verified through X–ray powder diffractometry (XRD) (Rigaku, Miniflex 300, Japan), with Ni–filtered Cu Ka radiation (λ = 1.54051 Å, 30 kV, 10 mA), using 2θ = 5–100°. Fourier transform infrared spectroscopy (FT–IR) (Shimadzu, Prestige 21, Japan) was used to identify the functional groups of the samples in the range of 400–4400 cm^{-1}. The SEM images of the samples were obtained on the VEGA-3 SBU equipment (TESCAN, Czech Republic) in an acceleration of 10 kV with gold coating treatment. The surface area was determined by the application of the BET method, using N_2 adsorption isotherms at 77 K (New Win, Quantachrome, USA).

4.2.3 Preparation of biochar derived from eucalypt sawdust

Firstly, eucalypt sawdust was washed with water to remove the impurities and dried at 105 °C for 24 h in an oven (Model 5, Brasdonto, Brazil). The dried sawdust was sieved into particle size smaller than 500 μm (Hsu et al., 2014). For the non-activated biochar production, the dried and sieved sawdust was pyrolyzed in a stainless-steel reactor placed in a tube furnace (Sanchis/Brazil) at 450ºC, for 30 min under N_2 atmosphere with a heating rate of 15 °C min^{-1}. The pyrolysis parameters were established based on preliminary tests taking into account the thermogravimetric curve of the raw material used in this study.

For the chemical activated biochar production, the sawdust was immersed in 40% phosphoric acid for 12 h with mass ratio of 2.5 of phosphoric acid to sawdust. The mixture was then dried at 80°C for 8 h, and thermally activated by pyrolysis process to 400°C for 3 h under a N_2 atmosphere with a heating rate of 10 °C min^{-1}. After activation,

the biochar was thoroughly washed with deionized water until neutral pH was obtained, and then dried at 120°C for 6 h (Han et al., 2020). The production of both biochar (non-activated and chemically activated) was performed in the same pyrolysis apparatus, as it can be seen from Figure 1.

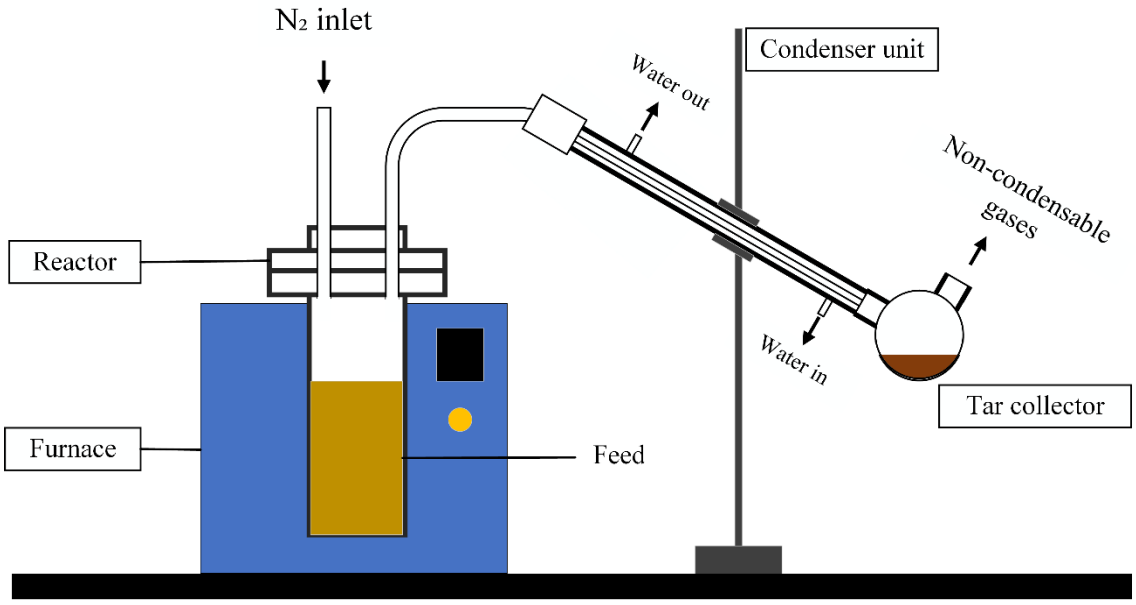

Figure 1 - Pyrolysis apparatus.

4.2.4 Synthesis of CaAl-LDH/biochar composites

CaAl-LDH/biochar composites were synthesized using a co-precipitation method which was adopted from Hoxha et al. (2020) and Meili et al. (2019). To produce the composites with proportion of 3 mol of Ca and 1 mol of Al (3:1), in a 50 mL beaker were weighed 6.61 g of calcium chloride and 3.62 g of aluminum chloride and then 20 mL of ultrapure water (resistivity of 18.25 MΩ·cm^{-1}) was added (Huang et al., 2019). The mixture was under constant stirring for 30 min until complete dissolution of the chemicals. After dissolution, this mixture was transferred to another beaker containing 1 g of the biochar (non-activated and chemically activated), under constant stirring. A sodium hydroxide solution (3 M) was dripped with a burette until the solution reached pH 12. After that, the solution was stirred for a further 2 h. Finally, the formed precipitate was filtered, washed with ultrapure water until neutral pH was obtained, then dried for 16 h at 60ºC. When leaving the oven, the material was macerated and sifted until reaching an average diameter < 0.50 mm.

4.2.5 Adsorption experiments

The adsorption of crystal violet (CV) dye was carried out in a batch process using a Shaker Incubator (Tecnal – TE 4200, Brazil). The pH effect, the equilibrium time through the kinetics experiments and the influence of temperature and concentration on the adsorption isotherm were evaluated. The adsorbent dosage (0.025 g) was fixed based in preliminary tests and in order to avoid operational costs (Puri and Sumana, 2018). CV (characteristics given in Table) dye was used as the adsorbate. A stock solution of CV (0.5 g L^{-1}) was first prepared by dissolving a known quantity in ultrapure water to simulate the wastewater and polluted groundwater. The stock solution was finally diluted to obtain the desired concentration.

Table 1 - Chemical properties and characteristics of crystal violet.

Generic name	Crystal violet
Chemical formula	$C_{25}H_{30}N_3Cl$
Molecular weight (g/mol)	407.98
Type of dye	Cationic
λ max (nm)	582
Chemical structure	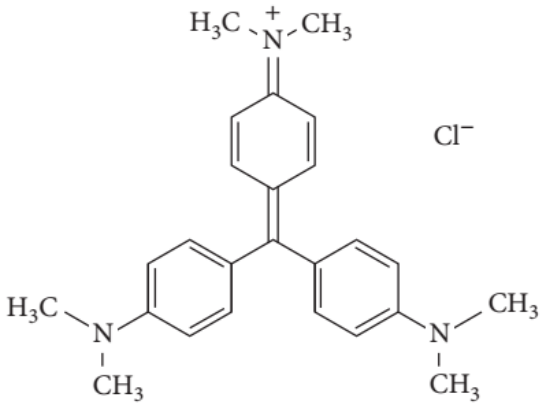

4.2.5.1 pH influence

The influence of pH on the CV dye adsorption was investigated adjusting the pH of the solutions for the values: 2, 4, 6, 8 and 10, using solutions of NaOH and HNO_3

(Brião et al., 2017). A volume of 50 ml of each CV solutions (50 mg L^{-1}) with pH adjusted were placed in a 125 mL Erlenmeyer flask containing 0.025 g of adsorbent. The dye solutions with adsorbents were taken into the incubator and shaken at 140 rpm for 4 h at 30°C. After this time, the samples were filtered using a filter paper and the absorbance was determined in a UV–Visible spectrophotometer (Shimadzu, UVmini-1240, Japan) at wavelength 582 nm. The adsorption capacity of the sorbent material (q_t) in mg g^{-1} was determined by Eq. 1. The point of zero charge (pH_{pzc})of the adsorbents were assessed according to Loulidi et al. (2020) and Ayaliew Werkneh (2015). The values of pH_{pzc} of an adsorbent are determined from the points where the initial pH of the solution equals the final pH. Therefore, it was assessed from the graph of final pH versus initial pH. The quantity adsorbed at equilibrium (q_e) was calculated by Eq. 2 (Chakraborty et al., 2011)

$$q_t = \frac{(Co - Ct).V}{W} \quad (1)$$

$$q_e = \frac{(Co - Ce).V}{W} \quad (2)$$

where C_0, C_e and C_t are the concentrations in mg L^{-1} of the solution at the beginning, at equilibrium and at time t, respectively. *W* is the mass in g of adsorbent used and *V* is the volume of the solution in liters.

4.2.5.2 Kinects studies

The adsorption kinetics curves of the CV dye in the sorbent samples were constructed by mixing 0.025 g of adsorbent in 50 mL of dye aqueous solution at pH 8, 30°C, and 50 mg L^{-1} of initial concentration. The mixture was placed in the incubator at 140 rpm for a contact time ranging from 0 to 240 min. The samples were filtered to ensure that no solid was present and the absorbance read. The kinetic data of dye adsorption were tested with pseudo first order (PFO) (Lagergren, 1898) and pseudo second order (PSO) (Ho and McKay, 1999) models, expressed in Eqs. 3 and 4.

$$q_t = q_1(1 - e^{-k_1.t}) \quad (3)$$

$$q_t = \frac{k_2.t.q_2^2}{(1 + k_2.t.q_2)} \quad (4)$$

where k_1 and k_2 are the rate constants of pseudo–first order (in min^{-1}) and pseudo–second order (in g $mg^{-1}.h^{-1}$), respectively. q_1 and q_2 are the theoretical values for the adsorption capacity (in mg g^{-1}).

4.2.5.3 Equilibrium studies

The adsorption isotherms were determined using 0.025 g of the composites mixed in 50 mL of dye solutions (pH 8) at different concentrations (50, 100, 250 and 500 mg L^{-1}) and at different temperatures (30, 40, and 50°C) with constant speed of 140 rpm for 2 h (Meili et al., 2019). Then, the samples were filtered and the absorbance was determined.

Equilibrium isotherm curves were fitted with Langmuir and Freundlich models. The Langmuir model is the most utilized, assuming a monolayer adsorption onto a homogeneous surface where the binding sites have equal affinity and energy (Langmuir, 1918). The Langmuir model is represented by Eq 5:

$$q_e = \frac{q_m k_L C_e}{1 + k_L C_e} \quad (5)$$

where, q_m is the maximum adsorption capacity (mg g^{-1}), C_e is the concentration (mg L^{-1}) of the solution at the at equilibrium and k_L is the Langmuir constant (L mg^{-1}).

The essential characteristic of the Langmuir isotherm can be expressed in terms of a dimensionless constant called equilibrium parameter (Hall et al., 1966) represented by Eq 6:

$$R_L = \frac{1}{1 + (k_L C_o)} \quad (6)$$

where k_L is the Langmuir constant and C_0 is the highest initial dye concentration (mg L^{-1}). The value of R_L indicates the type of isotherm to be either favorable ($0 < R_L < 1$), linear ($R_L = 1$), unfavorable ($R_L > 1$), or irreversible ($R_L = 0$).

The Freundlich model assumes that the adsorption occurs on a heterogeneous surface and that the amount of adsorbate adsorbed increase infinitely with the concentration (Freundlich, 1906). The Freundlich model is represented by Eq 7.

$$q_e = k_F C_e^{1/nF} \quad (7)$$

where, k_F is the Freundlich constant (mg g^{-1}) (mg L^{-1})$^{-1/nF}$, C_e is the concentration (mg L^{-1}) of the solution at the at equilibrium and 1/nF is the heterogeneity factor.

4.2.5.4 Thermodynamics parameters estimation

In order to identify the spontaneity, feasibility and organization of adsorbate-adsorbent during the adsorption thermodynamic parameters such as the standard values of Gibbs free energy (ΔG^0, kJ mol^{-1}), enthalpy (ΔH^0, kJ mol^{-1}) and entropy (ΔS^0, kJ mol^{-1} K^{-1}) are estimated. Therefore, these parameters were estimated according to the Eqs. 8 and 9 (Milonjić, 2007; Tran et al., 2017).

$$\Delta G^0 = -RTln(k^0) \quad (8)$$

$$ln(k^0) = \frac{\Delta S^0}{R} - \frac{\Delta H^0}{RT} \quad (9)$$

where, R is the universal constant (kJ mol^{-1} K^{-1}), T is the temperature (K) and kº is the thermodynamic equilibrium constant (dimensionless). For each adsorption system, kº was estimated from the parameters of the best fit equilibrium model.

4.2.6 Modeling and parameters estimation

Kinetic and equilibrium parameters were calculated through nonlinear regression of the experimental data based on the minimization of the least squares function. The calculations were made using the Statistic 9.1 software (Statsoft, USA). The fit quality was measured through determination coefficient (R^2), adjusted

determination coefficient (R^2_{adj}) and average relative error (ARE) (presented in Eq 10) (Peres et al., 2018).

$$ARE = \frac{100}{n}\sum_{i=1}^{n}\left|\frac{q_{i,model} - q_{i,exp}}{q_{i,exp}}\right| \quad (10)$$

where $q_{i,model}$ is each value of q provided by the adjustment, $q_{i,exp}$ is each value of q measured experimentally and n is the number of experimental points.

4.2.7 Salt ionic strength influence

The influence of salt ionic strength on the removal of CV by the adsorbents was studied with the sodium chloride concentration varying from 0 to 0.1 M. It was performed with 0.025 g of the composites mixed in 50 mL of dye solution (pH 8) at concentration of 50 mg L^{-1} and at 30°C with constant speed of 140 rpm for 2 h (X. fei Tan et al., 2016).

4.2.8 Regeneration of used CaAl/Biochar (H_3PO_4)

The durability of the adsorbent after long use was investigated by adsorption regeneration cycles. In the regeneration study, ethanol (CH_3CH_2OH) was used as an eluent, due to its effectiveness in the regeneration of adsorbents saturated with organic compounds. Studies already showed that the solvent weakens the interaction between adsorbent and solid surface (Girish and Murty, 2017; Larasati et al., 2020). Adsorption of the dye from the composite was performed by mixing 0.025 g of the adsorbent in 50 mL of the solution (50 mg L^{-1}) in a 125 mL Erlenmeyer flask under constant stirring at 140 rpm for 2 h at 30ºC. Then, the solution was filtered and the absorbance of the liquid phase was measured. The CV loaded CaAl/Biochar (H_3PO_4) was added in 20 mL of the ethanol and stirred for 2 h at 140 rpm. After this period of time, the sample was again filtered, washed and dried at 60°C for 2 h (Puri and Sumana, 2018). The dried material was used in another adsorption test, which was repeated four times.

4.3 RESULTS AND DISCUSSION

4.3.1 Materials characterization

The XRD patterns in the range of 5–100º of the different adsorbents samples are shown in Figure 2. There was not observed sharp peaks in the XRD pattern of biochar, characterizing the absence of inorganic material in the sample. In this way, the biochar prepared from eucalypt sawdust showed an amorphous structure represented by the broad nature of the peaks (Singh et al., 2016). However, adsorbents chemically activated presented the emergence of reflections in different regions. This cristalinity behavior was attributed to the precursor 40% phosphoric acid. A successful fabrication of the CaAl-LDH structure was confirmed by the presence of the peaks at 12 - 24º, since these peaks were absent in pure biochar. The results are in accordance with the literature (Iqbal et al., 2019; Mohadi et al., 2021).

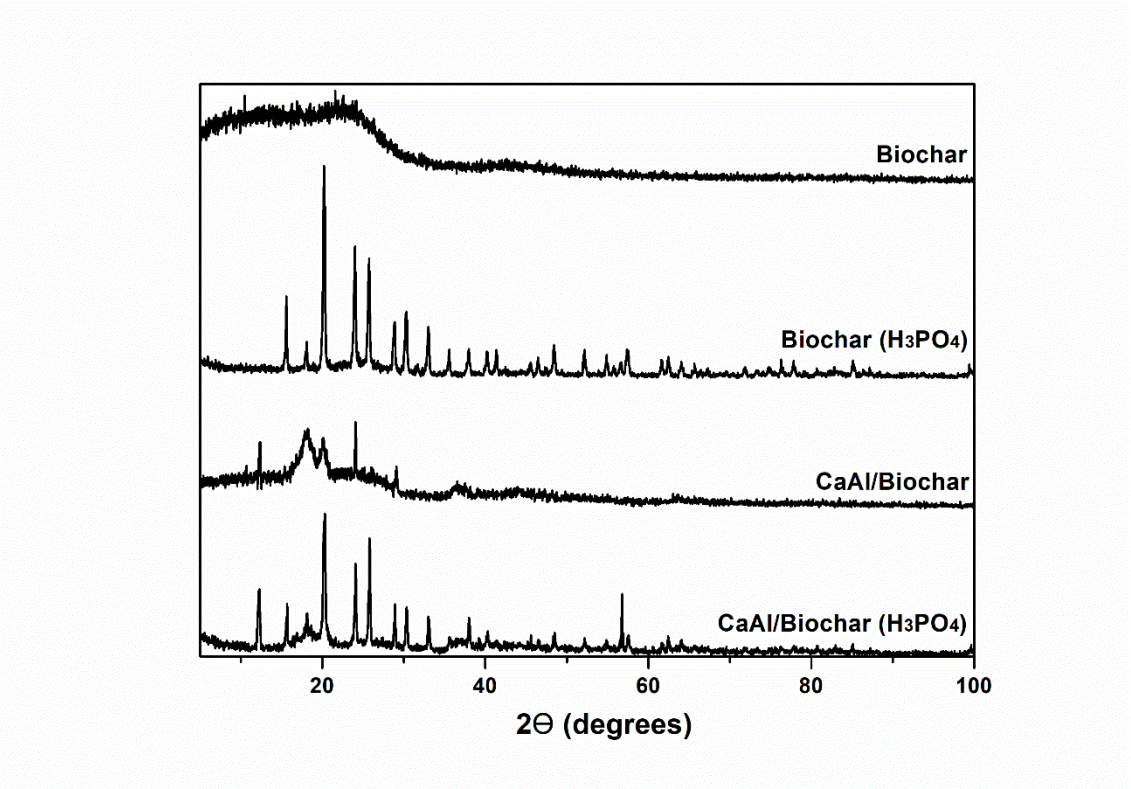

Figure 2 - XRD patterns of the adsorbents.

The FT-IR spectra of different adsorbents samples are presented in Figure 3. The characteristic peaks of stretching vibration of -OH were observed at the

absorbance bands at 3418 cm^{-1} and 1600 cm^{-1}. However, the intensity of these peaks was higher for CaAl/biochar, CaAl/biochar((H_3PO_4) and biochar (H_3PO_4) than for pristine biochar. Activation with phosphoric acid creates new groups on the surface and inside the pores of biochar which was suggested by the increasing intensity of -OH group (Sajjadi et al., 2019). Also, the LDH presence increases the intensity due to the interlayer of water or water adsorbed on the external surface of the samples (Meili et al., 2019). The peak at 1030 cm^{-1} were assigned to the stretching vibration of C-O, respectively (H. Chen et al., 2018). The absorbance band at 505 cm^{-1} is assigned to the symmetrical stretching and Al–O bending, indicating the formation of Al–O tetrahedrons (Luo et al., 2017). The peaks around at 740, 630 and 470 cm^{-1} represent the Ca-O lattice vibrations and Ca-O-H bending (H. Chen et al., 2018). Therefore, the presence of these absorption bands demonstrates the efficiency in the production of the composite biochar/LDH, which is responsible for the improvement of the adsorption capacity of the adsorbent. Similar result was found in the literature (Li et al., 2020).

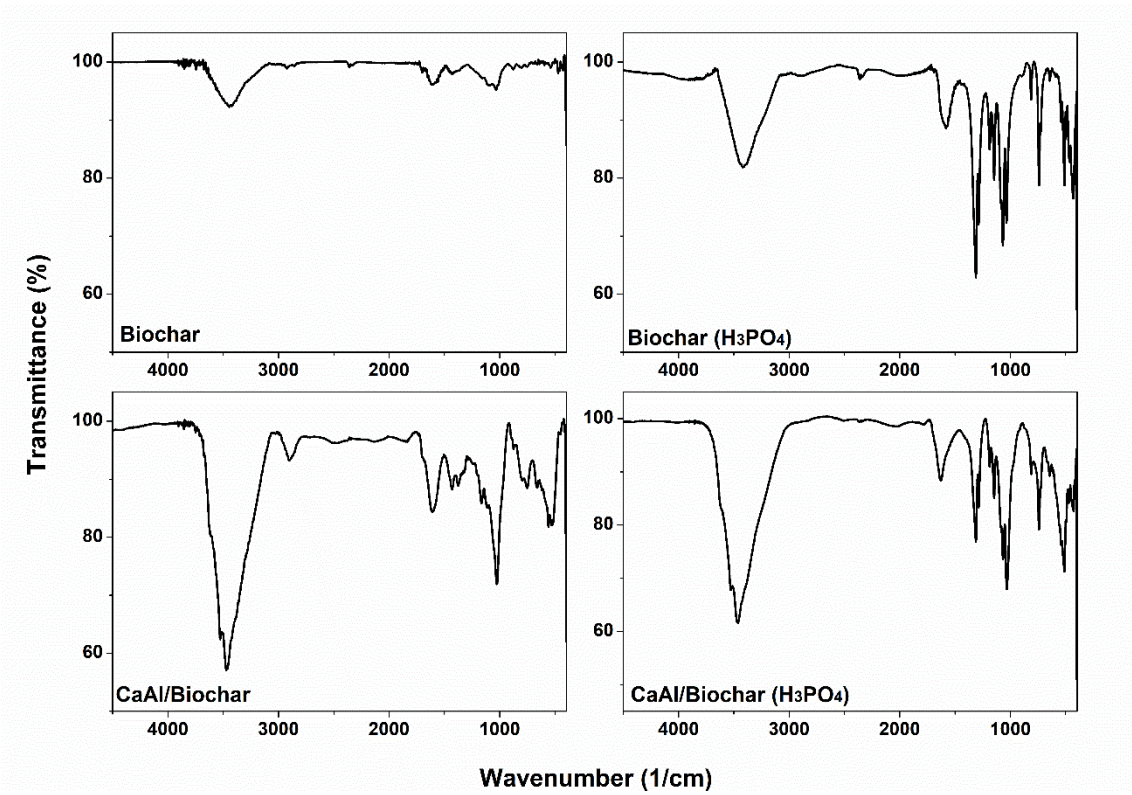

Figure 3 - FT-IR spectra of the adsorbents.

The SEM images of the morphologies of all the adsorbents, revealing differences in their surfaces, can be seen from Figure 4.

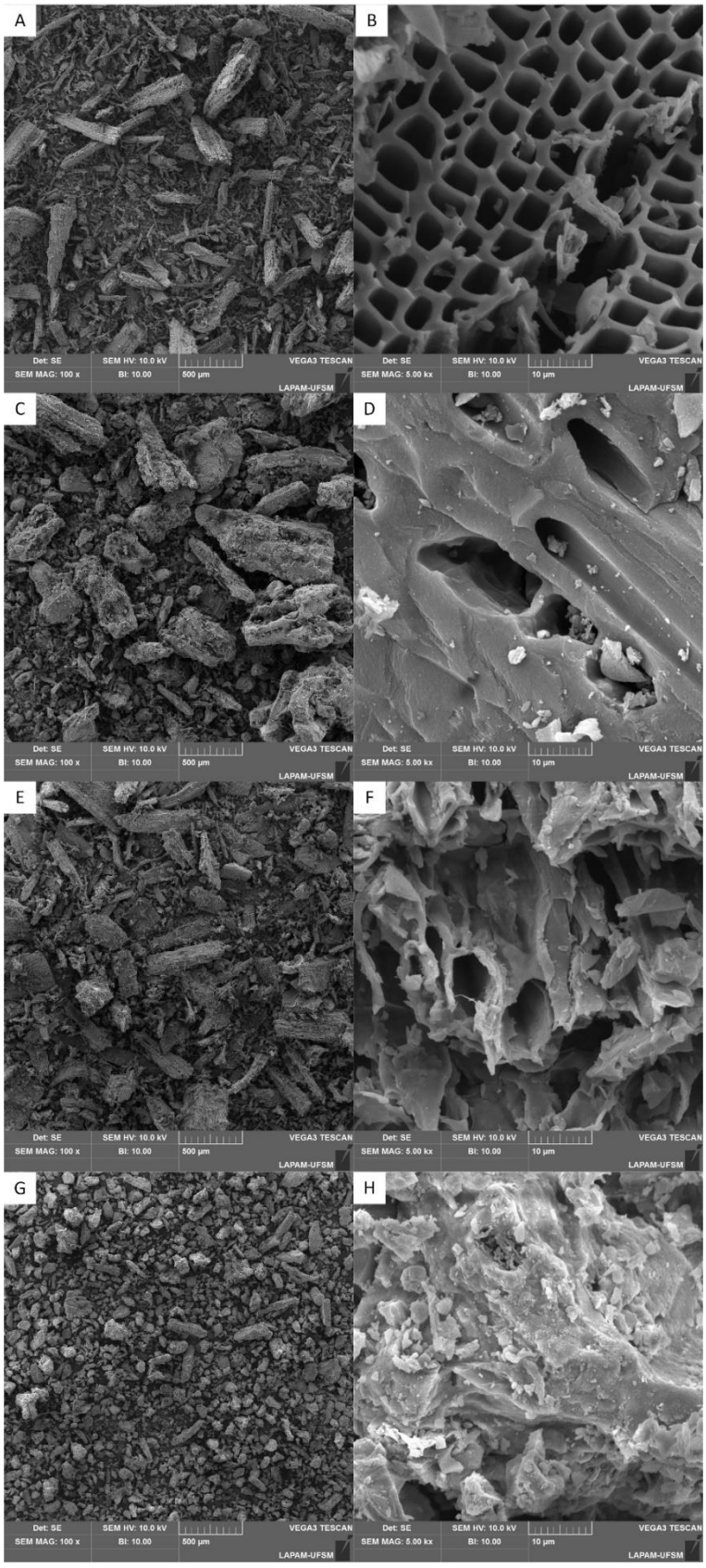

Figure 4 - SEM images of the biochar (A), biochar (H_3PO_4) (C), CaAl/biochar (E) and CaAl/biochar (H_3PO_4) (G), at 100× magnification. Images (B), (D), (F) and (H) are of the biochar, biochar (H_3PO_4), CaAl/biochar and CaAl/biochar (H_3PO_4), respectively, at a magnification of 5000×.

A smooth surface, well-organized channels and pores can be seen in biochar (Figure 4 (A) and (B)) (Amin et al., 2021), whereas biochar activated by phosphoric acid displayed rough surfaces with columnar or granular particles (Figure 4 (C) and (D)) (Han et al., 2020). The SEM images of CaAl/biochar (Figure 4 (E) and (F)) and CaAl/biochar (H_3PO_4) (Figure 4 (G) and (H)) exhibited irregular plate-like structures with different sizes, due to the CaAl-LDHs deposition on their surfaces (Kong et al., 2021; Li et al., 2020).

Specific surface areas were 136 m^2/g for the biochar, 468 m^2/g for the biochar (H_3PO_4), 486 m^2/g for the CaAl/biochar and 469 m^2/g for CaAl/biochar (H_3PO_4). An increase in surface area may be observed after activation of the biochar with phosphoric acid, because the dehydration produced by phosphoric acid is strong. It promotes bond cleavage reactions and the formation of crosslinks via processes such as cyclization and condensation and combines with organic species to form phosphate bridges, such as phosphate and polyphosphate esters (Ateş and Özcan, 2018). Also, the specific surface area of biochar increases from 136 to 486 m^2/g after modification by CaAl-LDH due to the loading of layered double hydroxides (Jia et al., 2019). In general lines, the LDH flakes increase the surface area of pristine biochar providing more adsorption active sites (Yang et al., 2019).

4.3.2 Adsorption experiments

4.3.2.1 pH influence

The pH is one of the most vital parameters in the optimization of adsorption process, since it exerts profound influence on the adsorptive uptake of adsorbate molecule due to its influence on the surface properties of the adsorbent and ionization degree of the adsorbate (Chakraborty et al., 2011). The influence of pH on the adsorption behavior of the CV dye on the adsorbents was investigated from 2 to 10, while keeping the other parameters at constant values, such as a stirring rate of 140 rpm, volume solution of 50 mL with a 50 mg L^{-1} concentration, adsorbent dosage of 500 mg L^{-1} and process time of 4 h at 30ºC. The results are depicted in Figure 5 and in Figure 6. The point zero charge pH_{pzc} of CaAl/Biochar (H_3PO_4) and CaAl/Biochar was 5.6 (inset in Figure 5) and 5.2 (inset in Figure 6), respectively.

The pH of a solution controls the magnitude of the electrostatic charges imparted by the ionized dye molecules. Both the adsorbent and adsorbate may have functional groups that can be protonated or deprotonated to produce different surface charges in solutions at different pH, resulting in electrostatic attraction or repulsion between the charged adsorbates and adsorbents (Loulidi et al., 2020). The adsorption capacity by CaAl/Biochar (H_3PO_4) and CaAl/Biochar presented similar trends, increasing with the increase in pH of the dye solution, appreciably up to pH 6.0. With further increase in pH from 6.0 to 10.0 the adsorption capacity became to a stable behavior. Under the solution pH < pH_{pzc}, the surface of the adsorbents was positively charged, resulted in the electrostatic repulsion between the positively charged surface and the dye cations, which led to the lower CV capacity adsorption (X. fei Tan et al., 2016). However, when the solution pH > pH_{pzc}, the surface of the composites is negatively charged, so attractive forces occur between the cationic dye and the negatively charged surface of the adsorbents, increasing the capacity adsorption of CV dye. Similar results were found by Brião et al. (Brião et al., 2017) in the adsorption of crystal violet dye onto a mesoporous ZSM–5 zeolite synthetized using chitin as template. Consequently, it was selected the pH 8 of the solution CV dye to perform the kinetic and isotherm experiments.

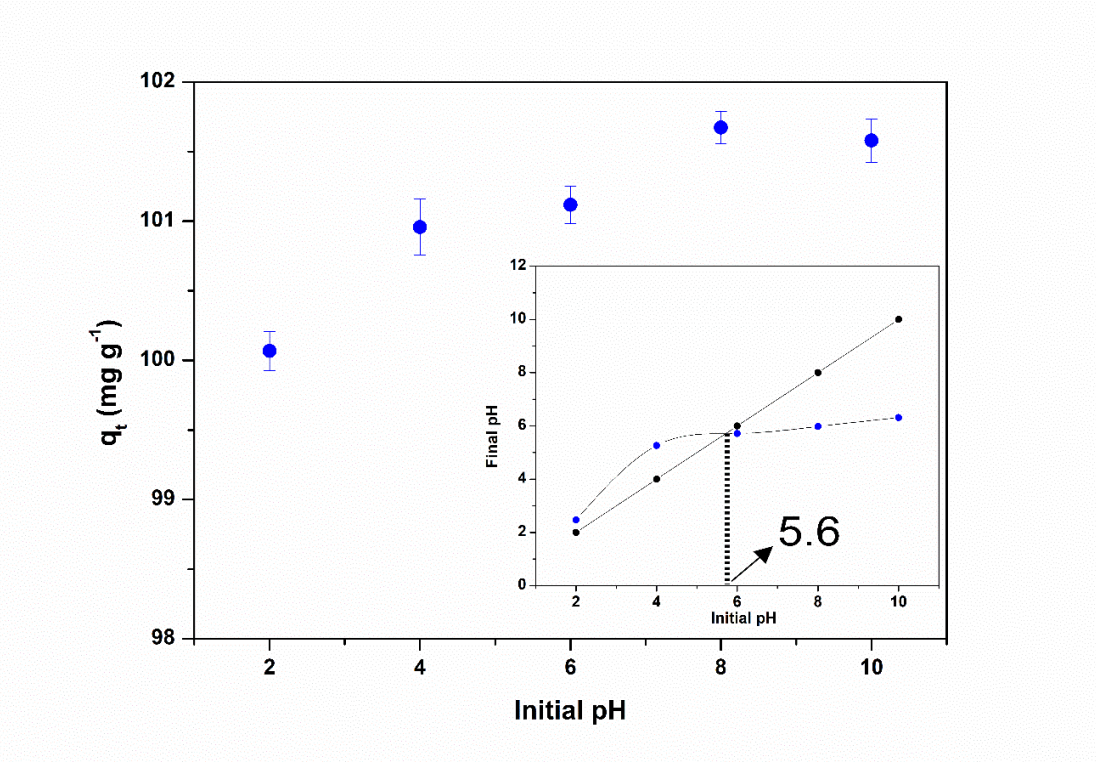

Figure 5 - pH influence on CV adsorption by CaAl/Biochar (H_3PO_4) (C_0 = 50mg L^{-1}, 30°C, 4 h, adsorbent dosage of 500 mg L^{-1}).

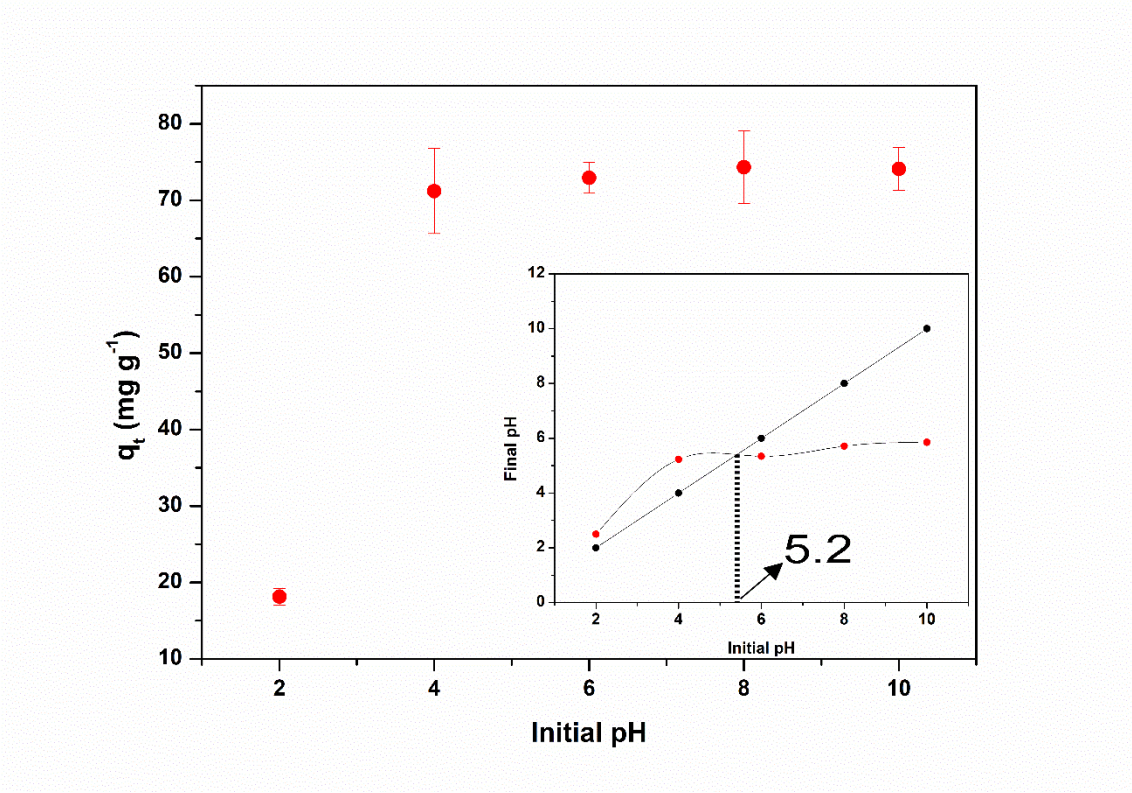

Figure 6 - pH influence on CV adsorption by CaAl/Biochar (C_0 = 50mg L^{-1}, 30°C, 4 h, adsorbent dosage of 500 mg L^{-1}).

4.3.2.2 Kinects studies

The adsorption kinetics is one of the most important factors in the evaluation of the efficiency of an adsorbent and it can be seen from Figure 7. The kinetic profiles of CV adsorption onto adsorbents were investigated at a range of contact time from 0 to 240 min, initial dye concentration of 50 mg L^{-1}, pH 8 of the solution, adsorbent dosage of 500 mg L^{-1}, agitation of 140 rpm and temperature of 298 K. The CaAl/Biochar (H_3PO_4) composite can adsorb a greater amount of dye when compared to the others adsorbents. This behavior is related to the addition of phosphoric acid before heating, which increased significantly the specific surface area of the activated carbons, and also related to the great capacity of ionic exchange acquired by the material when the LDH is incorporated to the biochar, providing a greatly increased adsorption of CV dye (Han et al., 2020; Meili et al., 2019).

Another important analysis that must be observed is that the adsorption of the crystal violet dye carried out by the CaAl/Biochar (H_3PO_4) gets into equilibrium approximately at 25 min. It is more quickly when compared to raw biochar,

approximately 40 min difference. These results demonstrate that the synthesized composites have a promising potential for the removal by dye adsorption.

Pseudo–first order (PFO), and pseudo–second order (PSO) models were investigated as reactions models to interpret the adsorption kinetic curves. The kinetic parameters for CV adsorption onto adsorbents are presented in Table . For the two evaluated models it can be seen that the values of determination coefficient (R^2) and average relative error (ARE) were suitable. However, it was found that PFO model was the more adequate to represent the adsorption kinetics of biochar, when compared to the PSO model, since it presented higher values of coefficient of determination (R^2), close values of q_e experimental and q_2 calculated, and smaller values of ARE (%). For the other composites, the PSO model presented the best results in terms of the capacity of experimental adsorption compared to the calculated one, as well as, R^2 and ARE (%). The q_2 values confirmed that the adsorption capacity of CaAl/Biochar (H_3PO_4) has increased 32% when compared to biochar.

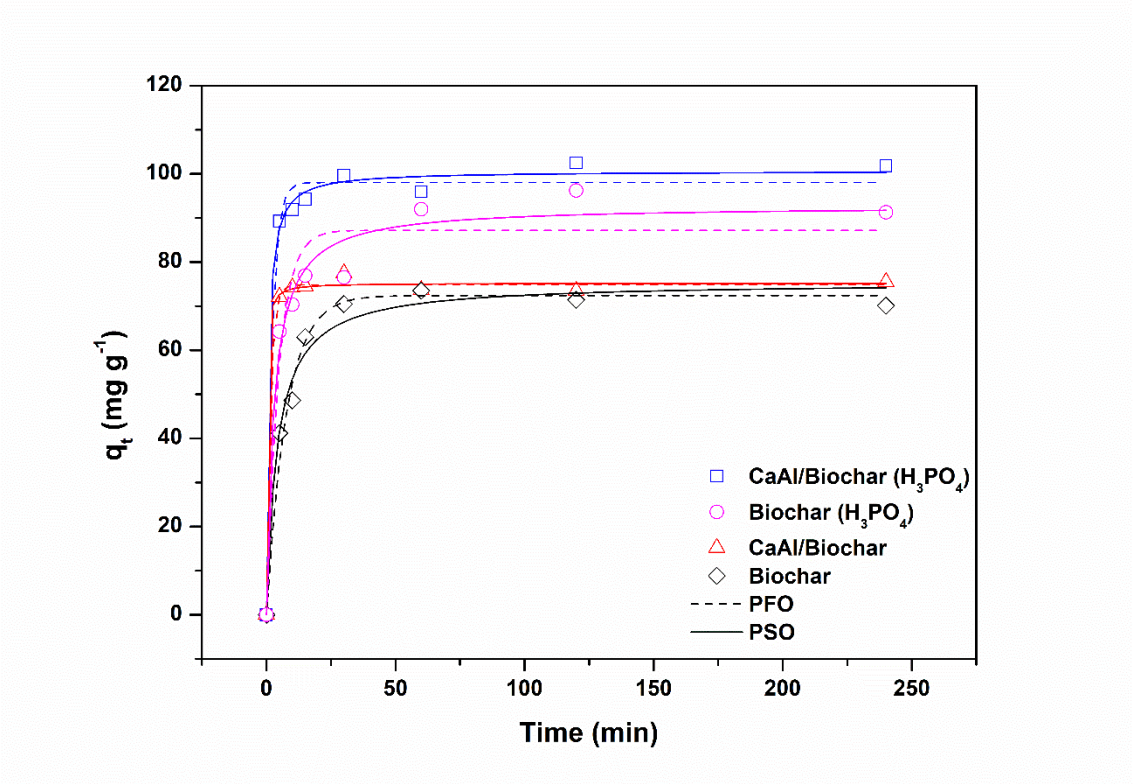

Figure 7 - Kinetic curves for the adsorption of CV onto different adsorbents (C_0 = 50 mg L^{-1}, 30°C and adsorbent dosage of 500 mg L^{-1}).

Table 2 - Kinetic parameters of samples of different adsorbents for the adsorption of CV.

Kinect model	Inicial CV concentration (50 mg L^{-1})			
	Biochar	Biochar (H_3PO_4)	CaAl/Biochar	CaAl/Biochar (H_3PO_4)
PFO				
q_1 (mg g^{-1})	71.3092	87.1810	74.8187	96.7557
k_1 (min^{-1})	0.1413	0.2130	0.6637	0.5631
R^2	0.9863	0.9444	0.9977	0.9900
R^2_{adj}	0.9839	0.9352	0.9973	0.9883
ARE (%)	3.5888	7.7168	1.1196	3.8027
PSO				
q_2 (g mg^{-1} min^{-1})	75.4208	92.7622	75.2136	99.6399
k_2 (min^{-1})	0.0032	0.0039	0.0753	0.0150
R^2	0.9814	0.9788	0.9975	0.9962
R^2_{adj}	0.9783	0.9753	0.9971	0.9956
ARE (%)	4.3048	4.1231	1.1641	2.8776
$q_{e\ experimental}$	70.1128	91.2660	75.5152	101.8218

Although the applied kinetic models do not describe the adsorption mechanism, they assume that the driving force causing the adsorption is the difference between the mean solid phase concentration and the equilibrium concentration. In summary, the adsorption rate would be proportional to the driving force for the PFO model and proportional to the square of the driving force for the PSO model (Chang and Juang, 2004; Meili et al., 2019). Similar results were also found in the literature (Puri and Sumana, 2018; X. fei Tan et al., 2016).

Therefore, the kinetic studies showed that CaAl/Biochar (H_3PO_4) was the better adsorbent for CV dye. In this way, and due to LDH production savings, the remaining tests were developed only with the CaAl/Biochar (H_3PO_4) composite.

4.3.2.3 Equilibrium studies

The adsorption equilibrium isotherms were obtained at different temperatures (30, 40 and 50ºC) with CV dye concentration range from 0 to 500 mg L^{-1}, CaAl/Biochar (H_3PO_4) dosage of 500 mg L^{-1}, pH of 8 and 140 rpm. The equilibrium curves are shown in Figure 8. The isotherms presented a L1 shape (Giles et al., 1960). There is an initial

curved portion at lower equilibrium concentrations, indicating the affinity adsorbate–adsorbent. The adsorption capacity at equilibrium (q_e) continued to increase at higher CV dye concentration in the solution (C_e). Therefore, it shows that the saturation of all adsorption sites was not reached in the experimental range applied (Silva et al., 2018). In this way, it can be concluded that CaAl/Biochar (H_3PO_4) has strong adsorption potential for CV dye.

The equilibrium isotherm was studied using two adsorption isothermal non-linear models including Langmuir and Freundlich models to fit the experimental data (Figure 8). The non-linear regression method was the best method to obtain the isotherm parameters and to select the optimum isotherm, compared to that of the linear regression (Nebaghe et al., 2016). The parameters and statistical values for the two different models are summarized in Table . The Freundlich model presented better statistical values compared to Langmuir model, as showed in Table , indicating the adsorption of CV dye onto the CaAl/Biochar (H_3PO_4) surface was probably a heterogeneous and multilayer adsorption process. The criteria that demonstrate which isotherm model best represents the adsorption process studied are the higher values of determination coefficient ($R^2 > 0.97$), adjusted determination coefficient ($R^2_{adj} > 0.96$) and the lower values of average relative error (ARE < 10%) (Brião et al., 2017). Therefore, the adsorbent accommodates more than one layer of molecules and not all adsorbed molecules are in contact with the surface layer of the adsorbent. Also, the Freundlich isotherm model predicts that the adsorbate concentration on the adsorbent will increase with the increasing of the adsorbate concentration in the solution (Freundlich, 1906). The kF parameter increased with the temperature, corroborating that the adsorption was favored at 50ºC (Table 3). Also, the magnitude of the exponent (1/nF) of Freundlich isotherm, indicated that the adsorption process was favorable, since the values of 1/nF were in the range of 0-1 (Ozdes et al., 2014). The maximum adsorption capacity was 496.55 mg g^{-1} at 50ºC.

Therefore, in order to attest the efficiency of CaAl/Biochar (H_3PO_4) for CV dye adsorption, a comparison between the maximum adsorption capacities (q_m) of several adsorbents was performed Table . Comparing CaAl/Biochar (H_3PO_4) with other adsorbents used for CV dye removal (Table 4), it can be stated that CaAl/Biochar (H_3PO_4) is an attractive adsorbent which can be used for the treatment of colored effluents containing CV dye.

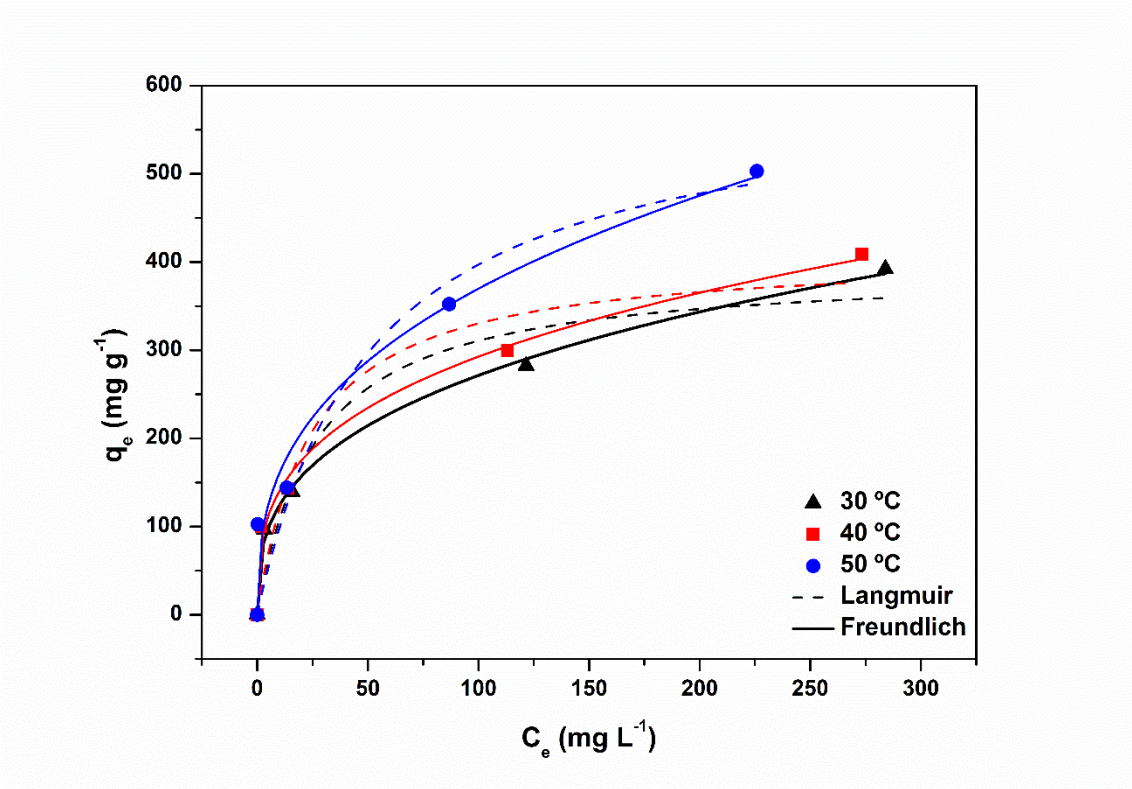

Figure 8 - Isotherm curves for the CV adsorption on CaAl/Biochar (H_3PO_4). (Adsorbent dosage of 500 mg L^{-1}, pH 8 and 140 rpm).

Table 3 - Isothermal parameters of the CaAl/Biochar (H_3PO_4) composite adjusted by the Langmuir and Freundlich models.

Isotherm model	Temperature (ºC)		
	30	40	50
Langmuir			
q_m (mg g^{-1})	392.5790	410.0495	599.4987
k_L (min $^{-1}$)	0.0379	0.0415	0.0196
R_L	0.0524	0.0480	0.0965
R^2	0.9706	0.9642	0.9664
R^2_{adj}	0.9226	0.9061	0.9120
ARE (%)	10.4529	11.9502	14.9638
Freundlich			
k_F (mg/g)(mg/L)$^{-1/nF}$	56.8332	67.3672	69.7607
nF	2.9454	3.1349	2.7613
1/nF	0.3395	0.3190	0.3621
R^2	0.9987	0.9976	0.9869
R^2_{adj}	0.9964	0.9935	0.9652
ARE (%)	2.5495	3.6621	9.9632

Table 4 - Comparison of CaAl/Biochar (H_3PO_4) with other adsorbents for CV dye adsorption.

Adsorbent	q_m (mg g^{-1})	Reference
CaAl/Biochar (H_3PO_4)	496.55	This work
ZSM–5 zeolite	141.80	(Brião et al., 2017)
MgAl/Biochar	374.69	(X. fei Tan et al., 2016)
Water Hyacinth	322.58	(Kulkarni et al., 2017)
Surfactant-modified nano-alumina	254.30	(Zolgharnein et al., 2015)
Almond shell	12.20	(Loulidi et al., 2020)
Biomass of *Ceriporia lacerate*	239.25	(Lin et al., 2011)
Khulays natural bentonite	263.00	(Al-Shahrani, 2020)
NMRH	44.87	(Chakraborty et al., 2011)

4.3.2.4 Thermodynamics studies

The thermodynamic parameters are important for a better understanding of the adsorption phenomena. Table shows the thermodynamic parameters (ΔG^0, ΔH^0 and ΔS^0), where the thermodynamics constant (k^0) values were estimated from the Freundlich parameters, as presented in Eq. 11 (Tran et al., 2017).

$$k^o = \frac{K_F \rho}{1000}\left(\frac{10^6}{\rho}\right)^{\left(1-\frac{1}{nF}\right)} \quad (11)$$

The negative ΔG^0 values show that the CV dye adsorption on CaAl/Biochar (H_3PO_4) was a spontaneous and favorable process. The ΔG^0 were more negative at higher temperatures, indicating that the process was favored at 323.15 K. Based on the ΔH° magnitude, it is possible infer about the adsorption mechanism. The value of ΔH^0 was positive, but lower than 20 kJ mol^{-1}, indicating that the ion exchange during the adsorption was of physical nature (weak attraction forces such as van der Waals interactions) and endothermic (Tran et al., 2016). The positive value of ΔS^0 indicates

that some rearrangements occurred in the solid-liquid interface during the adsorption process (Silva et al., 2018).

Table 5 - Thermodynamic parameters for CV dye adsorption on CaAl/Biochar (H_3PO_4) adsorbent.

T(K)	ΔG° (kJ mol⁻¹)	ΔH° (kJ mol⁻¹)	ΔS° (kJ mol⁻¹ K⁻¹)
303.15	-8.67	9.21	0.06
313.15	-9.35		
323.15	-9.85		

4.3.3 The effect of ionic strength on the adsorption capacity

The effect of the ionic strength of salt (sodium chloride), on the removal of CV dye by CaAl/Biochar (H_3PO_4), is presented in Figure 9. This analysis is important, because the real industrial aqueous waste and water polluted groundwater generally consists of a high concentration of salts, which can affect the adsorption of dyes. It is expected that the ionic strength would sensitively affect the thickness of the electrostatic plane and interfacial potential, resulting in a change of the intrinsic binding constants of the adsorbed species (Park et al., 2017). However, as can be seen, the adsorption capacity for CV remained stable with the increase of NaCl concentration, around 100 mg g^{-1}. This behavior can be attributed to the enhance of the electrostatic interaction between the CV cations and CaAl/Biochar (H_3PO_4) groups by promoting the protonation of CV molecules (X. fei Tan et al., 2016).

Therefore, it is suggested that CaAl/Biochar (H_3PO_4) could have excellent ability for the removal of CV dye from the actual industrial wastewater and polluted groundwater with high ionic strength.

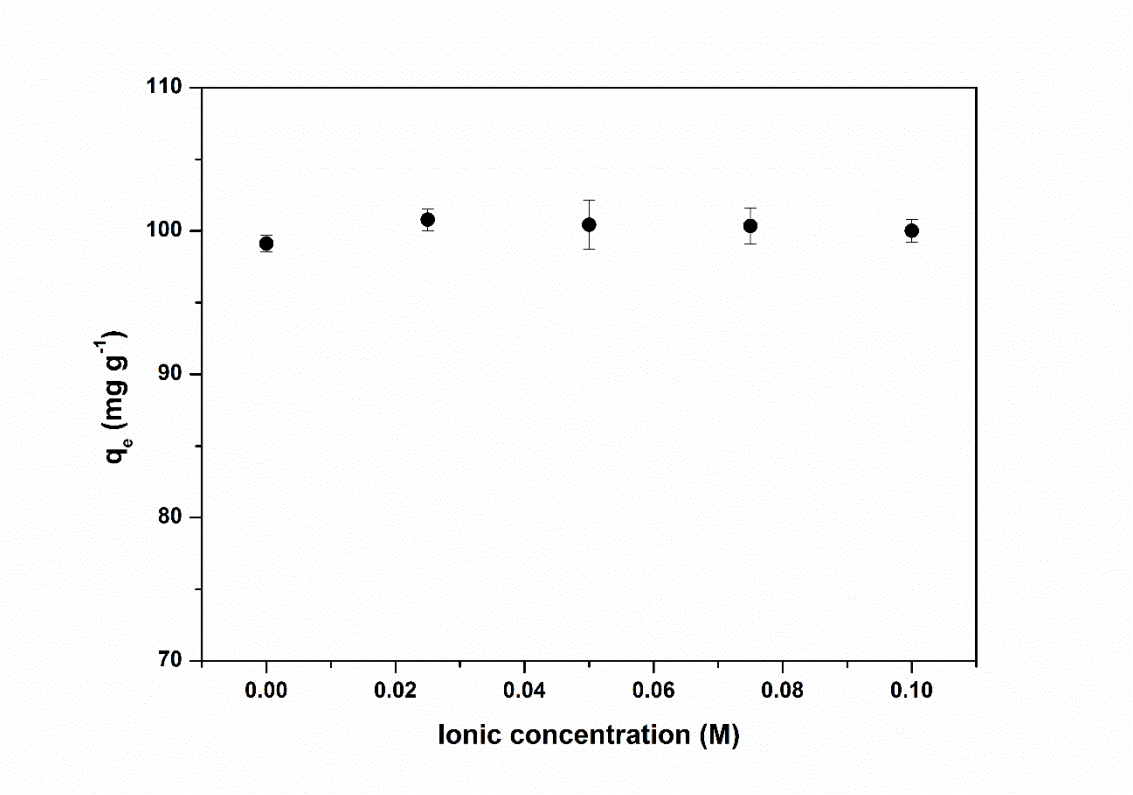

Figure 9 - The effect of ionic strength on the CV adsorption capacity of CaAl/Biochar (H_3PO_4).

4.3.4 Regeneration of used CaAl/Biochar (H_3PO_4)

The regeneration of adsorbents is an important process necessary for industrial applications, due to its economical and enhancement value, so that they can be reused in successive adsorption–desorption cycles. The results of the regeneration tests for ethanol are shown in Figure 10. As can be seen, after each cycle, the CV adsorption capacity of CaAl/Biochar (H_3PO_4) decreases. Studies have reported that LDH composites undergoing regeneration has difficulties maintaining its structure, as they are easily exfoliated (Takehira, 2017; Meili et al., 2019). However, the composite showed excellent regeneration capacity, after four cycles, it was able to maintain about 71% of the adsorptive capacity of the original cycle, probably due to the presence of the biochar that favored the permanence of the adsorptive capacity.

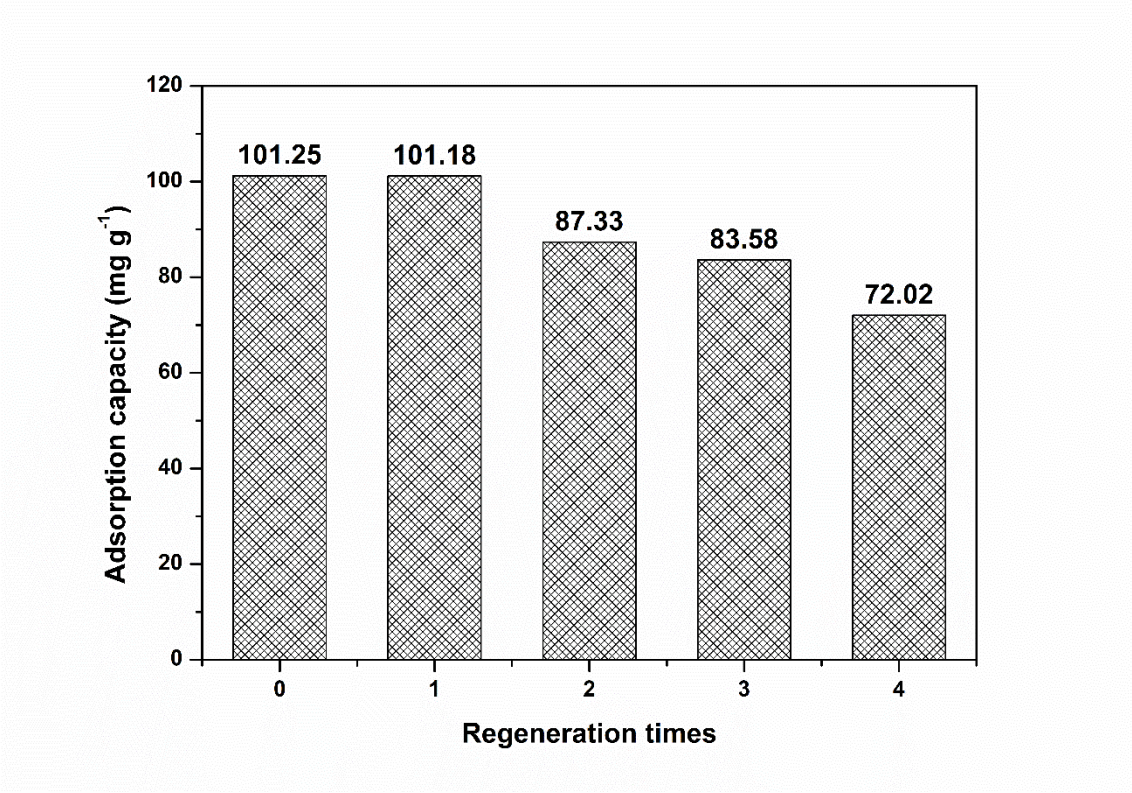

Figure 10 - Desorption cycles of the CaAl/Biochar (H_3PO_4) composite using ethanol as desorbent agent.

In summary, the results demonstrated that CaAl/LDH supported onto a chemically treated biochar with phosphoric acid (40%) promoted a highly efficient adsorbent for the removal of CV dye from aqueous solution, even after recovery cycles. Therefore, this work indicates that CaAl/Biochar (H_3PO_4) can be recycled and reused in environment reclamation and remediation.

4.4 CONCLUSION

In order to maintain a great adsorbent capacity and prevent LDH disintegration, over a range of recovery cycles, this work successfully developed a novel adsorbent material based on CaAl/LDH supported on the surface of a chemically treated biochar with phosphoric acid (40%).

The novel adsorbent was successfully synthesized using eucalypt sawdust as the raw biomass feedstock and the CaAl/LDH to improve biochar adsorption efficiency. The results showed that the adsorption was favored using adsorbent under pH of 8. The kinetic profile was well represented by the pseudo–second order model and the

equilibrium were in accordance with the Freundlich model. The adsorption was spontaneous, favorable and endothermic. The maximum adsorption capacity of the CaAl/Biochar (H_3PO_4), was of 496.55 $mg.g^{-1}$ obtained at 50ºC. The regeneration tests showed that after 4 cycles the removal capacity was able to maintain 71% of the adsorptive capacity of the original cycle.

When compared to other materials present in the literature, the CaAl/Biochar (H_3PO_4) showed great performance for CV dye removal from aqueous solutions, being a potential and sustainable adsorbent for the application in water treatments.

Acknowledgments

The authors are grateful for the financial support provided by CNPq (National Council of Scientific and Technological Development), CAPES (Brazilian Agency for Improvement of Graduate Personnel), FAPERGS (Foundation for Research Support of the State of Rio Grande do Sul), SDECT (Department of Economic Development, Science and Technology of the State of Rio Grande do Sul) and MADEIREIRA HAAS LTDA.

4.5 REFERENCES

Al-Shahrani, S., 2020. Phenomena of Removal of Crystal Violet from Wastewater Using Khulays Natural Bentonite. J. Chem. 1–8. https://doi.org/10.1155/2020/4607657

Amin, M.T., Alazba, A.A., Shafiq, M., 2021. Successful application of eucalyptus camdulensis biochar in the batch adsorption of crystal violet and methylene blue dyes from aqueous solution. Sustain. 13. https://doi.org/10.3390/su13073600

Angin, D., Şensöz, S., 2014. Effect of Pyrolysis Temperature on Chemical and Surface Properties of Biochar of Rapeseed (Brassica napus L.). Int. J. Phytoremediation 16, 684–693. https://doi.org/10.1080/15226514.2013.856842

Ateş, F., Özcan, Ö., 2018. Preparation and Characterization of Activated Carbon from Poplar Sawdust by Chemical Activation : Comparison of Different Activating Agents and Carbonization Temperature. EJERS 3, 6–11.

Ayaliew Werkneh, A., 2015. Removal of Water Hardness Causing Constituents Using Alkali Modified Sugarcane Bagasse and Coffee Husk at Jigjiga City, Ethiopia: A Comparative Study. Int. J. Environ. Monit. Anal. 3, 7. https://doi.org/10.11648/j.ijema.20150301.12

Brião, G.V., Jahn, S.L., Foletto, E.L., Dotto, G.L., 2017. Adsorption of Crystal Violet Dye onto a Mesoporous ZSM–5 Zeolite Synthetized using Chitin as Template. J. Colloid Interface Sci. 508, 313–322. https://doi.org/10.1016/j.jcis.2017.08.070

Burakov, A.E., Galunin, E. V., Burakova, I. V., Kucherova, A.E., Agarwal, S., Tkachev, A.G., Gupta, V.K., 2018. Adsorption of heavy metals on conventional and nanostructured materials for wastewater treatment purposes: A review. Ecotoxicol. Environ. Saf. 148, 702–712. https://doi.org/10.1016/j.ecoenv.2017.11.034

Chakraborty, S., Chowdhury, S., Saha, P. Das, Violet, C., 2011. Adsorption of Crystal Violet from aqueous solution onto NaOH-modified rice husk. Carbohydr. Polym. 86, 1533–1541. https://doi.org/10.1016/j.carbpol.2011.06.058

Chang, M.Y., Juang, R.S., 2004. Adsorption of tannic acid, humic acid, and dyes from water using the composite of chitosan and activated clay. J. Colloid Interface Sci. 278, 18–25. https://doi.org/10.1016/j.jcis.2004.05.029

Chen, H., Chen, Z., Zhao, G., Zhang, Z., Xu, C., Liu, Y., Chen, J., Zhuang, L., Haya, T., Wang, X., 2018. Enhanced adsorption of U(VI) and 241Am(III) from wastewater using Ca/Al layered double hydroxide@carbon nanotube composites. J. Hazard. Mater. 347, 67–77. https://doi.org/10.1016/j.jhazmat.2017.12.062

Chen, L., Li, Y., Chen, Lina, Li, N., Dong, C., Chen, Q., Liu, B., Ai, Q., Si, P., Feng, J., Zhang, L., Suhr, J., Lou, J., Ci, L., 2018. A large-area free-standing graphene oxide multilayer membrane with high stability for nanofiltration applications. Chem. Eng. J. 345, 536–544. https://doi.org/10.1016/j.cej.2018.03.136

Dotto, G.L., Santos, J.M.N., Rodrigues, I.L., Rosa, R., Pavan, F.A., Lima, E.C., 2015. Adsorption of Methylene Blue by ultrasonic surface modified chitin. J. Colloid Interface Sci. 446, 133–140. https://doi.org/10.1016/j.jcis.2015.01.046

Freundlich, H.M.F., 1906. Over the Adsorption in Solution. J. Phys. Chem. 57, 385–471.

Gao, W., Zhao, S., Wu, H., Deligeer, W., Asuha, S., 2016. Direct acid activation of kaolinite and its effects on the adsorption of methylene blue. Appl. Clay Sci. 126, 98–106. https://doi.org/10.1016/j.clay.2016.03.006

Giles, C.H., MacEwan, T.H., Nakhwa, S.N., Smith, D., 1960. Studies in adsorption part XI: a system of classification of solution adsorption isotherms, and its use in diagnosis of adsorption mechanisms and in measurement of specific surface areas of solids. J. Chem. Soc. 846, 3973–3993.

Girish, C.R., Murty, V.R., 2017. Desorption of phenol from Lantana camara, forest waste: Optimization using response surface methodology and kinetic studies. Int. J. Appl. Eng. Res. 12, 8257–8263.

Guo, X., Yin, P., Yang, H., 2017. Superb adsorption of organic dyes from aqueous

solution on hierarchically porous composites constructed by ZnAl-LDH/Al(OH)3 nanosheets. Microporous Mesoporous Mater. 259, 123–133. https://doi.org/10.1016/j.micromeso.2017.10.003

Hall, K.R., Eagleton, L.C., Acrivos, A., Vermeulen, T., 1966. Pore- and solid-diffusion kinetics in fixed-bed adsorption under constant-pattern conditions. Ind. Eng. Chem. Fundam. 5, 212–223. https://doi.org/10.1021/i160018a011

Han, Q., Wang, J., Goodman, B.A., Xie, J., Liu, Z., 2020. High adsorption of methylene blue by activated carbon prepared from phosphoric acid treated eucalyptus residue. Powder Technol. 366, 239–248. https://doi.org/10.1016/j.powtec.2020.02.013

Ho, Y.S., McKay, G., 1999. Pseudo-second order model for sorption processes. Process Biochem. 34, 451–465. https://doi.org/https://doi.org/10.1016/S0032-9592(98)00112-5

Hoxha, A., Gillam, D.G., Agha, A., Karpukhina, N., 2020. Novel fluoride rechargeable dental composites containing MgAl and CaAl layered double hydroxide (LDH). Dent. Mater. 36, 973–986. https://doi.org/10.1016/j.dental.2020.04.011

Hsu, S.H., Huang, C.S., Chung, T.W., Gao, S., 2014. Adsorption of chlorinated volatile organic compounds using activated carbon made from Jatropha curcas seeds. J. Taiwan Inst. Chem. Eng. 45, 2526–2530. https://doi.org/10.1016/j.jtice.2014.05.028

Huang, D., Liu, C., Zhang, C., Deng, R., Wang, R., Xue, W., Luo, H., Zeng, G., Zhang, Q., Guo, X., 2019. Cr(VI) removal from aqueous solution using biochar modified with Mg/Al-layered double hydroxide intercalated with ethylenediaminetetraacetic acid. Bioresour. Technol. 276, 127–132. https://doi.org/10.1016/j.biortech.2018.12.114

Iqbal, M.A., Sun, L., Fedel, M., 2019. Synthesis of novel cone - shaped CaAl - LDH directly on aluminum alloy by a facile urea hydrolysis method. SN Appl. Sci. 1, 1–5. https://doi.org/10.1007/s42452-019-1474-4

Jana, S., Purkait, M.K., Mohanty, K., 2010. Removal of crystal violet by advanced oxidation and microfiltration. Appl. Clay Sci. 50, 337–341. https://doi.org/10.1016/j.clay.2010.08.023

Jia, Y., Zhang, Y., Fu, J., Yuan, L., Li, Z., Liu, C., Zhao, D., Wang, X., 2019. A novel magnetic biochar/MgFe-layered double hydroxides composite removing Pb 2+ from aqueous solution: Isotherms, kinetics and thermodynamics. Colloids Surfaces A Physicochem. Eng. Asp. 567, 278–287. https://doi.org/10.1016/j.colsurfa.2019.01.064

Kong, X., Ge, R., Liu, T., Xu, S., Hao, P., Zhao, X., Li, Z., Lei, X., Duan, H., 2021. Super-stable mineralization of cadmium by calcium-aluminum layered double hydroxide and its large-scale application in agriculture soil remediation. Chem. Eng. J. 407. https://doi.org/10.1016/j.cej.2020.127178

Kulkarni, M.R., Revanth, T., Acharya, A., Bhat, P., 2017. Removal of Crystal Violet dye from aqueous solution using water hyacinth: Equilibrium, kinetics and thermodynamics study. Resour. Technol. 3, 71–77. https://doi.org/10.1016/j.reffit.2017.01.009

Lagergren, S., 1898. About the Theory of so Called Adsorption of Soluble Substances. K. Sven. Vetenskapsakademiens Handl. 24, 1–39.

Langmuir, I., 1918. The adsorption of gases on plane surfaces of glass, mica and platinum. J. Am. Chem. Soc. 40, 1361–1403. https://doi.org/https://doi.org/10.1021/ja02242a004

Larasati, A., Fowler, G.D., Graham, N.J.D., 2020. Chemical regeneration of granular activated carbon: Preliminary evaluation of alternative regenerant solutions. Environ. Sci. Water Res. Technol. 6, 2043–2056. https://doi.org/10.1039/d0ew00328j

Li, S., Dong, L., Wei, Z., Sheng, G., Du, K., Hu, B., 2020. Adsorption and mechanistic study of the invasive plant-derived biochar functionalized with CaAl-LDH for Eu(III) in water. J. Environ. Sci. (China) 96, 127–137. https://doi.org/10.1016/j.jes.2020.05.001

Lin, Y., He, X., Han, G., Tian, Q., Hu, W., 2011. Removal of Crystal Violet from aqueous solution using powdered mycelial biomass of Ceriporia lacerata P2. J. Environ. Sci. 23, 2055–2062. https://doi.org/10.1016/S1001-0742(10)60643-2

Liu, S., Wang, Z., Li, J., Zhao, C., He, X., Yang, G., 2018. Fabrication of slag particle three-dimensional electrode system for methylene blue degradation: Characterization, performance and mechanism study. Chemosphere 213, 377–383. https://doi.org/10.1016/j.chemosphere.2018.09.077

Loulidi, I., Boukhlifi, F., Ouchabi, M., Amar, A., Jabri, M., Kali, A., Chraibi, S., Hadey, C., Aziz, F., 2020. Adsorption of Crystal Violet onto an Agricultural Waste Residue: Kinetics, Isotherm, Thermodynamics, and Mechanism of Adsorption. Sci. World J. 1–9.

Luo, W., Yang, X., Wang, Z., Huang, W., Chen, J., Jiang, W., Wang, L., Cheng, X., Deng, Y., Zhao, D., 2017. Synthesis of ZSM-5 aggregates made of zeolite nanocrystals through a simple solvent-free method. Microporous Mesoporous Mater. 243, 112–118. https://doi.org/10.1016/j.micromeso.2017.01.040

Meili, L., Lins, P. V., Zanta, C.L.P.S., Soletti, J.I., Ribeiro, L.M.O., Dornelas, C.B., Silva, T.L., Vieira, M.G.A., 2019. MgAl-LDH/Biochar composites for methylene blue removal by adsorption. Appl. Clay Sci. 168, 11–20. https://doi.org/10.1016/j.clay.2018.10.012

Milonjić, S.K., 2007. A consideration of the correct calculation of thermodynamic parameters of adsorption. J. Serbian Chem. Soc. 72, 1363–1367. https://doi.org/10.2298/JSC0712363M

Mohadi, R., Palapa, N.R., Lesbani, A., 2021. Preparation of CaAl-Layered Double Hydroxides/Biochar Composite with High Adsorption Capacity and Selectivity toward Cationic Dyes in Aqueous. Bull. Chem. React. Eng. Catal. 16, 244–252. https://doi.org/10.9767/BCREC.16.2.10211.244-252

Nebaghe, K.C., El Boundati, Y., Ziat, K., Naji, A., Rghioui, L., Saidi, M., 2016. Comparison of linear and non-linear method for determination of optimum equilibrium isotherm for adsorption of copper(II) onto treated Martil sand. Fluid Phase Equilib. 430, 188–194. https://doi.org/10.1016/j.fluid.2016.10.003

Ozdes, D., Duran, C., Senturk, H.B., Avan, H., Bicer, B., 2014. Kinetics, thermodynamics, and equilibrium evaluation of adsorptive removal of methylene blue onto natural illitic clay mineral. Desalin. Water Treat. 52, 208–218. https://doi.org/10.1080/19443994.2013.787554

Panic, V., Velickovic, S., 2014. Removal of model cationic dye by adsorption onto poly(methacrylic acid)/zeolite hydrogel composites: Kinetics, equilibrium study and image analysis. Sep. Purif. Technol. 122, 384–394. https://doi.org/10.1016/j.seppur.2013.11.025

Park, C.M., Han, J., Chu, K.H., Al-Hamadani, Y.A.J., Her, N., Heo, J., Yoon, Y., 2017. Influence of solution pH, ionic strength, and humic acid on cadmium adsorption onto activated biochar: Experiment and modeling. J. Ind. Eng. Chem. 48, 186–193. https://doi.org/10.1016/j.jiec.2016.12.038

Peres, E.C., Hosseini–Bandegharaei, A., Dotto, G.L., Cunha, A.M., Slaviero, J.C., 2018. Microwave synthesis of silica nanoparticles and its application for methylene blue adsorption. J. Environ. Chem. Eng. 6, 649–659. https://doi.org/10.1016/j.jece.2017.12.062

Puri, C., Sumana, G., 2018. Highly effective adsorption of crystal violet dye from contaminated water using graphene oxide intercalated montmorillonite nanocomposite. Appl. Clay Sci. 166, 102–112. https://doi.org/10.1016/j.clay.2018.09.012

Sajjadi, B., Broome, J.W., Chen, W.Y., Mattern, D.L., Egiebor, N.O., Hammer, N., Smith, C.L., 2019. Urea functionalization of ultrasound-treated biochar: A feasible strategy for enhancing heavy metal adsorption capacity. Ultrason. Sonochem. 51, 20–30. https://doi.org/10.1016/j.ultsonch.2018.09.015

Shoukat, S., Bhatti, H.N., Iqbal, M., Noreen, S., 2017. Mango stone biocomposite preparation and application for crystal violet adsorption: A mechanistic study. Microporous Mesoporous Mater. 239, 180–189. https://doi.org/10.1016/j.micromeso.2016.10.004

Silva, J.S. da, Rosa, M.P. da, Beck, P.H., Peres, E.C., Dotto, G.L., Kessler, F., Grasel, F.S., 2018. Preparation of an alternative adsorbent from Acacia Mearnsii wastes through acetosolv method and its application for dye removal. J. Clean. Prod. 180, 386–394. https://doi.org/10.1016/j.jclepro.2018.01.201

Singh, V.K., Soni, A.B., Singh, R.K., 2016. Process optimization studies of Malachite Green dye adsorption onto eucalyptus (Eucalyptus globulus) wood biochar using response surface methodology. Orient. J. Chem. 32, 2621–2631. https://doi.org/10.13005/ojc/320534

Takehira, K., 2017. Recent development of layered double hydroxide-derived catalysts − Rehydration, reconstitution, and supporting, aiming at commercial application −. Appl. Clay Sci. 136, 112–141. https://doi.org/10.1016/j.clay.2016.11.012

Tan, X. fei, Liu, Y. guo, Gu, Y. ling, Liu, Shao bo, Zeng, G. ming, Cai, X., Hu, X. jiang, Wang, H., Liu, Si mian, Jiang, L. hua, 2016. Biochar pyrolyzed from MgAl-layered double hydroxides pre-coated ramie biomass (Boehmeria nivea (L.) Gaud.): Characterization and application for crystal violet removal. J. Environ. Manage. 184, 85–93. https://doi.org/10.1016/j.jenvman.2016.08.070

Tan, X., Liu, Y., Gu, Y., Xu, Y., Zeng, G., Hu, X., Liu, Shao-bo, Wang, X., Liu, Si-mian, Li, J., 2016. Biochar-based nano-composites for the decontamination of wastewater: A review. Bioresour. Technol. 212, 318–333. https://doi.org/10.1016/j.biortech.2016.04.093

Tan, X., Liu, Y., Zeng, G., Wang, X., Hu, X., Gu, Y., 2015. Application of biochar for the removal of pollutants from aqueous solutions. Chemosphere 125, 70–85. https://doi.org/10.1016/j.chemosphere.2014.12.058

Tran, H.N., You, S.-J., Hosseini-Bandegharaei, A., Chao, H.-P., 2017. Mistakes and inconsistencies regarding adsorption of contaminants from aqueous solutions: A critical review. Water Res. 120, 88–116. https://doi.org/https://doi.org/10.1016/j.watres.2017.04.014

Tran, H.N., You, S.J., Chao, H.P., 2016. Thermodynamic parameters of cadmium adsorption onto orange peel calculated from various methods: A comparison study. J. Environ. Chem. Eng. 4, 2671–2682. https://doi.org/10.1016/j.jece.2016.05.009

Xiang, W., Zhang, X., Chen, J., Zou, W., He, F., Hu, X., Tsang, D.C.W., Ok, Y.S., Gao, B., 2020. Biochar technology in wastewater treatment: A critical review. Chemosphere 252, 126539. https://doi.org/10.1016/j.chemosphere.2020.126539

Yan, K., Wu, G., Jin, W., 2016. Recent Advances in the Synthesis of Layered, Double-Hydroxide-Based Materials and Their Applications in Hydrogen and Oxygen Evolution. Energy Technol. 4, 354–368. https://doi.org/10.1002/ente.201500343

Yang, F., Zhang, S., Sun, Y., Tsang, D.C.W., Cheng, K., Ok, Y.S., 2019. Assembling biochar with various layered double hydroxides for enhancement of phosphorus recovery. J. Hazard. Mater. 365, 665–673. https://doi.org/10.1016/j.jhazmat.2018.11.047

Yek, P.N.Y., Peng, W., Wong, C.C., Liew, R.K., Ho, Y.L., Wan Mahari, W.A., Azwar, E., Yuan, T.Q., Tabatabaei, M., Aghbashlo, M., Sonne, C., Lam, S.S., 2020.

Engineered biochar via microwave CO2 and steam pyrolysis to treat carcinogenic Congo red dye. J. Hazard. Mater. 395, 122636. https://doi.org/10.1016/j.jhazmat.2020.122636

Yu, J., Zhu, Z., 2018. Mg – Fe layered double hydroxide assembled on biochar derived from rice husk ash : facile synthesis and application in efficient removal of heavy metals. Environ. Sci. Pollut. Res. 24, 1–12.

Zhang, Q., Zhang, T., He, T., Chen, L., 2014. Removal of crystal violet by clay/PNIPAm nanocomposite hydrogels with various clay contents. Appl. Clay Sci. 90, 1–5. https://doi.org/10.1016/j.clay.2014.01.003

Zolgharnein, J., Bagtash, M., Shariatmanesh, T., 2015. Simultaneous removal of binary mixture of Brilliant Green and Crystal Violet using derivative spectrophotometric determination, multivariate optimization and adsorption characterization of dyes on surfactant modified nano-γ-alumina. Spectrochim. Acta - Part A Mol. Biomol. Spectrosc. 137, 1016–1028. https://doi.org/10.1016/j.saa.2014.08.115

5 DISCUSSÃO DOS RESULTADOS

O presente trabalho envolveu a produção de dois artigos. O primeiro artigo teve como foco produzir um biochar, a partir da pirólise de um resíduo lignocelulósico para a produção de briquetes que combinassem, além do biochar, outros resíduos, afim de destiná-los de maneira correta, evitando assim impactos ambientais. Primeiramente, foi analisada a composição química do resíduo lignocelulósico utilizado, a serragem de eucalipto. Através dos resultados da composição química obtidos, ficou evidenciado a razão pela qual a serragem, quando usada de maneira direta, apresenta baixa eficiência energética, visto que, aproximadamente, 70% de sua composição é de hemiceluloses e celulose, ou seja, grande quantidade de matéria volátil. Dessa forma, a aplicação da pirólise é uma excelente maneira de agregar valor à serragem, transformando-a em biochar, com potencial aplicação para fins energéticos.

As temperaturas de pirólise avaliadas foram na faixa de 250 – 450 ºC. Nessa etapa, a taxa de aquecimento e o tempo de processo foram fixados em 15 ºC/min e 30 min, respectivamente. Os resultados obtidos, a partir dos ensaios de pirólise e da caracterização do biochar produzido, principalmente em termos de poder calorífico superior, indicaram que a temperatura de 400 ºC foi a melhor para seguimento do estudo, pois foi capaz de produzir um biochar com maior eficiência energética, quando comparada a um carvão comercial. O grande motivo para o aumento da eficiência energética do biochar para a serragem bruta, é que durante a pirólise, a 400 ºC, ocorre a degradação das hemiceluloses e celulose, componentes responsáveis pela matéria volátil do resíduo. Dessa forma, resta somente a lignina, composta principalmente por carbono, acarretando na melhora energética do material.

Posteriormente, foi analisado a aplicação do biochar na produção de briquetes, através da combinação do mesmo com amido e diferentes resíduos sólidos, como cera bruta e folha de eucalipto. A proporção de amido foi fixada em 8 %, já para a cera bruta e para a folha de eucalipto, foram testadas as proporções de 10, 20 e 30 %. A eficiência dos briquetes foi avaliada em termos de PCS e resistência mecânica. Dessa forma, o melhor resultado foi gerado pelo briquete com 62 % de carvão, 8% de amido e 30 % de cera bruta. O comportamento foi atribuído a composição química da cera bruta, a qual possui uma grande cadeia carbônica, acarretando assim no maior PCS. Além disso, testes de índice de quebra também foram efetuados e mostraram que o briquete, na composição mencionada, possuí resistência mecânica.

Portanto, através do primeiro artigo, é possível observar que a pirólise agregou valor a um resíduo lignocelulósico, a serragem, transformando-a em biochar com elevado poder calorífico para potencial uso em fins energéticos. Por fim, através dos briquetes, além do biochar, também pode ser aplicado resíduos, como cera bruta e folhas de eucalipto, dando um correto fim a esses materiais e minimizando impactos ambientais. Portanto, este estudo promoveu uma novidade para a destinação ecologicamente correta desses materiais, a fim de minimizar os problemas ambientais enfrentados nos dias atuais.

O segundo artigo teve como objetivo produzir um novo material adsorvente através de duas modificações sucessivas na estrutura do biochar, oriundo da pirólise da serragem de eucalipto. Sua eficiência foi avaliada na remoção do corante cristal violeta (CV) de soluções aquosas sintéticas. Primeiramente, foi realizado a ativação química com ácido fosfórico, conforme metodologia encontrada na literatura, seguido da impregnação do biochar ativado com hidróxidos duplos lamelares (HDLs), usando como cátions Ca^{2+} e Al^{3+}. A impregnação foi realizada através da metodologia de co-precipitação.

Os ensaios de adsorção, realizados em batelada, analisaram os seguintes parâmetros, pH da solução, cinética, equilíbrio e, por fim, parâmetros termodinâmicos. Os resultados da caracterização do novo material adsorvente mostraram que as modificações na estrutura do biochar foram realizadas com sucesso, e quando comparadas com o biochar bruto, apresentaram diferenças significativas em termos de área superficial e morfologia.

No pH = 8 da solução houve maior remoção do corante, visto que esse pH é superior ao pH do ponto de carga zero do adsorvente (5,6). Dessa forma, a superfície do material é carregada negativamente, ocorrem forças atrativas entre o corante catiônico e a superfície carregada negativamente dos adsorventes, aumentando a capacidade de adsorção do corante CV. O estudo da cinética mostrou que a adsorção do corante pelo novo adsorvente alcançou o equilíbrio em 25 minutos. Além disso, os dados estatísticos indicaram que a cinética foi melhor descrita pelo modelo de pseudo-segunda ordem. As isotermas de equilíbrio foram melhor representadas pelo modelo de Freundlich, com uma capacidade de adsorção de 496.55 $mg \cdot g^{-1}$ em 50°C, indicando que a adsorção do corante CV no material adsorvente foi provavelmente um processo de adsorção heterogêneo e multicamadas. Os resultados do estudo

termodinâmico também indicaram que o processo de adsorção foi favorável, espontâneo e endotérmico.

Além do exposto, o material adsorvente também foi avaliado em termos de regeneração, e os resultados mostraram que foi mantido 71% da capacidade adsortiva inicial mesmo após quatro ciclos de reuso. Dessa forma, o adsorvente desenvolvido é sustentável com alto desempenho para tratamento de efluentes contaminados por CV e remediação de águas subterrâneas.

Portanto, o estudo mostrou, novamente, que a pirólise é uma metodologia muito importante capaz de agregar valor à resíduos lignocelulósicos, convertendo-os em outros produtos, dentre eles o biochar com potencial para inúmeras aplicações. Nesse caso em específico, o mesmo passou por duas modificações de modo a melhorar sua eficiência na remoção do corante CV através da técnica de adsorção.

6 CONCLUSÃO

Este estudo teve como foco aplicar a técnica de pirólise com o intuito de agregar valor a um resíduo lignocelulósico, a serragem de eucalipto, convertendo-a em biochar e estudando a aplicação deste através da elaboração de briquetes (Artigo 1) e do seu uso como material adsorvente (Artigo 2). No Artigo 1, a produção de briquetes foi realizada a partir do biochar obtido a uma temperatura de pirólise de 400 ºC, com o objetivo de economizar energia e garantir um rendimento de carvão satisfatório. Nessa temperatura, o rendimento de biochar foi de 35% e o poder calorífico superior foi de 33,02 MJ/kg, 5% superior ao obtido para um carvão comercial de eucalipto. O efeito dos resíduos, cera bruta e folhas de eucalipto, cada um misturado com amido de milho, foi investigado em termos de eficiência energética e resistência mecânica do briquete de carvão. Resultados satisfatórios para PCS e resistência mecânica foram alcançados para o briquete de biochar produzido usando uma mistura de 30% de cera bruta e 8% de amido de milho. O PCS (23,45 MJ/kg) foi 11% maior do que o briquete comercial. Os resultados obtidos para o índice de estilhaçamento (97,80%) e densidade relaxada (713,70 kg/m³) confirmaram a boa resistência mecânica do produto final.

Portanto, a utilização dos resíduos apresentou resultados satisfatórios, confirmando que podem ser utilizados para aumentar a eficiência energética e a durabilidade dos briquetes de carvão de forma simples, eficiente e de fácil procedimento.

No Artigo 2, o novo adsorvente foi sintetizado com sucesso a partir da pirólise da serragem de eucalipto. O biochar sofreu ativação química com ácido fosfórico e impregnação com CaAl/HDL para melhorar a sua eficiência de adsorção. Os resultados mostraram que a adsorção foi favorecida usando adsorvente em pH 8. O perfil cinético foi bem representado pelo modelo de pseudo-segunda ordem e o equilíbrio foi de acordo com o modelo de Freundlich. A adsorção foi espontânea, favorável e endotérmica. A capacidade máxima de adsorção do novo material adsorvente, foi de 496,55 $mg.g^{-1}$ obtida a 50ºC. Os testes de regeneração mostraram que após 4 ciclos a capacidade de remoção foi capaz de manter 71% da capacidade adsortiva do ciclo original.

Dessa forma, o biochar modificado apresentou ótimo desempenho na remoção do corante cristal violeta (CV) de soluções aquosas, sendo um adsorvente potencial e sustentável para aplicação em tratamentos de água.

7 SUGESTÕES PARA TRABALHOS FUTUROS

A seguir são indicadas algumas sugestões como maneira de complementar esse estudo.

- Testar a aplicação do material adsorvente desenvolvido, no segundo artigo, na remoção de contaminantes orgânicos de um efluente real;
- Produzir um novo material adsorvente, a partir da pirólise de resíduos lignocelulósicos para geração de biochar, ativá-lo fisicamente e impregná-lo com HDL para aplicação na remoção de fosfato de soluções aquosas sintéticas;
- Avaliar o uso de biochar impregnado com HDL em adsorção em leito fixo;
- Avaliar o uso de biochar impregnado com HDL em processos de degradação fotocatalítica;
- Realizar estudos comparativos alternando o substrato de impregnação de HDL.

REFERÊNCIAS BIBLIOGRÁFICAS

ADELEKE, A. A. et al. Densification of coal fines and mildly torrefied biomass into composite fuel using different organic binders. **Heliyon**, v. 5, n. 7, p. e02160, 2019.

AGBOOLA, O. D.; BENSON, N. U. Physisorption and Chemisorption Mechanisms Influencing Micro (Nano) Plastics-Organic Chemical Contaminants Interactions: A Review. **Frontiers in Environmental Science**, v. 9, n. May, p. 1–27, 2021.

AL-HAMAMRE, Z. et al. Wastes and biomass materials as sustainable-renewable energy resources for Jordan. **Renewable and Sustainable Energy Reviews**, v. 67, p. 295–314, 2017.

ARANSIOLA, E. F. et al. Effect of binder type, binder concentration and compacting pressure on some physical properties of carbonized corncob briquette. **Energy Reports**, v. 5, p. 909–918, 2019.

BALLESTEROS, L. F. et al. **Lignocellulosic Materials and Their Use in Bio-based Packaging**. [s.l: s.n.].

BANSAL, R. C.; GOYAL, M. **Activated Carbon Adsorption**. 1. ed. [s.l.] CRC Press, Taylor & Francis Group, 2005.

BÓTA, A. et al. Active carbon from apricot pits. **Magy Kem F**, v. 103, n. 9, p. 470–479, 1997.

BRIDGWATER, A. V. Review of fast pyrolysis of biomass and product upgrading. **Biomass and Bioenergy**, v. 38, p. 68–94, 2012.

BRIDGWATER, A. V. Renewable fuels and chemicals by thermal processing of biomass. **Chemical Engineering Journal**, v. 91, p. 87–102, 2003.

BUKHTIYAROVA, M. V. A review on effect of synthesis conditions on the formation of layered double hydroxides. **Journal of Solid State Chemistry**, v. 269, p. 494–506, 2019.

CASTRO, J. P. et al. Massaranduba sawdust: A potential source of charcoal and activated carbon. **Polymers**, v. 11, n. 8, p. 1–14, 2019.

CHEN, Z. et al. Pyrolysis behaviors and kinetic studies on Eucalyptus residues using thermogravimetric analysis. **Energy Conversion and Management**, v. 105, p. 251–259, 2015.

DA SILVA MORAIS, A. P.; SANSÍGOLO, C. A.; DE OLIVEIRA NETO, M. Effects of autohydrolysis of Eucalyptus urograndis and Eucalyptus grandis on influence of chemical components and crystallinity index. **Bioresource Technology**, v. 214, p. 623–628, 2016.

DĄBROWSKI, A. Adsorption - From theory to practice. **Advances in Colloid and Interface Science**, v. 93, n. 1–3, p. 135–224, 2001.

DANISH, M.; AHMAD, T. A review on utilization of wood biomass as a sustainable precursor for activated carbon production and application. **Renewable and Sustainable Energy Reviews**, v. 87, n. April 2017, p. 1–21, 2018.

DAUD, M. et al. A review on the recent advances, challenges and future aspect of layered double hydroxides (LDH)– Containing hybrids as promising adsorbents for dyes removal. **Journal of Molecular Liquids**, v. 288, p. 110989, 2019.

DAWOOD, S.; SEN, T. K.; PHAN, C. Adsorption removal of Methylene Blue (MB) dye from aqueous solution by bio-char prepared from Eucalyptus sheathiana bark: kinetic, equilibrium, mechanism, thermodynamic and process design. **Desalination and Water Treatment**, v. 57, n. 59, p. 28964–28980, 2016.

DEMIRBAŞ, A. Estimating of structural composition of wood and non-wood biomass samples. **Energy Sources**, v. 27, n. 8, p. 761–767, 2005.

DOĞAN, M. et al. Adsorption kinetics of maxilon blue GRL onto sepiolite from aqueous solutions. **Chemical Engineering Journal**, v. 124, n. 1–3, p. 89–101, 2006.

DOS SANTOS LINS, P. V. et al. Evaluation of caffeine adsorption by MgAl-LDH/biochar composite. **Environmental Science and Pollution Research**, v. 26, n. 31, p. 31804–31811, 2019.

FARIA, D. et al. Cenários E Perspectivas Das Principais Culturas Do Rio Grande Do Sul Em Processos De Biorrefinaria. **Revista Eletrônica Científica da UERGS**, v. 2, n. 3, p. 291, 2016.

FLORENTINO-MADIEDO, L. et al. Influence of binder type on greenhouse gases and PAHs from the pyrolysis of biomass briquettes. **Fuel Processing Technology**, v. 171, n. September 2017, p. 330–338, 2018.

FLORENTINO-MADIEDO, L.; DÍAZ-FAES, E.; BARRIOCANAL, C. The effect of briquette composition on coking pressure generation. **Fuel**, v. 258, n. August, p. 116128, 2019.

FREUNDLICH, H. M. F. Over the Adsorption in Solution. **The Journal of Physical Chemistry**, v. 57, p. 385–471, 1906.

GARCA-PÈREZ, M.; CHAALA, A.; ROY, C. Co-pyrolysis of sugarcane bagasse with petroleum residue. Part II. Product yields and properties. **Fuel**, v. 81, n. 7, p. 893–907, 2002.

GHOLAMI, P. et al. Photocatalytic degradation of gemifloxacin antibiotic using Zn-Co-LDH@biochar nanocomposite. **Journal of Hazardous Materials**, v. 382, n. March 2019, p. 121070, 2020.

GUO, J. et al. Synthesis of a novel ternary HA/Fe-Mn oxides-loaded biochar composite and its application in cadmium(II) and arsenic(V) adsorption. **Journal of Environmental Sciences (China)**, v. 85, p. 168–176, 2019.

GUPTA, V. K.; ALI, I. Removal of endosulfan and methoxychlor from water on carbon slurry. **Environmental Science and Technology**, v. 42, n. 3, p. 766–770, 2008.

HAYKIRI-ACMA, H.; YAMAN, S.; KUCUKBAYRAK, S. Gasification of biomass chars in steam-nitrogen mixture. **Energy Conversion and Management**, v. 47, n. 7–8, p. 1004–1013, 2006.

HO, Y. S.; MCKAY, G. Pseudo-second order model for sorption processes. **Process Biochemistry**, v. 34, p. 451–465, 1999.

HU, B. et al. Engineering carbon materials from the hydrothermal carbonization process of biomass. **Advanced Materials**, v. 22, n. 7, p. 813–828, 2010.

HU, F. et al. High-efficient adsorption of phosphates from water by hierarchical CuAl/biomass carbon fiber layered double hydroxide. **Colloids and Surfaces A: Physicochemical and Engineering Aspects**, v. 555, p. 314–323, 2018.

HUANG, D. et al. Cr(VI) removal from aqueous solution using biochar modified with Mg/Al-layered double hydroxide intercalated with ethylenediaminetetraacetic acid. **Bioresource Technology**, v. 276, n. December 2018, p. 127–132, 2019.

IBGE. **Production of Vegetable Extraction and Silviculture - PEV's (in Portuguese)**. Disponível em: <https://biblioteca.ibge.gov.br/visualizacao/periodicos/74/pevs_2018_v33_informativo.pdf>.

ILOMUANYA, M. et al. Effect of pore size and morphology of activated charcoal prepared from midribs of Elaeis guineensis on adsorption of poisons using metronidazole and Escherichia coli O157:H7 as a case study. **Journal of Microscopy and Ultrastructure**, v. 5, n. 1, p. 32, 2017.

JANA, S.; PURKAIT, M. K.; MOHANTY, K. Removal of crystal violet by advanced oxidation and microfiltration. **Applied Clay Science**, v. 50, n. 3, p. 337–341, 2010.

JIA, Y. et al. A novel magnetic biochar/MgFe-layered double hydroxides composite removing Pb 2+ from aqueous solution: Isotherms, kinetics and thermodynamics. **Colloids and Surfaces A: Physicochemical and Engineering Aspects**, v. 567, n. December 2018, p. 278–287, 2019.

JIANG, T. Y. et al. Adsorption of Pb(II) on variable charge soils amended with rice-straw derived biochar. **Chemosphere**, v. 89, n. 3, p. 249–256, 2012.

JIBRIL, B. et al. Effects of H3PO4 and KOH in carbonization of lignocellulosic material. **Journal of Analytical and Applied Pyrolysis**, v. 83, n. 2, p. 151–156, 2008.

KALIYAN, N.; VANCE MOREY, R. Factors affecting strength and durability of densified biomass products. **Biomass and Bioenergy**, v. 33, n. 3, p. 337–359, 2009.

KAN, T.; STREZOV, V.; EVANS, T. J. Lignocellulosic biomass pyrolysis: A review of product properties and effects of pyrolysis parameters. **Renewable and Sustainable Energy Reviews**, v. 57, p. 1126–1140, 2016.

KIAN, L. K. et al. Isolation and characterization of nanocrystalline cellulose from roselle-derived microcrystalline cellulose. **International Journal of Biological Macromolecules**, v. 114, p. 54–63, 2018.

LAGERGREN, S. About the Theory of so Called Adsorption of Soluble Substances. **Kungliga Svenska Vetenskapsakademiens Handlingar**, v. 24, p. 1–39, 1898.

LAMINE, S. M. et al. Chemical activation of an activated carbon prepared from coffee residue. **Energy Procedia**, v. 50, p. 393–400, 2014.

LANGMUIR, I. The adsorption of gases on plane surfaces of glass, mica and platinum. **Journal of the American Chemical Society**, v. 40, p. 1361–1403, 1918.

LEHMANN, J.; JOSEPH, S. Biochar for environmental management: An introduction. **Biochar for Environmental Management: Science and Technology**, v. 1, p. 1–9, 2009.

LU, K. et al. Torrefaction and low temperature carbonization of oil palm fiber and eucalyptus in nitrogen and air atmospheres. **BIORESOURCE TECHNOLOGY**, v. 123, p. 98–105, 2012.

LUM, W. C. et al. **Lignocellulosic nanomaterials for construction and building applications**. [s.l.] Elsevier Inc., 2019.

MACEDO, J. S. et al. Biomorphic activated porous carbons with complex microstructures from lignocellulosic residues. **Microporous and Mesoporous Materials**, v. 107, n. 3, p. 276–285, 2008.

MACIÁ-AGULLÓ, J. A. et al. Activation of coal tar pitch carbon fibres: Physical activation vs. chemical activation. **Carbon**, v. 42, n. 7, p. 1361–1364, 2004.

MALL, I. D.; SRIVASTAVA, V. C.; AGARWAL, N. K. Removal of Orange-G and Methyl Violet dyes by adsorption onto bagasse fly ash - Kinetic study and equilibrium isotherm analyses. **Dyes and Pigments**, v. 69, n. 3, p. 210–223, 2006.

MASEL, R. I. **Principles of Adsorption and Reaction on Solid Surfaces**. [s.l.] John Wiley & Sons, 1996.

MASSARO, M. M.; SON, S. F.; GROVEN, L. J. Mechanical, pyrolysis, and combustion characterization of briquetted coal fines with municipal solid waste plastic (MSW) binders. **Fuel**, v. 115, p. 62–69, 2014.

MCCABE, W.; SMITH, J.; HARRIOTT, P. **Unit Operations of Chemical Engineering**. 7 edition ed. [s.l.] McGraw-Hill Education, 2004.

MEILI, L. et al. MgAl-LDH/Biochar composites for methylene blue removal by adsorption. **Applied Clay Science**, v. 168, n. October 2018, p. 11–20, 2019.

MICHELIN, M.; TEIXEIRA, J. A. Liquid hot water pretreatment of multi feedstocks and enzymatic hydrolysis of solids obtained thereof. **Bioresource Technology**, v. 216, p. 862–869, 2016.

MISHRA, G.; DASH, B.; PANDEY, S. Layered double hydroxides: A brief review from fundamentals to application as evolving biomaterials. **Applied Clay Science**, v. 153, n. June 2017, p. 172–186, 2018.

MUAZU, R. I.; STEGEMANN, J. A. Biosolids and microalgae as alternative binders for biomass fuel briquetting. **Fuel**, v. 194, p. 339–347, 2017.

MUNTEAN, S. G. et al. Evaluation of a functionalized copolymer as adsorbent on direct dyes removal process: Kinetics and equilibrium studies. **Journal of Applied Polymer Science**, v. 127, n. 6, p. 4409–4421, 2013.

MWAMPAMBA, T. H.; OWEN, M.; PIGAHT, M. Opportunities, challenges and way forward for the charcoal briquette industry in Sub-Saharan Africa. **Energy for Sustainable Development**, v. 17, n. 2, p. 158–170, 2013.

NAKASHIMA, G.; LARISSA, A.; HANSTED, S. Materiais Lignocelulósicos : Caracterização e Produção de Briquetes. **Revista Virtual de Química**, v. 9, n. 1, p. 150–162, 2017.

NASCIMENTO, R. F. DO et al. **Adsorção: Aspectos teóricos e aplicações ambientais**. [s.l: s.n.].

NORMARK, M. et al. Analysis, pretreatment and enzymatic saccharification of different fractions of Scots pine. **BMC Biotechnology**, v. 14, 2014.

OKOT, D. K.; BILSBORROW, P. E.; PHAN, A. N. Briquetting characteristics of bean straw-maize cob blend. **Biomass and Bioenergy**, v. 126, n. May, p. 150–158, 2019.

OLIVEIRA, E. B. DE. **O eucalipto e a embrapa: quatro décadas de pesquisa e desenvolvimento**. [s.l.] Embrapa, 2021.

PENG, Y. et al. Optimizing the synthesis of Fe/Al (Hydr)oxides-Biochars to maximize phosphate removal via response surface model. **Journal of Cleaner Production**, v. 237, p. 117770, 2019.

PIMCHUAI, A.; DUTTA, A.; BASU, P. Torrefaction of Agriculture Residue To Enhance Combustible Properties. **Energy and Fuels**, p. 4638–4645, 2010.

RANGABHASHIYAM, S. et al. Relevance of isotherm models in biosorption of pollutants by agricultural byproducts. **Journal of Environmental Chemical Engineering**, v. 2, n. 1, p. 398–414, 2014.

ROCHA, D. et al. Biomass briquetting and its perspectives in Brazil. **Biomass and Bioenergy**, v. 5, p. 1–7, 2011.

ROCHA, O. R. et al. Avaliação do processo adsortivo utilizando mesocarpo de coco verde para remoção do corante cinza reativo BF-2R. **Quimica Nova**, v. 35, n. 7, p. 1369–1374, 2012.

ROUSSET, P. et al. Enhancing the combustible properties of bamboo by torrefaction. **Bioresource Technology**, v. 102, n. 17, p. 8225–8231, 2011a.

ROUSSET, P. et al. LCA of eucalyptus wood charcoal briquettes. **Journal of Cleaner Production**, v. 19, n. 14, p. 1647–1653, 2011b.

RUTHVEN, D. M. **Principles of adsorption and adsorption processes**. [s.l.] John Wiley & Sons, 1984. v. 4

SALLEM-IDRISSI, N. et al. Lignin degradation and stability: Volatile Organic Compounds (VOCs) analysis throughout processing. **Polymer Degradation and Stability**, v. 130, p. 30–37, 2016.

SEKAR, M.; SAKTHI, V.; RENGARAJ, S. Kinetics and equilibrium adsorption study of lead(II) onto activated carbon prepared from coconut shell. **Journal of Colloid and Interface Science**, v. 279, n. 2, p. 307–313, 2004.

SETTE, C. R. et al. Energy enhancement of the eucalyptus bark by briquette production. **Industrial Crops and Products**, v. 122, n. May, p. 209–213, 2018.

SOARES, L. S. . et al. Use of waste coffee grounds and sawdust in briquettes molding and evaluation of properties. **Revista Materia**, v. 20, n. 2, p. 550–560, 2015.

STAMATE, A. E. et al. Highlights on the catalytic properties of polyoxometalate-intercalated layered double hydroxides: A review. **Catalysts**, v. 10, n. 1, 2020.

SUGUIHIRO, T. M. et al. An electroanalytical approach for evaluation of biochar adsorption characteristics and its application for Lead and Cadmium determination. **Bioresource Technology**, v. 143, p. 40–45, 2013.

THEISS, F. L.; AYOKO, G. A.; FROST, R. L. Iodide removal using LDH technology. **Chemical Engineering Journal**, v. 296, p. 300–309, 2016.

TÜKMEN, D. et al. **High Capacity Removal of Mercury(II) Ions by Poly(Hydroxyethyl Methacrylate) nanoparticles**. 1. ed. [s.l.] Elsevier, 2010.

TUMULURU, J. S. et al. A review on biomass torrefaction process and product properties for energy applications. **Industrial Biotechnology**, v. 7, n. 5, p. 384–401, 2011.

VOGEL, K. P.; JUNG, H. J. G. Genetic modification of herbaceous plants for feed and fuel. **Critical Reviews in Plant Sciences**, v. 20, n. 1, p. 15–49, 2001.

WANG, S. et al. Sorption of arsenic onto Ni/Fe layered double hydroxide (LDH)-biochar composites. **RSC Advances**, v. 6, n. 22, p. 17792–17799, 2016.

WANG, S. et al. Lignocellulosic biomass pyrolysis mechanism : A state-of-the-art review. **Progress in Energy and Combustion Science**, v. 62, p. 33–86, 2017.

WANG, T. et al. Biochar/MnAl-LDH composites for Cu (II) removal from aqueous solution. **Colloids and Surfaces A: Physicochemical and Engineering Aspects**, v. 538, p. 443–450, 2018.

WEBER, K.; QUICKER, P. Properties of biochar. **Fuel**, v. 217, n. September 2017, p. 240–261, 2018.

WILLIAMS, P. T. Hydrogen and Carbon Nanotubes from Pyrolysis-Catalysis of Waste Plastics: A Review. **Waste and Biomass Valorization**, n. 0123456789, 2020.

WORRELL, E.; REUTER, M. **Handbook of Recycling: State of the art for Practitioners, Analysts, and Scientists**. 1. ed. [s.l.] Elsevier, 2014.

WRÓBLEWSKA, H. et al. Application of post-consumer wood composts in canna lily (Canna x generalis L.H Bailey) cultivation. **Drewno**, v. 191, n. June, p. 5–25, 2014.

XIANG, W. et al. Biochar technology in wastewater treatment: A critical review. **Chemosphere**, v. 252, p. 126539, 2020.

YAN, K.; WU, G.; JIN, W. Recent Advances in the Synthesis of Layered, Double-Hydroxide-Based Materials and Their Applications in Hydrogen and Oxygen Evolution. **Energy Technology**, v. 4, n. 3, p. 354–368, 2016.

YÁÑEZ-S, M. et al. Physicochemical characterization of ethanol organosolv lignin (EOL) from Eucalyptus globulus: Effect of extraction conditions on the molecular structure. **Polymer Degradation and Stability**, v. 110, p. 184–194, 2014.

YANG, F. et al. Assembling biochar with various layered double hydroxides for enhancement of phosphorus recovery. **Journal of Hazardous Materials**, v. 365, p. 665–673, 2019.

YARGICOGLU, E. N. et al. Physical and chemical characterization of waste wood derived biochars. **Waste Management**, v. 36, p. 256–268, 2015.

YI, F.-Y. et al. Polyoxometalates-based Heterometallic Organic-Inorganic Hybrid Materials for Rapid Adsorption and Selective Separation of Methylene Blue from Aqueous Solution. **RSC Adv**, v. 51, p. 3336–3339, 2015.

ZAITON, S. et al. Eucalyptus in Malaysia: Review on Environmental Impacts. **Journal of Landscape Ecology**, v. 13, n. 2, p. 79–94, 2020.

ZHAO, S.; ZHANG, D. Supercritical CO2 extraction of Eucalyptus leaves oil and comparison with Soxhlet extraction and hydro-distillation methods. **Separation and Purification Technology**, v. 133, p. 443–451, 2014.

ZHENG, J. LU et al. Thermal conversion of rice husks and sawdust to liquid fuel. **Waste Management**, v. 26, n. 12, p. 1430–1435, 2006.